UNIVERSITY OF LEEDS

Economic Operation of Virtual Power Plants with Electric Vehicle Charging Stations

Han Wang

Submitted in accordance with the requirements for the degree of Doctor of Philosophy. Electronic and Electrical Engineering

The University of Leeds

Student of Engineering

School of Electronic and Electrical Engineering

May 2023

Abstract

Energy management of distributed energy resources (DERs) is challenging due to the distributed and uncertain nature of DERs. To optimally operate DERs and trade their energy as well as energy flexibility for financial benefits, energy management for virtual power plants (VPPs) and electric vehicle (EV) charging stations are investigated in this thesis. The research in this thesis can be summarized into three parts. Part I provides a VPP operation strategy in the electricity market environment. Part II proposes an EV charging station operation strategy considering EV user incentives. Part III develops a coordinated VPP and EV charging station operation framework based on the methods proposed in parts I and II.

(1) Economic VPP operation

In this part, an optimal VPP operation regime is proposed considering multiple electricity markets and multiple uncertainties. The proposed operation regime handles both the VPP market bidding and unit dispatching problems. To deal with uncertainties, a hybrid stochastic minimax regret optimization model is proposed. To reduce the conservativeness of the formulated optimization models, a self-adaptive algorithm is proposed.

(2) Economic EV charging station operation

In this part, an EV charging station operation strategy with an EV user incentive program is proposed to improve the EV charging station economic benefit. To maximize the long-term profit of the EV charging station, an optimal incentive price selection model is developed. In the solution methodology, a problem linearization method is first proposed. Then, a distributed solution methodology is developed based on the proposed adaptive alternating-direction-method-of-multipliers algorithm.

(3) Economic VPP operation considering EV charging stations

In this part, a multi-stakeholder VPP-charging station system is investigated. Firstly, a coordinated operation framework is proposed for the VPP-charging station system to maximize the total benefit of the system. Then, an improved EV user incentive program is proposed for acquiring EV energy flexibility. At the cost allocation stage, a τ-value cost allocation method is developed. To alleviate the computation burden in calculating the τ-values, a τ-values estimation approach is proposed.

The effectiveness of the energy management methods proposed in this thesis is verified through theoretical analysis and numerical simulations. Significant results suggest high potential for practical application in certain scenarios.

Keywords: **energy management, optimization, uncertainty, virtual power plants, electric vehicles, charging stations**

Intellectual Property

The candidate confirms that the work submitted is his/her own and that appropriate credit has been given where reference has been made to the work of others.

Signed Han Wang

Acknowledgements

I would like to express my deepest gratitude to my supervisors, Professor. Youwei Jia, Dr. Chun Sing Lai, Dr. Petros Aristidou, and Professor. Kang Li for their guidance, encouragement, and support throughout my PhD study. Their knowledge and expertise have been instrumental in shaping my research and helping me to achieve my goals. I am grateful for their patience, constructive feedback, and willingness to share their time and experience with me. It is a great honer of mine to have had the opportunity to work with such outstanding scholars

I also want to thank my colleagues for their support during my PhD study. Their insights and timely feedback have been invaluable to me. I am grateful for their willingness to share their insightful ideas, and for the inspiring discussions we have had over the years.

Finally, I would like to express my appreciation to my family, especially my wife Haoyu Ma, for their unwavering support and encouragement throughout my PhD journey. Haoyu has been my constant companion and source of strength during the most challenging times of my study. Her love, care and understanding have made it possible for me to focus on my research and complete my degree. I am truly blessed to have such a wonderful partner in life.

Abbreviations

The abbreviations used in this thesis are listed below.

ADMM	Alternating-direction-Method-of-Multipliers
ADMM-AP	Alternating-Direction-Method-of-Multipliers with Adaptive Penalty
C&CG	Column-and-Constrain Generation
CI	Controllability Index
DER	Distributed Energy Resource
ESS	Energy Storage System
EV	Electric Vehicle
iSOC	Initial State-of-Charge
MMR	Minimax-Regret
PFUR	Potential Flexibility Utilization Ratio
PV	Photovoltaic
SOC	State-of-Charge
V2G	Vehicle-to-Grid
VPP	Virtual Power Plant
VPP-CS	Virtual Power Plant-Charging Station

Nomenclature

α	Incentive price for the buy-out program
$\overline{\alpha}$	Incentive price upper bound for the buy-out program
α_g	Incentive price for the buy-out program in group g
β	Incentive price for the pay-as-use program
$\overline{\beta}$	Incentive price upper bound for the pay-as-use program
β_g	Incentive price for the pay-as-use program in group g
γ_m	Minimum acceptable incentive price for EV user in the pay-as-use program
γ_n	Minimum acceptable incentive price for EV user in the buy-out program
λ_t^{DA}	Energy price in the day-ahead electricity market
λ_t^{+}	Energy deficiency price in the balancing market
λ_t^{-}	Energy surplus price in the balancing market
π_s	Probability of price scenario
σ^{DA}	Uncertainty coefficient for day-ahead renewable generation
σ^{RT}	Uncertainty coefficient for real-time renewable generation
σ^{CS}	Uncertainty coefficient for day-ahead charging station energy demand
θ	Maximum regret for given VPP day-ahead decisions
θ_l	τ-value estimation accuracy
ϑ	Auxiliary variable in the C&CG algorithm
ϑ_n^B	Auxiliary variable for the bilinear terms in the buy-out program
$\vartheta_{m,t}^P$	Auxiliary variable for the bilinear terms in the pay-as-use program
$\varepsilon_{adaptive}$	Stopping threshold of the adaptive process in the ADMM-AP algorithm

ε_{admm}	Convergence threshold of the ADMM-AP algorithm
ε_{ccg}	Convergence threshold of the C&CG algorithm
ε_{coef}	Convergence threshold of the uncertainty coefficient adjusting algorithm
ε_{τ}	Accuracy threshold of the τ-value estimation approach
η	Charging/discharging efficiency of EV battery
ρ	Penalty factor in the ADMM and ADMM-AP algorithms
ω_n^B	Incentive payment for EV user n in the buy-out program
ω_m^P	Incentive payment for EV user m in the pay-as-use program
ψ^+	Penalty coefficient for energy deficiency
ψ^-	Penalty coefficient for energy surplus
ϕ	Coefficient for calculating τ-values
φ_g	Adaptive weight of group g in the adaptive algorithm of ADMM-AP
τ_l	τ-value of player l
τ_l^{conv}	τ-value obtained from the standard method
τ_l^{est}	τ-value obtained from the estimation method
ξ	Scaled dual variable in the ADMM algorithm
ζ	Lifted uncertain variable
$\Delta P_{m,t}$	Power change in the pay-as-use program
$\Delta P_{m,t}^D$	Downward power change in the pay-as-use program
$\Delta P_{m,t}^U$	Upward power change in the pay-as-use program
$\Delta P_{n,t}$	Power change in the buy-out program
Δt	Scheduling interval
$A_{g,v}$	Scaled dual variable in the ADMM-AP algorithm for the buy-out program
$B_{g,v}$	Scaled dual variable in the ADMM-AP algorithm for the pay-as-use program
$C_{m,t}^{bd}$	EV battery degradation cost
CR_m	Cost reduction in the pay-as-use program
CR_n	Cost reduction in the buy-out program

D	Day-ahead stage VPP decision variable
FG	Final gain of charging station in the adaptive process of the ADMM-AP algorithm
fv_t^r	Forecast value of renewable generation
fv_t^{cs}	Forecast value of charging station energy demand
J	Number of shortlisted member in the τ-value estimation approach
$P_{m,t}$	EV charging power in the pay-as-use program
$P_{n,t}$	EV charging power in the buy-out program
P_R	Reserve market energy request
P_t^B	Energy exchange in the balancing market
P_t^{DA}	Energy exchange in the day-ahead market
$P_{n,t}^{DA,CS}$	Day-ahead energy schedule of charging station
$P_{m,t}^{Dis}$	Energy discharged from EV
$P_{i,t}^G$	Energy generation of thermal power plants
P_t^s	Scheduled power of EV
P_t^{us}	Unscheduled power of EV
pf_n	Potential flexibility of EV in the buy-out program
rv_t^r	Real value of renewable generation
SOC_t	EV battery SOC
$\lvert S\rvert_{max}$	Maximum considered coalition size in the τ-value estimation approach
u_t^r	Renewable generation scenario
u_t^{cs}	Charging station energy demand scenario
y_i	On/off status of thermal power plant
y_m	Participation status of EV user in the pay-as-use program
y_n	Participation status of EV user in the buy-out program

Contents

1 Introduction **1**

1.1 Background 1

1.2 Motivations and Objectives 4

1.2.1 Motivations 4

1.2.2 Thesis Objectives 6

1.3 Thesis Contribution Summary 6

1.4 Preliminary Knowledge 8

1.4.1 Stochastic Optimization 8

1.4.2 Minimax-Regret Optimization 8

1.4.3 Column-and-Constraint-Generation Algorithm 9

1.4.4 Alternating Direction Method of Multipliers Algorithm 12

1.4.5 τ-Value Cost Allocation Model 13

1.5 Thesis Structure 15

2 Literature Review **17**

2.1 DER Aggregating Agents in Power Systems 17

2.1.1 Virtual Power Plants 18

2.1.2 Microgrids 19

2.1.3 EV Aggregators 20

2.1.4 EV Charging Stations 20

2.2 VPP Operation 21

2.2.1 Electricity Markets for VPPs 21

2.2.2 VPP Operation Uncertainties 23

2.3 EV Charging Station Operation 26

2.4 VPP Operation Considering EVs . . . 29

3 VPP Operation Strategy 31

3.1 Chapter Introduction . . . 31

3.2 Problem and Model Description . . . 36

3.2.1 Electricity Market Structure . . . 36

3.2.2 Virtual Power Plant Operational Model . . . 37

3.2.3 Uncertainty Modeling . . . 38

3.3 Problem Formulation . . . 39

3.3.1 Day-Ahead Bidding Model . . . 39

3.3.2 Real-Time Dispatch Model . . . 44

3.4 Solution Methodology . . . 46

3.4.1 Problem Reformulation . . . 46

3.4.2 C&CG Solution framework . . . 48

3.4.3 Self-Adaptive Algorithm . . . 51

3.5 Case Study . . . 53

3.5.1 Experiment Setup . . . 53

3.5.2 Results and Discussions . . . 54

3.6 Chapter Summary . . . 65

4 EV Charging Station Energy Management 67

4.1 Chapter Introduction . . . 67

4.2 Problem and Model Description . . . 72

4.2.1 Charging Station Operation Framework . . . 72

4.2.2 Proposed EV User Incentive Program . . . 74

4.3 Optimal Incentive Price Selection . . . 81

4.4 Proposed Solution Methodology . . . 83

4.4.1 Problem Linearization . . . 84

4.4.2 Distributed Solution Approach . . . 85

4.4.3 Adaptive Penalty Factors . . . 88

4.4.4 Convergence Discussion . . . 89

4.5 Case Study . . . 90

4.5.1 Experiment Setup . . . 91

4.5.2 Results and Discussions . . . 92
4.5.3 Comparative Case Study . . . 96
4.6 Chapter Summary . . . 102

5 VPP Operation Considering EV Charging Stations 103
5.1 Chapter Introduction . . . 103
5.2 Problem Description . . . 107
5.2.1 VPP-CSs System . . . 107
5.2.2 EV User Incentives . . . 112
5.3 Problem Formulation . . . 116
5.3.1 Charging Station Day-Ahead Energy Scheduling . . . 116
5.3.2 VPP Day-Ahead Bidding . . . 118
5.3.3 VPP-CSs Real-Time Balancing . . . 120
5.4 Cost Allocation Method . . . 123
5.4.1 τ-value Cost Allocation . . . 123
5.4.2 Proposed Maximum Right Cost Estimation Approach . . . 126
5.5 Case Study . . . 131
5.5.1 Experiment Setup . . . 131
5.5.2 Numerical Results . . . 132
5.5.3 τ-value Estimation . . . 138
5.6 Chapter Summary . . . 141

6 Conclusion 143

References 146

A Appendix Chapter 168
A.1 Two-Stage Minimax Regret Problem Reformulation . . . 168
A.2 Bilinear Term Transformation . . . 169

List of Figures

1.1 Distributed energy resources in power systems 2

1.2 Global DER market forecast 2

1.3 Estimated global EVs in use from 2013 to 2021 4

1.4 Generalized intermediary DER aggregating agent operating framework 5

1.5 Research structure illustration 15

3.1 Configuration of a general VPP 38

3.2 The hierarchical structure of the day-ahead bidding model 40

3.3 (a) the forecast data and the day-ahead forecast intervals (b) the real-time wind forecast intervals 54

3.4 Generated price scenarios and the actual price. 55

3.5 Bidding curves for hours 3, 15, and 21 56

3.6 The market allocated energy, called reserve, and required energy 56

3.7 The dispatching results of the thermal generators 57

3.8 The VPP's profit using the proposed methods (case 1) 58

3.9 The VPP's profit using the stochastic robust optimization model under the price-dependent framework (case 2) 59

3.10 The VPP's profit using the multistage stochastic programming approach (case 3) 60

3.11 The VPP's profit using the proposed stochastic MMR model under the price-independent framework (case 4) 61

3.12 The VPP's profit using the proposed price-dependent stochastic MMR model without performing real-time dispatch (case 5) 62

3.13 Profit loss in the dispatching stage using the adjusted and constant uncertainty coefficients 63

3.14 Reserve response results of the VPP 64

4.1 Operation framework of the charging station 73
4.2 EV Flexibility in the BO program 76
4.3 EV flexibility illustration in the pay-as-use program 79
4.4 Selected market energy price scenarios for 24 operating days. 91
4.5 Flexibility distributions for (a) different flexibility amounts and (b) different EV arrival time. 92
4.6 (a) EV user minimum acceptable prices and optimized incentive prices, (b) participation results 93
4.7 PFUR distribution for individual EV users in (a) the BO program and (b) the PAU program. 94
4.8 Convergence rates of (a) the proposed ADMM-AP algorithm and (b) the conventional ADMM algorithm 95
4.9 (a) Charging prices at the charging station. (b) EV response curve in the transactive control program. 96
4.10 200 EV charging scenarios. 97
4.11 Load shift results in the time-of-use pricing program 98
4.12 Load shift results in the transactive control program 99
4.13 Load shift results in the proposed hybrid incentive program. 100

5.1 Configuration of the VPP-CSs system 108
5.2 Operation framework of the considered VPP-CSs system. 109
5.3 Payments for using EV energy flexibility 114
5.4 Flowchart of the estimated τ-value cost allocation method. 130
5.5 (a) day-ahead renewable generation information, (b) forecast charging station load profiles and average forecast market price 131
5.6 (a) typical offering curves, (b) day-ahead scheduling results 133
5.7 Optimization results of the VPP-CSs system 134
5.8 (a) Profits using the estimated τ-value method and standard τ-value method, (b) profits using the estimated τ-value method and under no cooperation. 135
5.9 Attractive matrix for (a) all players and (b) charging stations only. 138

5.10 (a) Remainders and remainder drops for the VPP, (b) remainders for charging stations. 139
5.11 Estimated deviations under different J and $|S|_{max}$. 140
5.12 Computational performance comparison. 141

List of Tables

1.1 DER classifications . . . 3

3.1 VPP operation regime Summary . . . 35
3.2 Generator Characteristics . . . 54
3.3 Profit Results Using Different Strategies and Models . . . 62
3.4 Computation time analysis . . . 65

4.1 Key properties of different types of incentive programs . . . 71
4.2 EV model parameters . . . 92
4.3 Scheduling results . . . 100

5.1 Generator Characteristics . . . 132
5.2 Comparison of different cooperative levels . . . 136
5.3 Comparison of different incentive programs . . . 137

Chapter 1

Introduction

1.1 Background

The growing concerns over climate change are accelerating the worldwide trend for decarbonization (Zhang et al. 2020). In 2021, the electricity sector emitted 13 gigatonnes of carbon dioxide, accounting for over one-third of global energy-related carbon dioxide emissions (IEA 2022). In power systems, distributed energy resources (DERs) are small-scale, clean installations of electricity supply or demand resources such as small gas plants, solar arrays, small wind farms, energy storage devices, and electric vehicles (EVs), as shown in Fig. 1.1.

As compared to traditional centralized power plants, DERs have the potential to significantly reduce carbon emissions in the electricity sector by providing clean and renewable sources of energy. The use of DERs also allows for greater flexibility and reliability in power systems, as they can be located closer to where electricity is needed and can help to balance the grid by reducing peak demand. Due to advances in technology and falling costs, DERs have been gathering their momentum to be massively deployed in power systems in recent years, and this growing trend is expected to continue in the future (Navigant 2019), as shown in Fig. 1.2. DERs have the potential to provide a range of benefits. From the power system's perspective, DERs are the key components to achieve local supply of cleaner and more flexible energy, thus, making the power system more sustainable and more reliable. For electricity consumers, DERs can reduce the bills they pay for electricity, as well as improve the power quality.

Generally, DERs can be divided into dispatchable units and non-dispatchable units (Rahman

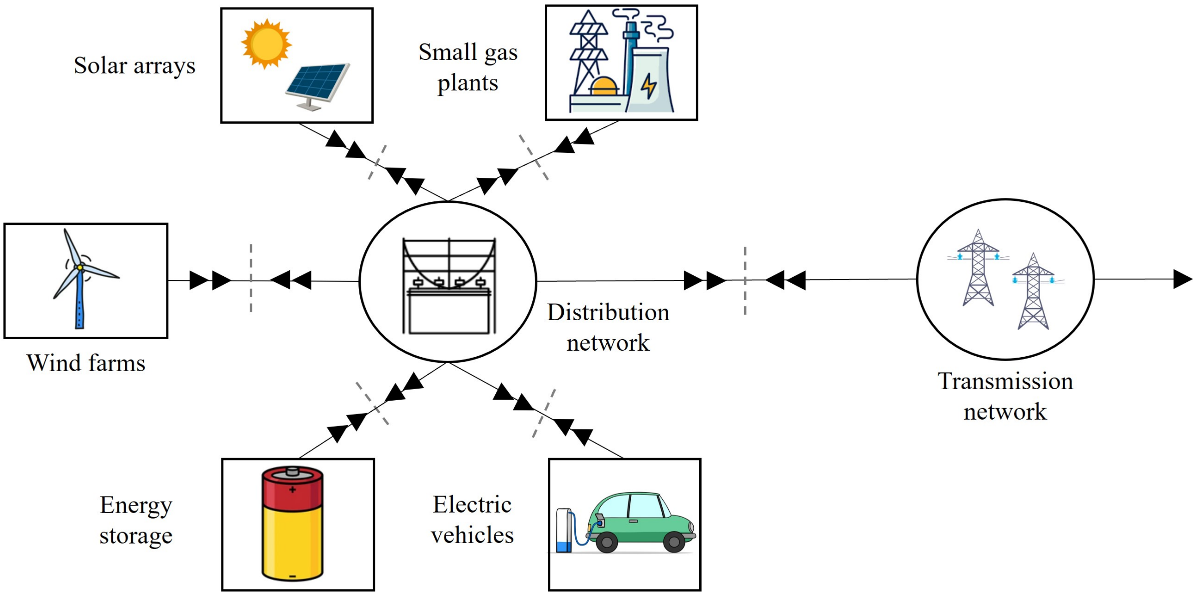

Figure 1.1: Distributed energy resources in power systems

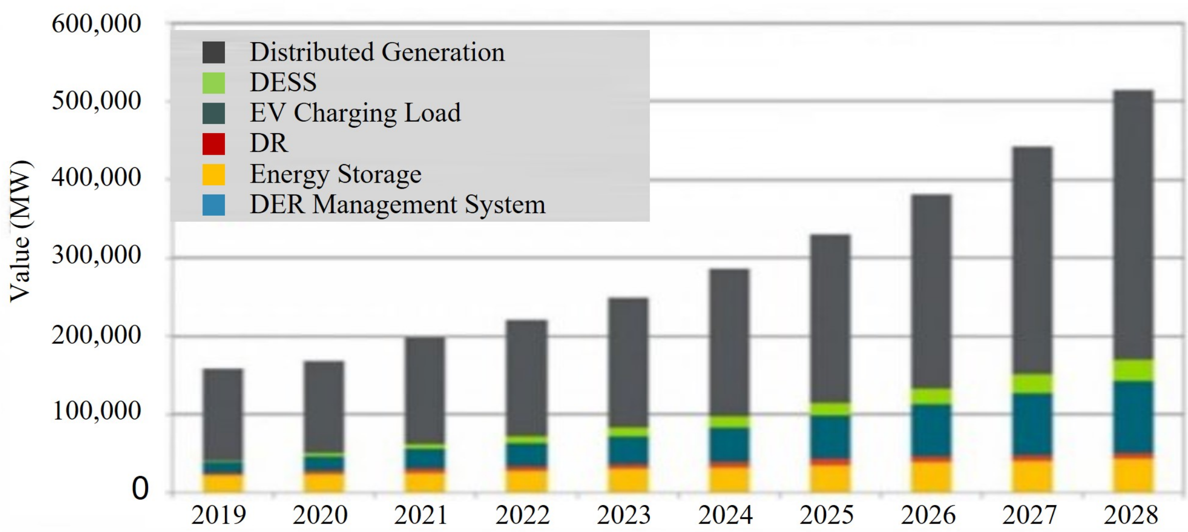

Figure 1.2: Global DER market forecast

Table 1.1: DER classifications

Classification	Power range	Typical installations
Micro DERs	Less than 2kW and connected to low voltage network	Rooftop solar photovoltaic (PV), battery storage
Mini DERs	Greater than 2kW and up to 30kW	Fuel cells, EVs
Small DERs	Greater than 30kw but no more than 1MW	small hydro, combined heat and power system
Medium DERs	Greater than 1MW but no more than 5MW	Biomass, hydro, local wind generating units
Large DERs	Greater than 5MW	Co-generation, hydro, solar thermal

et al. 2015). For dispatchable DER like small thermal plants and energy storage devices, their power output can be adjusted by the DER operators. For non-dispatchable DERs such as solar arrays and small wind farms, their power output cannot be controlled by their operators because their power output is subject to fluctuations due to weather conditions, time of day, and other factors outside of the operator's control.

According to their sizes, DERs can be classified as micro DERs, mini DERs, small DERs, medium DERs, and large DERs (*DER classification* 2021), as summarized in Table 1.1.

Micro DERs refer to DERs with installed capacities less than 2kW, which normally refers to rooftop solar panels and small battery storage devices. Mini DERs are DERs with installed capacity ranging from 2 kW to 30 kW, fuel cells and EVs normally fall into this category. Small DERs have capacities larger than 30kW but less than 1MW. Typical small DERs include combined heat and power systems and small hydro plants. Medium DERs are DERs with capacities larger than 1MW but less than 5MW. Biomass plants and local wind farms can belong to this class. Finally, there are some DERs with installed capacities larger than 5MW, such as co-generation plants and some hydro plants. These DERs are classified as large DERs.

Though individual EV power capacities are small, EVs are of particular interest thanks to their accelerating growing trend in recent years. From 2013 to 2021, the estimated number of EVs in use worldwide increased from 0.4 million to 16.4 million (*Global electric car stock* 2022), with an annual growth rate of 59%, as shown in Fig. 1.3.

With the fast adoption of DERs in power systems, traditional centralized management methods

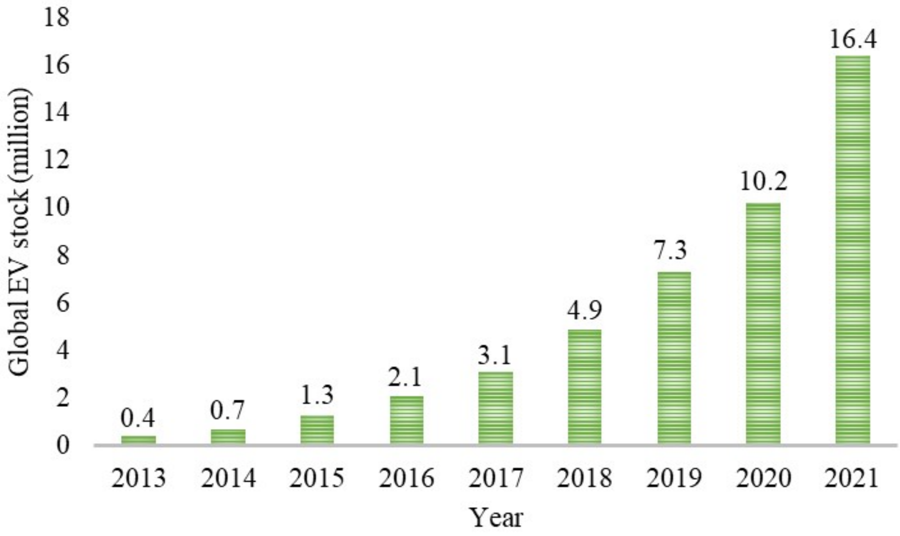

Figure 1.3: Estimated global EVs in use from 2013 to 2021

can no longer satisfy the operation requirements due to the distributed, heterogeneous, and uncertain nature of DERs (Stekli et al. 2022). Hence, more advanced energy management methods await to be developed to effectively operate DERs and maximize their energy as well as energy flexibility utilities.

1.2 Motivations and Objectives

1.2.1 Motivations

Despite the huge benefits DERs can bring to power systems and electricity consumers, the management of DERs in bulk power systems remains to be a challenging problem due to their small capacity, uncertainty, heterogeneity, and distributed nature (Zhang et al. 2018; Jia et al. 2020; Quint et al. 2019). For system operators, DERs are normally too small and too many to be centrally dispatched. In electricity markets, constraints of small installed capacity and uncertainty make the entrance (which historically has been on the order of 500kW to 1 MW for power capacity (Stekli et al. 2022)) and operation of the power market difficult for DERs (Ju et al. 2016a; Braslavsky, Wall, and Reedman 2015). To address the difficulties in managing DERs, intermediary aggregating agents that can actively manage DERs and interact with bulk power system operators become necessary.

Internally, the intermediary DER aggregating agents are expected to forecast and optimize the operation of DERs. Externally, the intermediary DER aggregating agents should exchange the

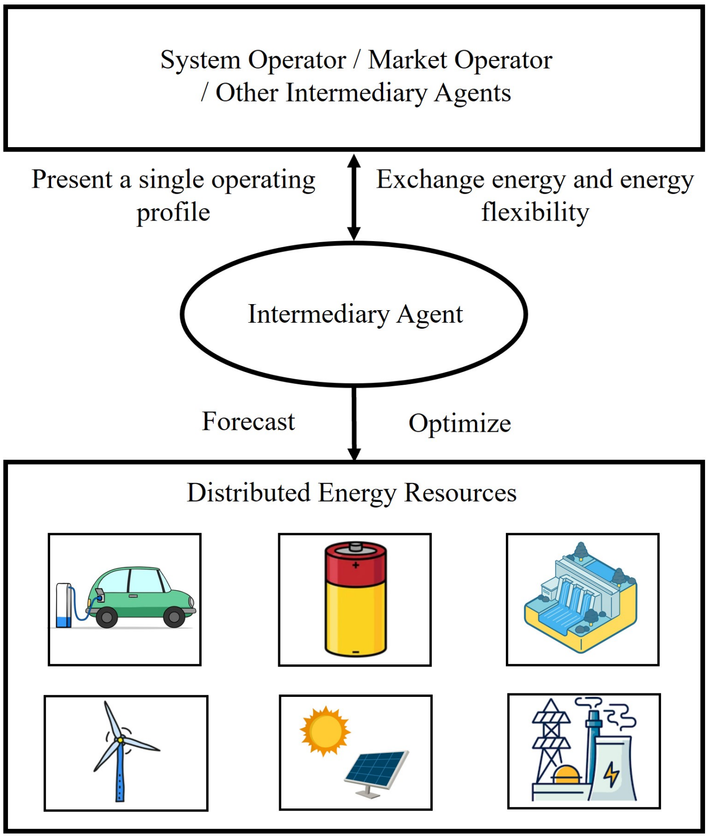

Figure 1.4: Generalized intermediary DER aggregating agent operating framework

aggregated DER energy as well as energy flexibility with bulk system operators or other DER aggregating agents to maximize the DER utility. In this way, the intermediary DER aggregating agents can bridge DERs with bulk system operators by presenting a single, aggregated DER operating profile at the bulk system operator side. The general operating framework of intermediary DER aggregating agents is shown in Fig. 1.4.

The advantages of introducing intermediary DER aggregating agents are multi-fold. From the bulk system operator's perspective, the benefits include reduced operating problem complexity, reduced communication cost, increased visibility of system components, and increased controllability. For DERs, through the aggregation of intermediary DER aggregating agents, they can more actively participate in the operation of bulk power systems. More proactive operation means increased utilization of DER energy and energy flexibility, which can create more benefits for DER owners.

However, the operation of intermediary DER aggregating agents also faces many challenges. For example, uncertainties in stochastic DERs and external factors like electricity markets must be addressed. The operating problem dimensionality can also be a problem if the aggregated DERs are too many and the number of operation decision variables is huge. In some cases, multiple intermediary agents with different interests are simultaneously incorporated, which leads to cooperative or non-cooperative game problems and increases the operating problem complexity.

This thesis is dedicated to proposing advanced energy management methods that can help intermediary DER aggregating agents handle operating challenges, and the DER aggregating agents investigated in this thesis include virtual power plants (VPPs) and EV charging stations. The methods proposed in this thesis is focused on maximizing the financial benefits of VPPs and EV charging stations by maximizing the utility of DER energy as well as energy flexibility. This thesis maximizes the financial benefits of VPPs and EV charging stations by developing profit-oriented energy management methods that allow VPPs and EV charging stations to maximize the utility of DERs integrated into this framework.

1.2.2 Thesis Objectives

This thesis aims to aggregate DERs as single operating entities such as VPPs and EV charging stations for improving the economic benefits of DERs. To realize this target, the objectives of this thesis are listed as follows:

- Identifying the factors that can affect the economic performance of DERs.
- Proposing methods that can improve the economic benefits of DERs.
- Evaluating the effectiveness of the proposed methods through experimental demonstrations.
- Demonstrating the potential of applying the proposed methods to practical scenarios.

1.3 Thesis Contribution Summary

This thesis is dedicated to developing energy management methods for VPPs considering the operation of EV charging stations. To realize this target, the research works are divided into three major parts. The first part develops an optimal operating regime for VPPs to optimally operate renewable resources and thermal power plants in electricity markets under multiple uncertainties. The second part aims to propose an efficient EV charging station operation strategy considering using incentives in exchange for EV user cooperation. In the third part, a cooperative operating framework is proposed to allow the VPP and EV charging stations to coordinately operate renewable resources, thermal power plants, and EVs. The technical contributions of each part can be summarized as follows:

The original contributions of the first part include:

- An optimal VPP operation regime under multiple uncertainties is proposed, which consists of a day-ahead price-dependent bidding strategy and a real-time dispatching model.
- A stochastic minimax-regret optimization model is proposed to help the VPP make optimal day-ahead bidding decisions.
- A self-adaptive algorithm is proposed to control the conservativeness introduced by the minimax nature of the minimax-regret-based dispatching model in the real-time stage.

The original contributions of the second part include:

- A hybrid incentive program is proposed to encourage EV users to sell their charging flexibility to the charging station. The proposed hybrid incentive program combines the advantages of both static and dynamic incentive programs, namely, it has the features of simplicity, consistency, and controllability.
- An optimal incentive price selection model is developed to minimize the charging station's operating cost. The optimization results of the proposed model can serve as a reference for policymakers who adopt the proposed hybrid incentive program.
- An alternating-direction-method-of-multipliers with adaptive penalties solution algorithm is presented to efficiently solve the problem in a distributed manner for large EV fleets.

The original contributions of the third part include:

- A multi-stakeholder VPP-charging station system consisting of a DER-based VPP and multiple charging stations is investigated based on the methods proposed in chapters 3 and 4. A cooperative operation framework is proposed to handle the interactive day-ahead bidding and real-time balancing problems of the VPP-charging station system.
- An EV user incentive program is proposed. As compared to the methods proposed in chapter 4, the proposed incentive program can achieve more EV user cost reduction, higher EV energy flexibility utilization, and lower total system cost.
- An estimated τ-value cost allocation method is proposed to efficiently address the cost

allocation problem of the VPP-charging station system.

With the efforts made in this thesis, it is expected that my work will help DERs to be effectively integrated into existing power systems and promote more sustainable usage of electrical energy.

1.4 Preliminary Knowledge

This section provides some theoretical fundamentals for the optimization models and solution algorithms applied in this thesis.

1.4.1 Stochastic Optimization

The scenario-based stochastic optimization approach is used to handle uncertain random variables described by using probability distributions (Luis and Morteza 2021). In the scenario-based stochastic optimization approach, each scenario represents a plausible realization of the uncertain factors and has an associated probability of occurrence. In the formulation of a stochastic optimization problem, the optimal decision is made such that the expected objective value is optimized over all the representative scenarios.

Let X be the domain of all feasible decisions and x be the decision variables. Let S be the set of representative uncertainty scenarios and s be a specific representative uncertainty scenario. Denote the probability for each scenario s as π_s. Let $C(x, s)$ be the cost function. Then, the general stochastic optimization problem formulation can be written as:

$$\min_{x \in X} \left\{ \sum_{s \in S} \pi_s C(x, s) \right\} \tag{1.1}$$

1.4.2 Minimax-Regret Optimization

The minimax-regret optimization approach is used to handle uncertain random variables described by using uncertainty intervals. In the minimax-regret optimization approach, the uncertainty interval defines all possible outcomes of the uncertain factors. The solution of a minimax-regret optimization problem considers all the possible realizations of the uncertain factors within the uncertainty interval. The objective of a minimax-regret optimization problem is to minimize the worst-case regret under all possible uncertainty outcomes, in which the regret is defined as the objective value difference between the optimal solution with perfect uncertainty information and the solution obtained with incomplete uncertainty information.

Depending on the availability of uncertainty information in the decision-making process, minimax-regret optimization problems can be classified into two groups. The first group is minimax-regret optimization problems without recourse. In this group of problems, all the decisions should be made before any uncertain information is available. Let U be the set of all possible outcomes of uncertain factors and u be a specific uncertainty scenario within the uncertainty set. Denote x^u as the optimal solution for a specific uncertainty realization u. Then, the general formulation of the minimax-regret optimization problem without recourse can be written as:

$$\min_{x \in X} \left\{ \max_{u \in U} \{C(x, u) - C(x^u, u)\} \right\} \tag{1.2}$$

Another group of minimax-regret problems is minimax-regret optimization problems with recourse, which is also known as two-stage minimax-regret optimization problems (Jiang et al. 2013; Chen et al. 2014). In two-stage minimax-regret optimization problems, the second-stage decision variables can be adjusted after some uncertainty information becomes available. Denote Y as the domain of all feasible first-stage decisions and y be a specific first-stage decision action. Let x be the adjustable second-stage decision variables with domain X. Let $C_1(y)$ denote the cost function of the first stage. Let $C_2(y, x, u)$ denote the cost function of the second stage. Denote y^u and x^u as the optimal first- and second-stage solutions under uncertainty scenario u. The general formulation of a two-stage minimax-regret optimization problem can be formulated as:

$$\min_{y \in Y} \left\{ C_1(y) + \max_{u \in U} \left\{ \min_{x \in X} C_2(y, x, u) - \min_{x^u \in X, y^u \in Y} [C_1(y^u) + C_2(y^u, x^u, u)] \right\} \right\} \tag{1.3}$$

1.4.3 Column-and-Constraint-Generation Algorithm

The column-and-constraint-generation (C&CG) solution algorithm is meant to solve convex two-stage robust optimization problems (Zeng and Zhao 2013) with the following form:

$$\min_{y\in Y}\left\{C_1(y)+\max_{u\in U}\left\{\min_{x\in X}C_2(y,x,u)\right\}\right\} \tag{1.4}$$

s.t.

$$A_1y \geq d_1 \tag{1.5}$$

$$A_2x + A_3y + A_4u \geq d_2 \tag{1.6}$$

Where A_1,A_2,A_3, and A_4 are matrices and d_1,d_2 are vectors.

In the C&CG algorithm, the two-stage robust optimization problem is firstly decomposed into a primary problem and a secondary problem by introducing an auxiliary variable ϑ. After decomposition, the primary problem can be written as:

$$\min_{y\in Y} C_1(y) + \vartheta \tag{1.7}$$

s.t.

$$A_1y \geq d_1 \tag{1.8}$$

$$\vartheta \geq C_2(y, x_v, u^*_{v-1}) \tag{1.9}$$

$$A_2 x_v + A_3 y + A_4 u^*_{v-1} \geq d_2 \tag{1.10}$$

Where x_v are new variables added in iteration v. u^*_{v-1} are the optimized uncertainty realizations in the last iteration $v-1$.

The secondary problem can be written as:

$$\max_{u \in U} \left\{ \min_{x \in X} \left[C_2(y, x, u) \right] \right\} \tag{1.11}$$

s.t.

$$A_2 x + A_3 y^*_v + A_4 u \geq d_2 \tag{1.12}$$

where y^*_v is the optimal solution of the primary problem in iteration v.

After the decomposition, the C&CG algorithm solves the decomposed problems by using the following steps:

(1) Set lower bound (LB) to $LB = -\infty$, upper bound (UB) to $UB = \infty$. Iteration number $v = 0$. Set the convergence threshold ε.

(2) Solve the primary problem with added new variables x_v and new constraints (1.9), (1.10). Derive the optimal solutions $\{y^*_v, x^*_v, \vartheta^*\}$. Update the lower bound as $\max[LB, C_1(y^*_v) + \vartheta^*]$

(3) Solve the secondary problem with the latest optimal first-stage solution y^*_v. Derive the optimal secondary solutions x^*_v and the worst-case uncertainty scenario u^*_v. Update the upper bound as $\min\{UB, C_1(y^*_v) + C_2(y^*_v, x^*_v, u^*_v)\}$

(4) If $UB - LB \leq \varepsilon$, return y^*_v and terminate the process. Otherwise, update iteration $v = v+1$, add new variables x_{v+1} and new constraints (1.9), (1.10) to the primary problem. Go back to step (2).

1.4.4 Alternating Direction Method of Multipliers Algorithm

The alternating-direction-method-of-multipliers (ADMM) algorithm solves optimization problems with separable objective functions.

Denote x_1 and x_2 as two sets of variables in an optimization problem. Let $F_1(x_1)$ and $F_2(x_2)$ denote the separated objective functions of the optimization problem. Then, a separable optimization problem with the following form can be solved by using the ADMM algorithm (Boyd et al. 2011):

$$\min_{x_1,x_2} \{F_1(x_1) + F_2(x_2)\} \tag{1.13}$$

s.t.

$$A_5x_1 + A_6x_2 = d_3 \tag{1.14}$$

Where A_5 and A_6 are matrices and d_3 is a vector.

In the ADMM solution algorithm, the augmented Lagrangian of the original problem can be written as:

$$L_\rho(x_1, x_2, x_3) = F_1(x_1) + F_2(x_2) + x_3^T(A_5x_1 + A_6x_2 - d_3) + \frac{\rho}{2}\|A_5x_1 + A_6x_2 - d_3\|_2^2 \tag{1.15}$$

Where x_3 are dual variables of the original optimization problem, ρ is the update step length, which is also known as the penalty factor. By introducing the scaled dual variable x_4, the augmented Lagrangian can be rewritten as:

$$L_\rho(x_1, x_2.x_4) = F_1(x_1) + F_2(x_2) + \frac{\rho}{2}\|A_5x_1 + A_6x_2 - d_3 + x_4\|_2^2 + Constant \tag{1.16}$$

with the scaled dual variable $x_4 = \frac{x_3}{\rho}$.

Under the ADMM solution framework, the problem can be solved by using the following steps:

(1) Set iteration $v = 1$. Set the penalty factor ρ and convergence threshold ε.

(2) Solve $arg\min F_1(x_1) + \frac{\rho}{2}\left\|A_5x_1 + A_6x_2^{v-1} - d_3 + x_4^{v-1}\right\|_2^2$ with x_2^{v-1} and x_4^{v-1}. Derive the optimal solution x_1^v. Where x_2^{v-1} and x_4^{v-1} are the optimal solutions obtained in iteration $v-1$.

(3) Solve $arg\min F_2(x_2) + \frac{\rho}{2}\left\|A_5x_1^v + A_6x_2 - d_3 + x_4^{v-1}\right\|_2^2$ with x_1^v and x_4^{v-1} to derive the optimal solution x_2^v.

(4) Update the scaled dual variable $x_4^v = x_4^{v-1} + A_5x_1^v + A_6x_2^v - d_3$.

(5) If $A_5x_1^v + A_6x_2^v - d_3 \leq \varepsilon$, terminate the iteration and return $\{x_1^v, x_2^v\}$. Otherwise, go back to step (2).

1.4.5 τ-Value Cost Allocation Model

The τ-value method is a cost allocation method in cooperative games. Denote a grand coalition with $|Z|$ members as Z. Let the characteristic function $v : 2^Z \rightarrow R$ of this grand coalition be the cost generated from any sub-coalition $S \in Z$ with $v(\emptyset) = 0$. Then, a cooperative game can be defined as the ordered pair $\langle Z, v\rangle$, in which the real number $v(S)$ represents the cost generated from the members of S when they cooperate.

In this cooperative game $\langle Z, v\rangle$, for each player $l \in Z$ in the sub-coalition $S : \{S \in Z, l \in S\}$, the marginal cost contribution $M_l(S, v)$ of player l to the coalition S is:

$$M_l(S, v) = v(S) - v(S\backslash\{l\}) \tag{1.17}$$

where the last term represents the cost generated by the rest members of S without player l. When the considered sub-coalition is the grand coalition Z, this marginal contribution of player l is defined as its utopia cost $M_l^u(Z, v)$:

$$M_l^u(Z, v) = v(Z) - v(Z\backslash\{l\}) \tag{1.18}$$

The utopia cost represents the cost contribution of a considered player to the total cost of the grand coalition. Namely, when a new player is added to the grand coalition, the utopia cost of the added new player is the increment of the total grand coalition cost due to the addition of this new player. The utopia cost $M_l^u(Z, v)$ is the minimum cost player l should pay. Because if player l wants to pay less, then it is more advantageous for other players in the grand coalition Z to remove player l. Hence, the utopia cost $M_l^u(Z, v)$ provides a lower bound of the cost allocated to player l. Next, an upper bound of the cost allocated to player l is found by identifying the maximum cost player l should pay.

The remainder $R(S, l)$ of player l in a sub-coalition S is defined as the cost remanent for player l in the coalition S if all other players $h : \{h \in S, h \neq l\}$ only pay their utopia costs:

$$R(S, l) = v(S) - \sum_{h \in S \setminus \{l\}} M_h^u(Z, v) \tag{1.19}$$

Then, for each $\in Z$, the maximum right cost $M_l^{mrc}(v)$ is defined as the minimum remainder player l can have from all possible sub-coalitions that contain player l:

$$M_l^{mrc}(v) = \min_{S: l \in S} R(S, l) \tag{1.20}$$

The maximum right cost of player l is the maximum cost player l needs to pay in the grand coalition. Because if player l pays more than $M_l^{mrc}(v)$, then the sub-coalition S with $R(S, l) = M_l^{mrc}(v)$ would form a more solid coalition by making all other players in S pay their utopia costs. Hence, $M_l^{mrc}(v)$ can serve as an upper bound of the cost allocated to the player l.

After obtaining the utopia costs and maximum right costs, the lower and upper bounds of costs allocated to each player in the grand coalition can be determined. With the upper and lower bounds, it is reasonable to find a compromise between the lower and upper bounds to be the solution for the cost allocation problem. By using the lower and upper bounds of costs allocated to players, the τ-values for each player $l \in Z$ can be computed such that each player pays a cost that lies between their lower- and upper-cost bounds:

$$\tau_l(v) = \phi M_l^{mrc}(v) + (1-\phi)M_l^u(Z, v) \tag{1.21}$$

where the coefficient $\phi \in [0, 1]$ can be uniquely determined by satisfying the efficiency criterion:

$$\sum_{l \in Z} \tau_l(v) = v(Z) \tag{1.22}$$

In the cost allocation problem, the obtained τ-value $\tau_l(v)$ for player l is the cost allocated to that player.

1.5 Thesis Structure

This thesis is meant to aggregate DERs through VPPs and EV charging stations for improving the economic benefits of DERs. The research structure of this thesis is illustrated in Fig. 1.5. The rest of this thesis is organized as follows:

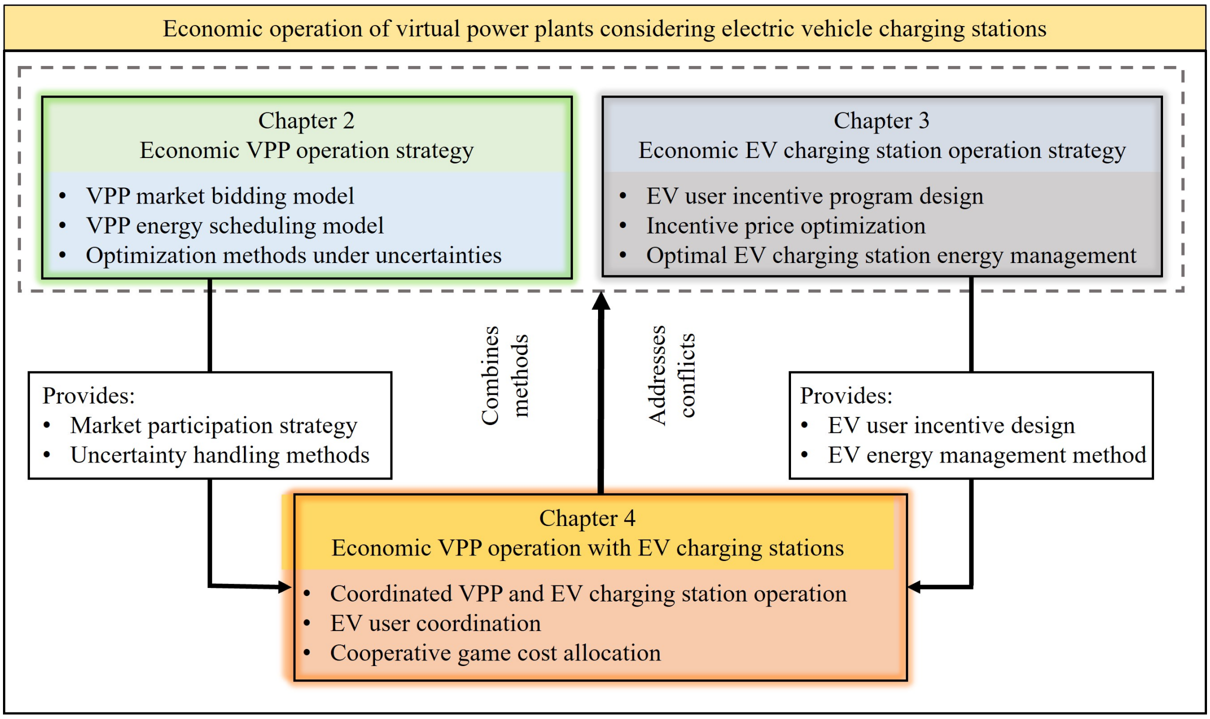

Figure 1.5: Research structure illustration

Chapter 2 first reviews the most common intermediary DER aggregating agents in the literature by giving their definitions, analyzing their problem objectives, and presenting their operation constraints. Then, as the focus of this thesis, the energy management methods for VPPs, EV charging stations, and VPPs considering EVs will be reviewed.

Chapter 3 proposes an optimal VPP operation regime to optimally operate renewable energy sources and thermal power plants in electricity markets considering multiple uncertainties.

Chapter 4 proposes an EV charging station operation strategy with an EV user incentive program for encouraging EV user participation in EV charging station charging scheduling.

Based on the methods proposed in chapters 3 and 4, chapter 5 proposes a coordinated VPP and EV charging stations operating framework to cooperatively operate renewable energy sources, thermal power plants, and EVs in electricity markets under multiple uncertainties. Besides, the conflicting interests between the VPP and EV charging stations are also addressed in chapter 5.

Chapter 6 concludes this thesis and provides some possible future extensions.

Chapter 2

Literature Review

In the literature, there has been a wide range of pioneering works devoted to developing efficient energy management methods for DER aggregating agents. For different types of intermediary DER aggregating agents, the proposed energy management methods may be different in their problem objectives and operating constraints. This section first introduces some common intermediary DER aggregating agents by providing their definitions, analyzing their problem objectives, and presenting their operation constraints. Then, as the focus of this thesis, the energy management methods for VPPs, EV charging stations, and VPPs considering EVs will be reviewed.

2.1 DER Aggregating Agents in Power Systems

Intermediary DER aggregating agents are meant to help bulk system operators to manage DERs more efficiently and visibly. To accommodate various operating conditions and purposes, different DER aggregating agents should be carefully selected to achieve better management performances.

In the literature, the most common DER aggregating agents include VPPs and microgrids. For these aggregating agents, all kinds of DERs such as small-scale thermal power plants, renewable generation, demand response resources, and EVs can be integrated into their operation. There are also some special DER aggregating agents like EV aggregators and EV charging stations. Normally, EV aggregators and EV charging stations can only collectively manage the charging/discharging operation of EVs. In some special cases (Mouli, Bauer, and Zeman 2016;

Fathabadi 2017; Singh et al. 2020; Shin, Choi, and Kim 2019; Sun 2021), the EV charging stations may also be equipped with energy storage devices and solar arrays, which enable them to operate a wider range of DERs other than EVs. These DER aggregating agents will be introduced next by providing their definitions, discussing their problem objectives, and explaining their operating constraints.

2.1.1 Virtual Power Plants

VPPs are cloud-based aggregating platforms of DERs (Bhuiyan et al. 2021). The cloud-based feature makes it possible for the components of VPPs to be distributed in different geographical locations without physical connections between them. The category for VPP is subdivided into commercial VPPs and technical VPPs (Pourghaderi et al. 2018). Commercial VPPs are a portrayal of DERs that participates in electricity markets similar to traditional transmission power plants. In commercial VPPs, network constraints are not modeled in the operating strategies (Pourghaderi et al. 2021), and the focus is to earn as much profit as possible from electricity markets by selling the DER energy and energy flexibility. Technical VPPs are responsible for the network balance and clarity of DERs to the operators, which makes technical VPPs more engaged in the system management of power system networks (Foroughi et al. 2021).

For VPPs, there are two major objectives in the operation problems, including developing external bidding strategies in electricity markets and making internal energy management decisions for the DERs under control (Naval and Yusta 2021). In the bidding problems, the aim is to maximize the operating profit while reducing energy production forecast errors and economic penalties due to the forecast errors. The constraints in the bidding problems include a series of technical and temporal constraints for the generators, such as power output limits, ramp limits, unit commitment status, reserve requirement, and energy balancing constraints (Camal, Michiorri, and Kariniotakis 2018; Nezamabadi and Setayesh Nazar 2016; Karimyan et al. 2016). In energy management problems, the aim is to optimize the scheduling of different generation facilities, storage systems, and electricity demand to maximize the final VPP profit. The energy management models are typically technical-economic dispatching problems that determine the final power output of each dispatchable unit. In energy management problems, the VPP operation is subject to energy balancing constraints and technical constraints, such as generator availability, electricity exchange with the markets, and state-of-charge (SOC) of energy storage devices.

2.1.2 Microgrids

A microgrid is a concept that accommodates renewable and conventional energy resources on a small scale while merging the integral parts of the power system to attain reliable operation throughout the generation to load demand (Muhtadi et al. 2021). Specifically, all the components of a microgrid should be constrained within a predefined geographical area and should be physically connected (Nosratabadi, Hooshmand, and Gholipour 2017). Depending on the connection states, microgrids can be classified as grid-connected microgrids that can interchange energy with the utility grid, and islanded microgrids that can operate independently to maintain their system stability (Ferruzzi et al. 2016). For some grid-connected microgrids, the connection can be switched off to disconnect the microgrid from the main grid in case of main-grid failure to maintain the stability of the microgrid. Based on the type of energy resources and consumers, some works classify microgrids as AC or DC microgrids, where AC stands for alternating current and DC stands for direct current.

In the microgrid operation, the objective function can be roughly classified into two categories, including cost minimization problems and power quality maximization problems (Jirdehi et al. 2020). In cost minimization problems, the objective is formulated as a cost function that may involve various costs like energy procurement, generator fuel, maintenance, energy storage device degradation, generator start-up, power curtailment, user comfort violation, and energy not supplied (Nwulu and Xia 2017; Wang et al. 2017b; Aboli, Ramezani, and Falaghi 2019; Yuan et al. 2022; Gazijahani and Salehi 2017; Wang et al. 2017a). In power quality maximization problems, the objectives are mostly formulated to control the voltages (Olival, Madureira, and Matos 2017; Merritt, Chakraborty, and Bajpai 2017; Chen, Hou, and Hui 2016) and regulate the frequencies (Heidari, Seron, and Braslavsky 2017; Li et al. 2017; Khooban et al. 2017). For microgrids, the operating constraints are more complicated than VPPs since network security should be guaranteed. The electric power balancing constraints ensure that the energy production is equal to the sum of demands and network losses. The generation limits for generators include the maximum/minimum power output and the ramping limits. The energy storage constraints such as the power of charging/discharging and terminal SOC. In the grid-connected mode, the energy exchange with the main-grid is limited by the capacity of the point-of-common-coupling. Considering the network security, voltage, frequency, bus angle, and power line current should be involved in the problem formulations.

2.1.3 EV Aggregators

An EV aggregator is a cloud-based platform that can aggregate EV fleets to optimize their charging behavior and participate in electricity markets on behalf of the EV fleets. EV aggregators can remotely monitor and control the charging/discharging states of EV batteries (Zheng, Wang, and Yang 2023). Hence, EV aggregators can utilize the EV energy flexibility to minimize the total operating cost (Zheng, Wang, and Yang 2023; Aliasghari, Mohammadi-Ivatloo, and Abapour 2020; Zheng et al. 2020; Cao et al. 2020; Wang et al. 2022c) or provide a series of grid services (Wenzel et al. 2017) like frequency regulation (Wang et al. 2020; Ko, Han, and Sung 2016), voltage control (Hashemi, Shahabi, and Teimourzadeh-Baboli 2019; Xu et al. 2019) and supporting renewable integration (Rezaei et al. 2020; Shamshirband, Salehi, and Gazijahani 2018).

In EV aggregator operating problems, the objective is normally formulated to maximize the total benefit of the EV aggregator. The benefit terms can include a wide range of factors such as energy market cost/revenue, ancillary service market revenue, EV user energy bill, incentives paid to EV users for utilizing the EV charging/discharging energy flexibility, and penalty for loss of commitment to the offered ancillary service capacity (Zheng, Wang, and Yang 2023; Aliasghari, Mohammadi-Ivatloo, and Abapour 2020; Shamshirband, Salehi, and Gazijahani 2018). In EV aggregator operating problems, the constraints may include electricity market capacity constraints, EV charging rate constraints, EV battery capacity constraints, reserve margin constraints, power balancing constraints, and EV charging demand constraints.

2.1.4 EV Charging Stations

EV charging stations are an important type of physical charging infrastructure where EV users go to recharge their EVs. Similar to EV aggregators, EV charging stations can also monitor and manage the charging/discharging states of EVs to maximize their benefit or provide some grid service (Wu and Sioshansi 2019; Wu et al. 2022). Based on the target customers, EV charging stations can be classified as private charging stations, semi-public charging stations, and public charging stations (Ministry 2021). Private EV charging station usage is limited to personal EV or EV fleets owned by one entity, such as some bus charging stations. Semi-public charging station usage is normally limited to a restricted set of EV users such as apartment residents and university staff. Public charging stations are charging infrastructures that are open to all EV users. Depending on the system configurations, EV charging stations can be pure EV charging stations, PV-EV charging stations (Mouli, Bauer, and Zeman 2016; Fathabadi 2017), and PV-ESS-EV charging stations (Singh et al. 2020; Shin, Choi, and Kim 2019; Sun 2021), where ESS stands for energy storage systems. Based on the charging modes, EV charging stations can also be classified as AC, DC, and inductive EV charging stations (Rajendran et al. 2021).

The operating objectives of EV charging stations can involve operation cost minimization, power loss minimization, optimal power flow, renewable integration, peak load shaving, and valley load filling (Wu et al. 2022). The operating constraints in EV charging station management problems normally include the EV charging rate limits, EV battery SOC limits, EV battery capacity constraints, and EV charging demand limits. When energy storage is included, the operation constraints should also include the energy storage device limits such as initial and terminal SOC, charging/discharging rate, and energy capacity limits.

In this thesis, the primary focus is the operation of VPPs and EV charging stations, and the goal is to develop energy management methods that optimally operate DERs through VPPs and EV charging stations. Hence, the rest of this section specifically reviews the VPP operation methods, the EV charging station management methods, and the VPP operation considering EVs.

2.2 VPP Operation

VPPs can network DERs to forecast and optimize their operation, and trade the energy as well as energy flexibility of DERs in electricity markets to generate profits. To achieve this goal, VPPs need to interact with various electricity markets. During the interactions with electricity markets, a major challenge of VPP operation is how to deal with the uncertainties that arise from both DERs and electricity markets (Yu et al. 2019). This subsection first reviews different electricity markets VPPs can participate in, then discuss the VPP uncertainty problem by presenting the uncertainty models and corresponding optimization techniques.

2.2.1 Electricity Markets for VPPs

VPP can participate in multiple electricity markets to increase revenue sources and improve profitability. However, participating in multiple markets can also bring more technical and temporal constraints on the VPP operation problem, making the problem more complicated to coordinate between different markets. To develop better VPP operating strategies, it is necessary to know about what the electricity markets are and understand how they work.

According to the time difference between the market-clearing and physical delivery of energy/energy flexibility, electricity markets can be classified as forward markets, day-ahead markets, intraday markets, and real-time markets (Naval and Yusta 2021).

The forward market is designed for energy exchange over a specified period at a fixed price. Participating in the forward market enables securing long-term prices and product quantities. Hence, hedging the risk of dealing with more volatile spot market prices (Toubeau, De Grève, and Vallée 2017). In the forward market, energy transactions can be made at times that are several weeks to several years before the physical delivery happens. In (Toubeau, De Grève, and Vallée 2017; Jafari and Foroud 2020), VPP operating models considering the forward market is proposed to increase the VPP profitability.

The day-ahead market is meant to conduct electricity transactions between suppliers and consumers for each hour of the following day. In the day-ahead market pool, each participant submits their energy offers or demand bids, and the pool matches these offers and bids to form energy transactions between market participants. In most VPP works, the revenue from the energy day-ahead market is the major source of VPP income.

The intraday market trades energy at a time horizon that is closer than the day-ahead market. In the intraday stage, there is more available information than in the day-ahead stage. Hence, some unexpected energy deviations in the day-ahead stage can be settled in the intraday market. As the penetration level of renewable generation increases, the stochasticity in generation makes the intraday market more and more important. In (Nguyen, Le, and Wang 2018; Wozabal and Rameseder 2020; Wei et al. 2018; Kong et al. 2019), the intraday market is included to make up for day-ahead forecast errors and reduce the VPP operating cost.

As the last opportunity for balancing energy production and consumption, the real-time market has the shortest time horizon between the market clearing and the physical delivery. Normally, this time interval ranges between five to thirty minutes (Naval and Yusta 2021). In (Rahimiyan and Baringo 2015; Kasaei, Gandomkar, and Nikoukar 2017; Shafiekhani et al. 2019; Zhou et al. 2020; Baringo and Baringo 2016), the VPP participates in the real-time market to settle its energy deviations that cannot be economically covered by using its own DER energy flexibility.

Electricity markets can also be classified by the type of products they trade. Energy markets trade electricity energy, and ancillary service markets trade ancillary services that can help to ensure the power quality, security, and reliability of the electricity generation and transmission system.

By participating in energy markets, VPP earns profits by selling DER energy. Almost all VPP operating frameworks consider energy markets in the operating problems. Some VPP works involve ancillary service markets to diversify the VPP income sources. In ancillary service markets, the DER energy flexibility can be traded to increase VPP profit. In (Camal, Michiorri, and Kariniotakis 2018; Wang et al. 2017b; Liang and Guo 2016; Shayegan-Rad, Badri, and Zangeneh 2017), reserve markets are considered in VPP operating problems to increase the VPP income. In (Shayegan-Rad, Badri, and Zangeneh 2017; Tajeddini, Rahimi-Kian, and Soroudi 2014; Wang, Riaz, and Mancarella 2020), the frequency-regulation market is involved in the VPP operating model.

2.2.2 VPP Operation Uncertainties

Uncertainty problem is a major challenge in VPP research and applications. In VPP operation problems, there are many uncertainty sources such as renewable power, market price, and load demand (Yu et al. 2019). Uncertainties can have negative impacts such as increasing threats to the safety and stability of system operation, reducing the estimation accuracy of variables during the VPP operation and scheduling, and increasing the operation cost of the VPP. To measure the influences of uncertainties in VPP operation, uncertainty models should be used to describe the uncertainties. Then, to restrict the negative impacts of uncertainties, optimization techniques should be developed based on the uncertainty description models to make optimal operation decisions under uncertainties.

In the literature, the most popular descriptions for uncertainties in VPPs include the probability distribution models and uncertainty interval models. In probability distribution models, the random variables in the VPP operation are generally described by probability density functions such as Normal distribution, uniform distribution, and Weibull distribution (Yu et al. 2019). These probability density distributions can give information on how likely it is for uncertain factors to take specific values. Hence, probability descriptions allow the VPP to decide what actions to take for different uncertainty values with corresponding probabilities. Generally, probability descriptions allow VPPs to optimize the expected objective values. In uncertainty interval models, the probability distributions of random variables are not required. Instead, only the upper and lower bounds of uncertainties need to be determined. With all possible uncertainty scenarios considered in the problem, uncertainty interval descriptions allow VPPs to optimize the worst-case objective values, which usually tend to make the solutions conservative (Wang et al. 2021b).

To handle uncertainties described by using probability distributions, the most common optimization technique in the literature is the stochastic optimization approach. In the stochastic optimization approach, uncertainties are represented by several scenarios with certain probabilities (Zhou, Zhai, and Wu 2022; Koraki and Strunz 2017). In that case, stochastic optimization problems aim to optimize the expected objective value under the generated uncertainty scenarios considering their probabilities. The stochastic optimization approach has been applied to VPP operation problems in (Ju et al. 2016a; Nguyen, Le, and Wang 2018; Wozabal and Rameseder 2020; Koraki and Strunz 2017; Abbasi et al. 2019; Rahimi, Ardakani, and Ardakani 2021; Baringo, Baringo, and Arroyo 2018a; Ju et al. 2019; Kardakos, Simoglou, and Bakirtzis 2015; Hadayeghparast, Farsangi, and Shayanfar 2019) to deal with uncertainties by optimizing the expected objective values.

For uncertainties described with uncertainty intervals, the robust optimization approach is an effective method to make operational decisions. In the robust optimization approach, solutions that are insensitive to uncertain factor disturbances are found to guarantee the minimum performance under all possible circumstances. To realize this target, the worst-case scenarios are identified, and the optimal solutions are found to guarantee the VPP performance under the worst-case scenarios. In (Rahimiyan and Baringo 2015; Baringo, Baringo, and Arroyo 2018a; Ju et al. 2019; Jun, Jun, and Linpeng 2019; Liu, Xu, and Tomsovic 2015), the robust optimization technique is used to handle uncertainties by ensuring the optimal VPP performance under the worst-case scenarios.

Besides the robust optimization approach, the minimax-regret optimization approach is also an effective optimization technique for handling distribution-free uncertain factors. In the minimax-regret optimization approach, regret is defined as the objective value difference between the optimal solution with perfect uncertainty information and the solution obtained with incomplete uncertainty information (Jiang et al. 2013; Fan et al. 2014). Similar to the robust optimization approach, the minimax-regret optimization approach also needs to identify the worst-case uncertainty scenario and make optimal operational decisions against the worst-case scenario. The difference is that the robust optimization approach directly optimizes the objective values, but the minimax-regret optimization approach minimizes the difference between the objective values of the optimal solution with perfect information and the solution with partial information. That is, the minimax-regret optimization approach always seeks to choose actions that are closer to the optimal feasible solution. This mechanism of the minimax-regret optimization approach makes it less conservative than the robust optimization approach. In (Jiang et al. 2013; Fan et al. 2014), the minimax-regret optimization approach is applied to deal with renewable uncertainties that are modeled using uncertainty intervals.

In the early stages of VPP research, the operating frameworks are relatively simple. Some early VPP works only consider participation in the day-ahead energy market (Peik-Herfeh, Seifi, and Sheikh-El-Eslami 2013; Peikherfeh, Seifi, and Sheikh-El-Eslami 2011; Giuntoli and Poli 2013; Vasirani et al. 2013). Then, to bridge the information gap between the day-ahead forecast and real-time operation, the intraday and real-time markets are introduced to enhance the VPP performance (Rahimiyan and Baringo 2015; Kardakos, Simoglou, and Bakirtzis 2015; Pandžić et al. 2013; Dabbagh and Sheikh-El-Eslami 2015). Further, to explore more possibilities for generating income, the ancillary service markets are also involved in VPP operation (Camal, Michiorri, and Kariniotakis 2018; Shayegan-Rad, Badri, and Zangeneh 2017; Baringo, Baringo, and Arroyo 2018a; Dabbagh and Sheikh-El-Eslami 2015; Baringo, Baringo, and Arroyo 2018b). For the uncertainty problem, some early VPP works choose not to include uncertainties in the problem (Nezamabadi and Setayesh Nazar 2016; Mashhour and Moghaddas-Tafreshi 2010; Mashhour and Moghaddas-Tafreshi 2010; You, Traeholt, and Poulsen 2009). Then, optimization models that can only handle one type of uncertainty model such as probability distributions or uncertainty intervals are applied in the VPP operation (Rahimiyan and Baringo 2015; Kardakos, Simoglou, and Bakirtzis 2015; Hadayeghparast, Farsangi, and Shayanfar 2019; Zamani et al. 2016; Nosratabadi, Hooshmand, and Gholipour 2016; Shabanzadeh, Sheikh-El-Eslami, and Haghifam 2015). To date, hybrid optimization models have been proposed for VPPs to handle multiple uncertainties that are described by probability distributions and uncertainty intervals (Baringo and Baringo 2016; Kong et al. 2020; Tan et al. 2020).

2.3 EV Charging Station Operation

With the increasing stock of EVs, unscheduled EV charging load can degrade the power grid performance and lead to collapses of the existing power grid (Fachrizal et al. 2020). Previous research has shown that most EVs have energy flexibility available for performing load scheduling to mitigate the pressure brought by increasing EV charging load (Heinisch et al. 2021; Richardson 2013). Though it is not practical for power system operators to directly manage the EV energy flexibility, aggregating agents can take over this task by acting as the intelligent mediator between the power grid and EVs (Solanke et al. 2020).

As natural aggregators of EV charging load, EV charging stations are promising control agents for managing EV energy flexibility (Wang et al. 2022a). In the literature, many energy management methods have been proposed for EV charging stations. In the proposed energy management methods, the main idea is to perform load shift and vehicle-to-grid (V2G) operations to achieve a series of goals such as enhancing the system security, improving the financial benefit, ensuring EV user charging satisfaction, and supporting renewable energy integration.

From the perspective of EV charging stations, the financial benefit is a primary focus of the operation. In (You et al. 2015; Zhang and Li 2015b; Tan et al. 2017; Liu et al. 2018; Liu et al. 2019), cost minimization scheduling strategies are proposed for EV charging stations to control the financial cost, which is normally the energy procurement cost.

To mitigate the pressure on the power system operation, a major application of EV charging station scheduling is to provide grid services. These services can include load-flattening (Wang et al. 2022b; Jovanovic and Bayram 2019; Hu et al. 2016), voltage control (Dong et al. 2018; Singh, Jagota, and Singh 2018), frequency regulation (Divshali and Evens 2020) (Iqbal et al. 2020), and mitigating transformer degradation (Li et al. 2022; Zheng et al. 2021). By providing these grid services, EV charging stations can help stabilize the grid operation to avoid or delay heavy investment costs for strengthening the grid (Kong and Karagiannidis 2016; Nunes and Brito 2017; Brinkel et al. 2020).

In some works, due to the mismatching between charging infrastructure and EV charging demand, EV user waiting time becomes a major concern. In such cases, improving user satisfaction is the focus of the EV charging station operating strategies. In (Zhang and Li 2015a; Wang and Thompson 2018; Moghaddam et al. 2017), the limited EV charging station service capability is optimally scheduled to achieve as much EV user satisfaction as possible.

For PV-EV charging stations, a major operating target is to ensure the utilization of self-equipped PV energy generation. In the operating strategies proposed for PV-EV charging stations (Li et al. 2020; Rui et al. 2019; Torreglosa et al. 2016; Liu et al. 2015; Wang et al. 2021a), EV energy flexibility is used to cover the generation uncertainty of PV arrays to assist the consumption of PV energy generation. Meanwhile, by using the energy generated from the self-equipped PV arrays, the operating cost of the EV charging stations can be reduced due to reduced energy bills.

Recently, multi-objective operating strategies that can simultaneously consider several factors in EV charging scheduling operations become a hot research topic. The optimization models in multi-objective operating strategies seek to find a compromise between a combination of multiple objectives such as the financial cost and user satisfaction (Moghaddam et al. 2017), the grid operation performance and user satisfaction (Luo et al. 2020), the PV energy consumption and EV user satisfaction (Kouka et al. 2020), as well as the grid operation performance and financial cost (Oliveira Farias et al. 2021).

Besides exploring different EV charging scheduling applications, another research field that has attracted much attention in EV charging station scheduling research is developing incentive programs for EV users in exchange for their EV energy flexibility. Due to limited EV battery capacities and long recharging time, EV users normally prefer to recharge their EVs as quickly as possible to mitigate their range anxieties (Chung et al. 2018). However, in EV charging station scheduling problems, the common scheduling scenarios include delaying the charging load through smart charging and injecting EV battery energy back into the grid through the V2G operation (Solanke et al. 2020). Both smart charging and V2G can increase the time needed to recharge EVs and reduce EV user satisfaction. Hence, incentives are necessary for EV user cooperation. Otherwise, EV users will not be motivated to participate in the charging station scheduling process.

Depending on the incentive signal update frequency, EV user incentive programs can be categorically classified as static programs and dynamic programs. The incentive signal update frequency of static incentive programs is relatively low, which keeps the incentive programs unchanged over a relatively long period. The advantages of such programs are that they are consistent and simple to implement, and EV users can easily use them as a reference for scheduling their charging plans.

Practices of static incentive programs include time-of-use pricing and critical peak pricing. In (Su, Lie, and Zamora 2020), an optimal time-of-use tariff plan decision model is proposed to shift the EV charging load from high-price hours to low-price hours. In (Dubey et al. 2015), an optimal time-of-use tariff plan is proposed by evaluating various aspects of EV charging behavior under the time-of-use tariff. In (Muñoz et al. 2016), several strategies including time-of-use tariff are applied to EV charging load to mitigate the transformer burden imposed by the high penetration level of EVs. In (Song, Shangguan, and Li 2021), a time-of-use charging price program with a price reduction strategy is applied to reduce energy procurement costs and distribute the benefits between EV users and charging infrastructure operators. In (Sheidaei and Ahmarinejad 2020), both time-of-use and critical-peak-pricing mechanisms are applied to the EVs to improve the VPP's profitability. Similarly, both time-of-use and critical-peak-pricing programs are used in (Sadati et al. 2019) to increase the profit of a distribution company. In static incentive programs, consumers are allowed to sacrifice a certain degree of convenience in return for reduced charging fees in a simple way. However, existing static programs cannot provide EV charging stations with enough controllability to maximize their benefit from the short-term market and system fluctuations.

Compared with static programs, dynamic programs update incentive signals more frequently in response to short-term market and system information. The most popular dynamic programs are dynamic pricing and transactive control programs. In (Zhao et al. 2017), a charging station uses real-time energy and reserve price signals to incentivize EV users for altering their charging schedules. In (Liu et al. 2021), dynamic price signals are used to encourage EV users to change their charging plan or authorize the battery access right to the aggregator. In (Moghaddam et al. 2019), a dynamic pricing model is proposed for multiple charging stations to coordinately shift EV charging load from residential load peaks. A dynamic pricing framework for charging stations is proposed in (Limmer and Rodemann 2019) to concurrently maximize the profit of charging stations and reduce the peak load. In (Liu et al. 2018), the EV charging load is managed by clearing a transactive market according to the day-ahead energy procurement and real-time requests of EV users. The charging load in (Wu et al. 2018) is controlled through a transactive market to which EV users need to submit their real-time charging requirements and preference setting of demand response. A sensitivity-based real-time transactive control framework is proposed in (Hoque et al. 2021) to coordinate the EV charging behavior through a local energy market.

Comparing dynamic and static incentive programs, dynamic programs can change the incentive signals on a shorter time horizon, which enables more controllable charging scheduling actions to handle short-term market and system fluctuations. Hence, dynamic incentive programs can encourage more proactive participation of EV users in offering flexible services to the power grid. Although dynamic programs are more controllable, they lack simplicity and consistency compared to static programs. Besides, dynamic incentive programs assume that EV users can actively respond to the price signals and alter their charging behavior responsively (Zhou et al. 2019), which is too optimistic as it takes effort and specific knowledge to complete these tasks. Furthermore, to make optimal decisions to maximize the benefit, EV users have to be constantly updated with the latest market information, which demands extra effort from EV users.

2.4 VPP Operation Considering EVs

In VPP operation, there are some renewable energy generators with stochastic power output. The uncertainty in renewable generation can cause energy deviations between the forecast and actual values. Such energy deviations can have negative impacts on VPP operation such as increased operating costs. As energy consumers and providers, EVs can play a crucial role in the operation and scheduling of VPPs by reducing such energy deviations (Yang and Zhang 2021). Hence, integrating EVs into VPP operation can provide a practical and economical solution to improve VPP performance.

In the literature, there have been some pioneering studies that integrate EVs into VPPs for operation scheduling and optimization in conjunction with other DERs like renewables and thermal power plants. In (Kong et al. 2019; Ju et al. 2016b; Sheidaei and Ahmarinejad 2020; Alahyari, Ehsan, and Mousavizadeh 2019; Sadeghi et al. 2021), EVs are scheduled with other DERs in the VPP to coordinately maximize the VPP benefit.

When EVs are incorporated into VPPs, there are generally two control structures, including direct control and hierarchical control structures (Yang and Zhang 2021). In the direct control structure, the VPP can directly exchange information with EVs to schedule their charging/discharging behavior (Shayegan-Rad, Badri, and Zangeneh 2017; Vasirani et al. 2013; Sadati et al.

2019; Alahyari, Ehsan, and Mousavizadeh 2019; Sadeghi et al. 2021; Yang et al. 2020a). This kind of control structure is feasible when the number of EVs under the VPP control is small. However, if a large number of EVs are considered, the centralized control structure becomes impractical due to expensive communication and computation costs. Besides, the ownerships of VPP and EV charging facilities may be different, making it difficult for VPPs to directly control the EV charging/discharging behavior.

To address large-scale EV fleet integration into VPPs, some researchers proposed a hierarchical control structure that introduces mediators to bridge VPPs and EVs. In the hierarchical structure, the mediators are responsible for optimizing and controlling the charging/discharging behavior of individual EVs. Under the aggregation of mediators, the VPP only needs to deal with a single operating profile for each aggregating mediator. Hence, the VPP management burden can be significantly reduced.

The hierarchical control structure has been applied in (Wang et al. 2022d; Fan et al. 2020), where the considered EV aggregating mediators are EV charging stations. In (Wang et al. 2022d; Fan et al. 2020), the VPP first optimizes the operation of DERs, then sends the optimized scheduling signals to the EV charging stations. After receiving the scheduling signals, EV charging stations dispatch the EV load to meet the VPP requirements. A drawback of the operation framework proposed in these works is that the EV charging stations can only passively respond to VPP price signals instead of proactively interacting with the VPP operator, which can weaken the functionality of EVs as energy buffers.

Chapter 3

VPP Operation Strategy

In this thesis, VPP plays an important role in bridging DERs with electricity markets. To realize efficient DER energy management in a VPP, this chapter presents a VPP operation framework that deals with the VPP market bidding, energy scheduling, and unit dispatching problems. Uncertainties from renewable energy resources and electricity markets are also involved in the VPP operation problem formulations.

3.1 Chapter Introduction

Growing pressure on secured energy supply and environmental issues is now boosting the development of DERs (Rahimi, Ardakani, and Ardakani 2021). In the past few decades, both the bulk injection and penetration level of the DERs have been dramatically increased (Qiu et al. 2017). Moreover, many major energy consumption parties, such as China and the European Union, have recently announced their carbon neutralization plans. In the foreseeable future, the number of DERs will continue to grow to a great extent.

DERs normally feature small power capacities and inherent intermittency (Yang et al. 2020b). From the perspective of the system operator, the massive integration of DERs into the power system will cast great challenges on system operation security (Wang, Riaz, and Mancarella 2020). From individual DER points of view, they can hardly access the wholesale market and benefit from the market competition. As a promising solution to the aforementioned occasion, VPP can aggregate multiple DERs to become a single market participant with an integrated operating profile (Kardakos, Simoglou, and Bakirtzis 2015). Through such VPP aggregation, the power fluctuations induced by DERs can be absorbed. Moreover, the aggregated DERs can be admitted into the wholesale market for economic operation instead of “free-running”.

In electricity markets, joining multiple markets rather than only the day-ahead energy market has become an efficient approach to improve the profitability of the market participants. In (Ottesen, Tomasgard, and Fleten 2018), authors develop a multi-market bidding strategy for demand side aggregators participating in a sequential of capacity reserve market, day-ahead, and real-time flexibility markets. In (Fleten and Kristoffersen 2007), a bidding strategy is proposed for a hydropower producer to participate in both the day-ahead and balancing markets in the NORDPOOL system. In (Hedegaard, Pedersen, and Petersen 2017), a model predictive control scheme is proposed to enable parallel participation of Denmark demand response providers in both the day-ahead and intraday markets. In (Aasgård et al. 2019), the authors review the optimization models for hydropower producers bidding in multiple markets. It is concluded that participating in multiple markets offers opportunities in the form of possibilities to trade their way to profitable and flexible production schedules.

Owing to the fast-responding capability of the DERs, the VPP is of high potential to arbitrage through the ancillary service markets (Sadeghi et al. 2021). In the literature, several attempts have been engaged in VPP operation by considering the provision of reserve. At the early stage, attempts to incorporate reserve provision in the VPP operation regime normally focus on developing joint optimization models to maximize the VPP’s profit while neglecting the uncertainties. In the works reported in (Mashhour and Moghaddas-Tafreshi 2010), authors develop an optimization problem to maximize the profit from both selling the energy and proving reserve under no uncertainty. In (Nezamabadi and Setayesh Nazar 2016), a more comprehensive model that includes energy, reserve, and reactive power provision is developed to help the VPP arbitrage in multiple markets without considering uncertainties. Later, the operating strategies of VPPs with reserve become more complex by involving uncertainties in the decision-making process. Whereas in this stage, these works normally concern only the day-ahead stage, and the real-time stage is rarely included. In (Zamani et al. 2016), a modified scenario-based method is proposed to optimize the VPP’s day-ahead energy and reserve scheduling decisions in confronting renewable and market price uncertainties. The work in (Hadayeghparast, Farsangi, and Shayanfar 2019) reports a stochastic optimization-based day-ahead scheduling strategy for VPP with multiple uncertainties including renewable generation, market price, and electrical load. In the day-ahead self-scheduling model developed in (Baringo, Baringo, and Arroyo 2018a), scenarios and confidence bounds are used to jointly describe the uncertainties in price, wind generation, and reserve calls.

To date, VPP works considering reserve provisions are becoming more mature. The gap between the day-ahead stage forecast and the real-time stage information is handled by using multi-stage models. In (Vahedipour-Dahraie et al. 2020), the authors propose a two-stage risk-constrained stochastic optimization model for the VPP energy and reserve scheduling in both day-ahead and real-time stages. In (Zhao et al. 2020), authors study a multi-energy VPP participating in the day-ahead energy and reserve markets. In the intraday operation, adjustments are introduced to the day-ahead baseline schedule with more accurate uncertainty information.

Indeed, researchers have progressed significantly in studying the VPP's bidding and dispatching with reserve. However, most of the existing works concern price-independent bidding strategies in the operation of VPPs with reserve. That is, the energy exchange volume is initially fixed regardless of the market-clearing results. Nevertheless, in some electricity markets (e.g., NORDPOOL, PJM, etc.), price-dependent offers can be more effective to reach economic outcomes. In the literature, some preliminary attempts have been made for VPP by deploying the price-dependent energy bidding strategy (Pourghaderi et al. 2018; Baringo and Baringo 2016). As compared to price-independent offers, price-dependent offers are advantageous in reflecting the suppliers' aspiration to sell electricity at different price levels.

Based on the existing literature, this chapter aims to develop an optimal VPP operation regime under several uncertainties. The proposed operation regime includes a novel price-dependent bidding strategy and a real-time dispatching model. Towards this end, one should first resolve the most challenging issue arising from the uncertainties of market price, renewable generation, and calls for reserve deployment by the system operator. Currently, the stochastic optimization approach (e.g., (Jafari and Foroud 2020; Hadayeghparast, Farsangi, and Shayanfar 2019; Ju et al. 2016b)) is widely employed to handle uncertainties in the relevant works of VPP. However, in some cases, one can hardly obtain the precise probability distribution for uncertain factors. Hence, the effectiveness is obviously limited by solely adopting stochastic optimization. To tackle this issue, hybrid stochastic robust optimization models are proposed (e.g. (Baringo, Baringo, and Arroyo 2018a; Jun, Jun, and Linpeng 2019; Liu, Xu, and Tomsovic 2015)), in which the probability distribution is unnecessarily needed. However, considerable conservativeness is inevitable due to the robust nature of these models. As an alternative to handling uncertainties without accurate probability distributions, the minimax regret (MMR) approach features distribution-free and less conservative. Thus, this method has also been duly deployed in several power engineering applications (e.g., transmission expansion planning in (Chen et al. 2014), unit commitment problem in (Jiang et al. 2013), and thermal generator bidding problem in (Fan et al. 2014), etc).

In the day-ahead bidding stage, it is assumed that the uncertainty intervals are used for modeling renewable generation uncertainty and probability distributions for market price and reserve deployment calls. Hence, on the one hand, confidence bounds are introduced to represent the renewable generation, which serves as a prerequisite input of the MMR model. On the other hand, the market price and uncertain calls for reserve deployment are described by using scenarios complying with certain probability distributions, which enables the utilization of the stochastic optimization model. In combining these two mechanisms, a novel hybrid stochastic MMR model is proposed in this chapter to jointly resolve the aforementioned uncertainty issues. In this chapter, risk-management tools are not considered in the proposed operation regime to minimize the conservativeness of the obtained operating solutions.

To show the differences and contributions of our work, a summary of VPP operational works is provided in Table 3.1, where four factors are involved for comparison, including price-dependent bidding strategy in the day-ahead stage, real-time dispatch, reserve provision, and considering multiple uncertainty models simultaneously.

At the power dispatching stage, to remain consistent with the MMR-based bidding model, a similar mechanism is applied to the scheduling strategy to obtain the optimal VPP dispatching solutions. To control the conservativeness arising from the minimax nature of the MMR approach, a self-adaptive algorithm is proposed to instantly adjust the uncertainty interval size based on the revealed uncertainty information. The contributions of this chapter include:

- An optimal VPP operation regime under multiple uncertainties is proposed, which consists of a day-ahead price-dependent bidding strategy and a real-time dispatching model.
- A novel stochastic MMR-based optimization model is proposed for the day-ahead optimal bidding decision-making in VPP
- A self-adaptive algorithm is proposed to control the conservativeness introduced by the

Table 3.1: VPP operation regime Summary

Reference	Price-dependent bidding	Real-time dispatch	Reserve provision	Multiple uncertainty models
(Shafiekhani et al. 2019; Sheidaei and Ahmarinejad 2020; Sadeghi et al. 2021)	-	-	-	-
(Pourghaderi et al. 2018)	✓	-	-	-
(Dabbagh and Sheikh-El-Eslami 2015)	-	✓	-	-
(Nezamabadi and Setayesh Nazar 2016; Mashhour and Moghaddas-Tafreshi 2010; Baringo, Baringo, and Arroyo 2018a; Zamani et al. 2016; Zhao et al. 2020)	-	-	✓	-
(Hadayeghparast, Farsangi, and Shayanfar 2019; Jun, Jun, and Linpeng 2019; Kong et al. 2020)	-	-	-	✓
(Vahedipour-Dahraie et al. 2020)	-	✓	✓	-
(Baringo and Baringo 2016) ✓	-	-	✓	
The proposed method	✓	✓	✓	✓

minimax nature of the MMR-based dispatching model in the real-time stage

The rest of this chapter is organized as follows. In Section 3.2, the studied model is discussed in detail. Section 3.3 presents the formulations of the optimization problems. The proposed solution methodology and the self-adaptive algorithm are presented in Section 3.4. Section 3.5 provides simulation results and discussions of the case studies. Section 3.6 concludes the work.

3.2 Problem and Model Description

This section first discusses what electricity markets that the VPP participates in, then provides the VPP operation model under the considered electricity markets. Uncertainty models for renewable generation and electricity markets will also be given in this section.

3.2.1 Electricity Market Structure

The day-ahead energy market considered in this chapter adopts a uniform pricing mechanism and the market-clearing resolution is one hour, i.e., there are 24 clearing periods for each day. For each hour, all the energy suppliers are expected to submit stepwise bidding curves indicating the amount of energy they are willing to sell at different price levels. In normal practices, each bidding curve comprises at most five steps (e.g., (Baringo and Baringo 2016) and (Peikherfeh, Seifi, and Sheikh-El-Eslami 2011)). Hence, it is assumed that the energy market considered in this chapter only accepts offers with at most five bidding steps. As reported in existing works (e.g., (Kardakos, Simoglou, and Bakirtzis 2015) and (Pandžić et al. 2013)), the dual pricing mechanism is applied for energy deviations at the *ex-post* settlement stage to encourage the suppliers to provide the energy allocated during the bidding process. In this chapter, a similar dual pricing scheme (as presented in (Kardakos, Simoglou, and Bakirtzis 2015)) is adopted to settle the energy deviations based on market-clearing results. The settlement prices are expressed as follows:

$$\lambda_t^+ = \psi^+ \cdot \lambda_t^{DA} \tag{3.1}$$

$$\lambda_t^- = \psi^- \cdot \lambda_t^{DA} \tag{3.2}$$

$$\psi^{+} \geq 1 \tag{3.3}$$

$$\psi^{-} \leq 1 \tag{3.4}$$

where λ_t^{DA} is the day-ahead energy market-clearing price at time t; The balancing prices for energy deficiency/surplus are given by λ_t^{+} / λ_t^{-}, respectively. Parameters ψ^{+} and ψ^{-} are the market penalty coefficients for energy deficiency and surplus deviations, respectively.

3.2.2 Virtual Power Plant Operational Model

VPPs are generally equipped with distributed thermal generators, renewable generators like wind turbines and photovoltaic panels, as well as energy storage systems. A general configuration for VPPs is shown in Fig. 3.1.

The VPP considered in this chapter participates in the forward reserve market and contracts 20% of its dispatchable generation capacity as the secondary reserve. The reserve considered in this chapter is similar to the thirty-minute reserve (*PJM thirty minute reserve* 2019) in the PJM market except that the resolution has been adjusted to one hour. The VPP receives revenue for providing the potential reserve. Besides, once the reserve is called at a specific operating time, the change in energy production will be settled at the day-ahead market-clearing price. Inversely, failure to deliver the called reserve can result in energy deviations that will be settled in the balancing stage at penalty prices.

In this study, the VPP operation is divided into two stages (i.e., the day-ahead bidding stage and the real-time dispatching stage). At the day-ahead bidding stage, the VPP is faced with multiple uncertainties relating to energy market price, wind energy generation, and calls for reserve deployment by the system operator. At the real-time dispatching stage, the market has been cleared and the system operator has informed the VPP of the called reserve volume. Operation uncertainty is all induced by wind power generation at this stage.

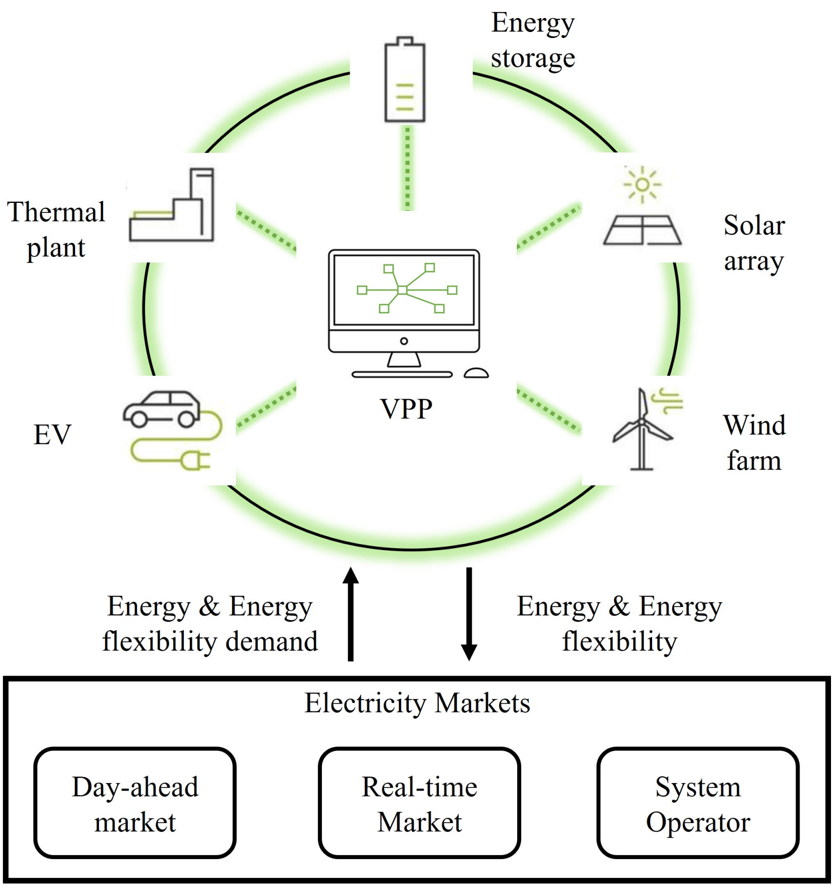

Figure 3.1: Configuration of a general VPP

3.2.3 Uncertainty Modeling

In this chapter, representative scenarios are used to model the wholesale energy market price and call for reserve deployments. As inspired by (Vahedipour-Dahraie et al. 2020), a similar scenario generation method is utilized in our study. Since all the bidding decisions are made in the day-ahead stage, it is assumed that the probability distribution functions of reserve calls remain unchanged during the next day. Specifically, five typical scenarios are generated for the market price and the reserve deployment uncertainties, respectively. The values of the generated scenarios are ordered as very high, high, medium, low, and very low, which can capture the main features of the price and reserve uncertainty distributions as well as cover most of the possible scenarios in our situation.

To represent the uncertainty induced by wind power generation, confidence bounds are adopted to measure the output range. In our model, the confidence bounds are characterized by a forecasting value fv^r and an uncertainty coefficient σ, which indicates the size of the uncertainty intervals. For given fv^r and σ, the real wind power generation rv^r is assumed to reside between the bounds expressed as:

$$\left[(1-\sigma)\, fv_t^r, \min\left\{(1+\sigma)\, fv_t^r, P^{r,ic}\right\}\right] \tag{3.5}$$

where $P^{r,ic}$ is the installed capacity of the wind generator.

At the bidding stage, a constant empirical forecasting accuracy σ^{DA} is considered for all the decision periods because no uncertainty information is revealed in this stage. At the dispatching stage, to reduce the conservativeness stemming from the minimax nature of the dispatching model, the confidence bounds are adjusted by the proposed self-adaptive algorithm based on the uncertainty realizations. The intuition behind the self-adaptive algorithm is that the forecast accuracy of renewable generations is temporally related (Ma et al. 2017; Tastu et al. 2011).

3.3 Problem Formulation

Further to section 3.2, this section presents detailed formulations for VPP day-ahead bidding and real-time dispatching problems, respectively.

3.3.1 Day-Ahead Bidding Model

At the day-ahead bidding stage, the bidding problems of different hours are solved individually. Because three different uncertain factors are considered in this chapter, a three-level model is proposed to investigate the uncertainties at different scales. Firstly, the regret model is adopted where only the renewable uncertainty is involved (i.e., Level 1). In concerning both renewable and reserve uncertainties, the stochastic MMR model is formulated (i.e., Level 2). Last, in the presence of all operational uncertainties including price uncertainty, the VPP bidding curves are formed (i.e., Level 3). The hierarchical structure of the proposed bidding strategy is illustrated below and presented in Fig. 3.2. It is worth mentioning that the optimal bidding result obtained from the day-ahead bidding model is determined by factors including thermal generator production, renewable generator production, and reserve deployment scenarios.

(1) Level 1: Regret Maximization

In our problem, regret is defined as the profit difference between the optimal solution with full

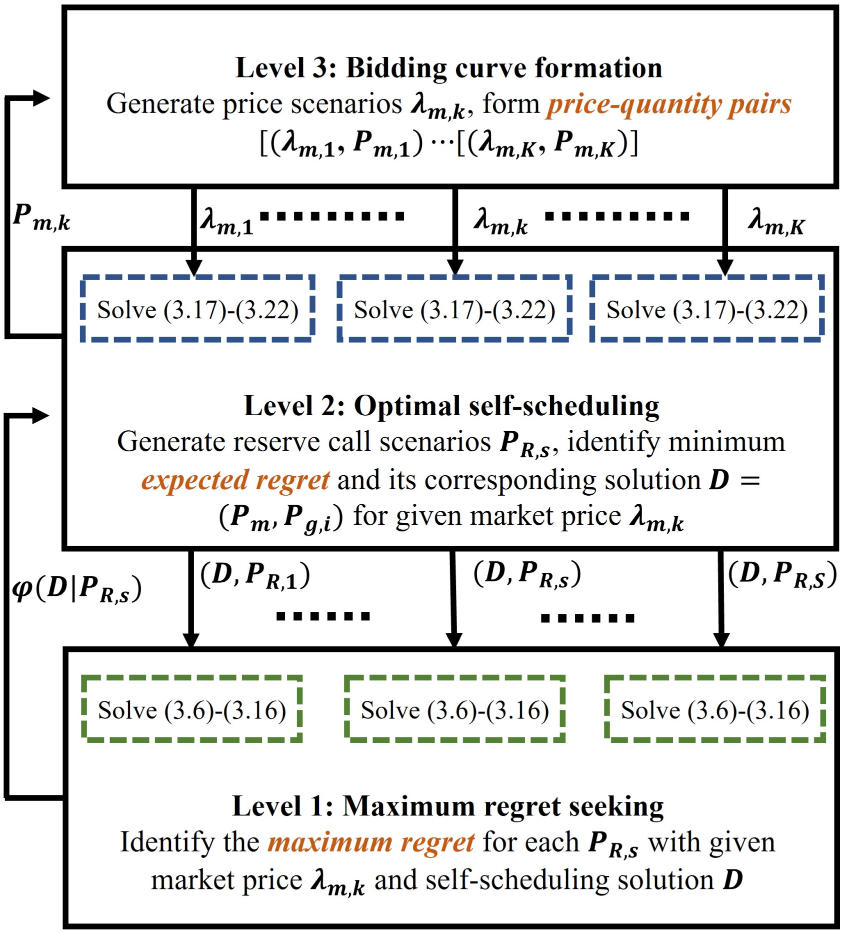

Figure 3.2: The hierarchical structure of the day-ahead bidding model

knowledge of uncertainties and the solution obtained with incomplete information. At this level, both the market-clearing price and reserve volume requested by the system operator are given, the only uncertainty is related to wind power generation. The regret model identifies the worst-case scenario regarding wind uncertainty for a given self-scheduling solution $D = \{P^{DA}, P_i^G\}$, where P^{DA} denotes the energy offered in the market and P_i^G denotes the power generation of the ith thermal generator.

Given the market-clearing price λ^{DA} and a called reserve volume P_R, the maximum regret $\theta(D|P_R)$ for the self-scheduling decision D can be acquired by solving the following optimization problem:

$$\max_u \left\{ \begin{array}{c} \min_{P^{DA,u}, P_i^{G,u}, P^{B,u}, y_i^u} \left\{ \sum_i f^G\left(P_i^{G,u}\right) + f^B\left(P^{B,u}\right) - f^M\left(P^{DA,u}\right) - f^R\left(P_R\right) \right\} \\ -\min_{P^B} \left\{ \sum_i f^G\left(P_i^G\right) + f^B\left(P^B\right) - f^M\left(P^{DA}\right) - f^R\left(P_R\right) \right\} \end{array} \right\} \quad (3.6)$$

s.t.

$$(3.1) - (3.4) \tag{3.7}$$

$$f^M(P^{DA}) = \lambda^{DA} \cdot P^{DA} \tag{3.8}$$

$$f^R(P_R) = \lambda^{DA} \cdot P_R \tag{3.9}$$

$$f^G(P_i^G) = c_i(P_i^G)^2 + b_i \cdot P_i^G + a_i \tag{3.10}$$

$$f^B\left(P^B\right) = \begin{cases} P^B \cdot \lambda^+, P^B \geq 0 \\ P^B \cdot \lambda^-, P^B \leq 0 \end{cases} \tag{3.11}$$

$$P^{B,u} + \sum_i P_i^{G,u} + \eta u = P^{DA,u} + P_R \tag{3.12}$$

$$P^B + \sum_i P_i^G + \eta u = P^{DA} + P_R \tag{3.13}$$

$$y_i^u P_i^{G,min} \leq P_i^{G,u} \leq y_i^u P_i^{G,max} \tag{3.14}$$

$$(1 - \sigma^{DA}) f v_t^r \leq u \leq min \left\{ (1 + \sigma^{DA}) f v_t^r, P^{r,ic} \right\} \tag{3.15}$$

$$y_i^u \in (0, 1) \tag{3.16}$$

The energy exchanged in the market is denoted as P^{DA}, and the power generation of the ith thermal generator is denoted as P_i^G. Renewable energy production is represented by u, and η is the conversion efficiency of the DC/AC converters. The energy deviation is represented by P^B. In this formulation, terms with the superscript u mean that they are optimization variables in the optimal self-scheduling problem under the renewable generation scenario u. The binary variable y_i^u is used to indicate the on/off status of the dispatchable generators.

The revenue from the energy market, revenue from responding to the reserve calls, the fuel cost of thermal generators, and balancing the cost of energy deviations are represented by $f^M(P^{DA})$, $f^R(P_R)$, $f^G(P_i^G)$, and $f^B(P^B)$, respectively. Eqs. (3.12) and (3.13) are energy-balancing constraints in the VPP. Constraints in (3.14) restrict the power outputs of the thermal generators. Constraint (3.15) gives the interval for wind power production.

The first inner minimization problem aims to reach the optimal self-scheduling decisions such that the profit of VPP can be maximized under the uncertainty scenario u. The second inner minimization problem is meant to find the optimal recourse action that minimizes the balancing cost under scenario u and first-stage decision D. The overall objective function is the regret of the decision D under the wind generation scenario u. Therefore, the outer maximization problem aims to locate a renewable generation scenario such that the profit difference between the optimal solution and the given solution is maximized.

The regret model presented at this level will be solved multiple times using different reserve deployment scenarios to yield multiple maximum regrets under the wind generation uncertainty. The obtained maximum regrets will be passed to level 2 for further processing.

Level 2: Stochastic MMR Optimization

At level 2, the model is extended to include the uncertain call for reserve deployments. To this end, scenarios complying with a certain probability distribution are used to represent the reserve call uncertainty. As concerned in the level-1 problem, for a given self-scheduling decision D under the reserve call scenario $P_{R,s}$, its maximum regret $\theta(D|P_{R,s})$ can be obtained by solving the problem (3.6) - (3.16). For a total number of S reserve call scenarios, S regrets can be obtained by solving the problem for S individual times. Since each reserve call scenario corresponds to a certain probability π_s, the 'Expected regret' for the self-scheduling decision D can be obtained by summing up the products of each regret and their corresponding probability. Therefore, the resulting model becomes a hybrid stochastic MMR optimization problem, which aims to make such a decision, in which the expected regret is minimized.

$$\min_{D} \{\theta(D|P_{R,1})\pi_1 + ... + \theta(D|P_{R,S})\pi_S\} \tag{3.17}$$

s.t.

$$(3.6) - (3.16) \tag{3.18}$$

$$y_i P_i^{G,min} \leq P_i^G \leq y_i P_i^{G,max} \tag{3.19}$$

$$\sum_i P_i^G + (1-\sigma^{DA}) f v_t^r \leq P^{DA} - P_{R,s} \leq \sum_i P_i^G + \min_u \left\{(1+\sigma^{DA}) f v_t^r, P^{r,ic}\right\} \tag{3.20}$$

$$\pi_1 + ... + \pi_S = 1 \tag{3.21}$$

$$y_i \in (0, 1) \tag{3.22}$$

In this formulation, $P_{R,s}$ and π_s are the sth reserve call scenario and its probability. The term $\theta(D|P_{R,s})$ represents the maximum regret of the self-scheduling decision D under the reserve call scenario $P_{R,s}$. Constraints in (3.19) restrict the power generation of the thermal generators. Constraint (3.20) limits the energy bidding quantity. Constraint (3.21) ensures that the sum of the reserve call scenario probabilities equals to one.

The stochastic MMR optimization model presented at this level is solved several times to obtain the optimal bidding quantities under different market-clearing price scenarios. The acquired bidding quantities will be communicated with level 3 for the final construction of the stepwise bidding curve.

Level 3: Bidding Curve Construction

At this level, to handle the price uncertainty, price scenarios ranging from low to high are generated to represent different price levels. The generated price scenarios are used as the bidding prices in the stepwise bidding curves, and the bidding volumes corresponding to each price scenario can be obtained by solving problem (3.17) – (3.22) independently for each price scenario. As S price scenarios are considered as the input of problem (3.17) – (3.22), the same number of price-quantity pairs can be acquired. By combining the obtained price-quantity pairs, the bidding curves can be hereby constructed.

It should be noted that the order to explain the bidding model is inverse to the actual implementation order of it for ease of understanding. Hence, starting from level 3, the price uncertainty is firstly addressed by generating different price scenarios to form the bidding curves, then the reserve deployment uncertainty is addressed by the stochastic optimization in level 2. Finally, level 1 deals with the wind generation uncertainty using the regret model.

3.3.2 Real-Time Dispatch Model

The market-clearing results are passed from the day-ahead stage to the real-time stage. At the real-time stage, the system operator has also informed the VPP of the called reserve volume. Hence, thermal generators shall be duly dispatched given the wind generation uncertainty to meet both the day-ahead market-clearing results and the real-time reserve deployment requests. The MMR-based dispatching problem is formulated as follows:

$$\min_{P_{i,t}^G} \left\{ \sum_i f^G(P_{i,t}^G) + \max_{u_t} \left\{ \min_{P_t^B} f^B(P_t^B) - \min_{P_{i,t}^{G,u}, P_t^{B,u}} \left\{ \sum_i f^G(P_{i,t}^{G,u}) + f^B(P_t^{B,u}) \right\} \right\} \right\} \tag{3.23}$$

s.t.

$$(3.7) - (3.11) \tag{3.24}$$

$$y_{i,t}^u P_{i,t}^{G,min} \leq P_{i,t}^{G,u} \leq y_{i,t}^u P_{i,t}^{G,max} \tag{3.25}$$

$$y_{i,t} P_{i,t}^{G,min} \leq P_{i,t}^G \leq y_{i,t} P_{i,t}^{G,max} \tag{3.26}$$

$$-RD_i \leq P_{i,t+1}^G - P_{i,t}^G \leq RU_i \tag{3.27}$$

$$-RD_i \leq P_{i,t+1}^{G,u} - P_{i,t}^{G,u} \leq RU_i \tag{3.28}$$

$$P_t^{DA,u} + P_{R,t} = \sum_i P_{i,t}^G + P_t^{B,u} + u_t \tag{3.29}$$

$$P_t^{DA} + P_{R,t} = \sum_i P_{i,t}^G + P_t^B + u_t \tag{3.30}$$

$$(1 - \sigma^{RT}) f v_t^r \leq u_t \leq min\left\{(1 + \sigma^{RT}) f v_t^r, P^{r,ic}\right\} \tag{3.31}$$

$$[y_{i,t}^u, y_{i,t}] \in (0, 1) \tag{3.32}$$

3.4 Solution Methodology

The C&CG algorithm (Zeng and Zhao 2013) has been proven efficient for solving two-stage minimax problems, yet it cannot be directly applied to the formulated MMR models because of the extra step that is needed to locate the "optimal solution" under scenario u. Hence, in this section, a reformulation methodology is firstly proposed to transform the bidding and dispatching problems into two-stage robust optimization problems, then a detailed C&CG framework is developed to solve the reformulated problems. The proposed self-adaptive algorithm is given at the end of this section.

3.4.1 Problem Reformulation

It can be observed that both the bidding and dispatching MMR optimization problems can be written in the following compact form:

$$\min_y \left\{ f_1(y) + \max_u \left\{ \min_x f_2(x) - \min_{y^u, x^u} \left\{ f_1(y^u) + f_2(x^u) \right\} \right\} \right\} \tag{3.33}$$

s.t.

$$A_1 y \leq p, y \in S_Y \tag{3.34}$$

$$A_2y + A_3x - A_4u \leq q \tag{3.35}$$

$$A_1y^u \leq p, y^u \in S_Y \tag{3.36}$$

$$A_2y^u + A_3x^u - A_4u \leq q \tag{3.37}$$

$$A_5u \leq l, u \in S_U \tag{3.38}$$

where y represents the first-stage decision variables. The recourse actions are represented by x. The uncertainty scenario is represented by u and the optimal solution under the uncertainty realization u is given by (y^u, x^u). The negative utility functions of the first- and second-stage variables are given by $f_1(y)$ and $f_2(x)$, respectively.

Proposition: Given that the recourse action solution set is always non-empty, problem (3.33) – (3.38) is equivalent to the following two-stage robust optimization problem:

$$\min_y \left\{ f_1(y) + \max_\zeta \left\{ \min_x \left\{ f_2(x) - f_1(y^u) - f_2(x^u) \right\} \right\} \right\} \tag{3.39}$$

s.t.

$$(3.34), (3.35) \tag{3.40}$$

$$E^{'}\zeta \leq l^{'} \tag{3.41}$$

$$\zeta = [u^T, (y^u)^T, (x^u)^T]^T \tag{3.42}$$

$$E^{'} = \begin{bmatrix} 0 & A_1 & 0 \\ -A_4 & A_2 & A_3 \\ A_5 & 0 & 0 \end{bmatrix} \tag{3.43}$$

$$l^{'} = \begin{bmatrix} p \\ q \\ l \end{bmatrix} \tag{3.44}$$

Proof: See appendix 1.

3.4.2 C&CG Solution framework

To solve the problem (3.39) – (3.44), a detailed C&CG framework is developed in this subsection. Under the C&CG framework, the original problem will be decomposed into primary and secondary problems. In this chapter, the primary problem is meant to find the optimal first-stage decisions that will minimize the maximum regret, and it can be written as:

$$\min_{y,\vartheta} \{f_1(y) + \vartheta\} \tag{3.45}$$

s.t.

$$(3.34) \tag{3.46}$$

$$\vartheta \geq -H \tag{3.47}$$

$$A_2 y + A_3 x_{v+1} - A_4 u_v^c \leq q \tag{3.48}$$

$$\vartheta \geq f_2(x_{v+1}) - f_1(y_v^{u,c}) - f_2(x_v^{u,c}) \tag{3.49}$$

$$x_{v+1} \in S_X \tag{3.50}$$

where ϑ is the auxiliary variable. Variables x_{v+1} are new variables created in the $(v+1)th$ iteration. Terms u_v^c x_v^c, $y_v^{u,c}$, and $x_v^{u,c}$ are the optimal values calculated in the vth iteration from the secondary problem. The symbol H represents a big enough number to ensure that the primary problem is bounded in the first iteration. Note that in the first iteration, only constraints (3.46) and (3.47) are considered.

Since the primary problem is a relaxation of the original problem, its optimal objective value will be no bigger than the actual optimal objective value of the original problem. Therefore, the lower bound will be updated after solving the primary problem:

$$LB = \max\left\{LB, f_1(y_{v+1}^c) + \vartheta_{v+1}^c\right\} \tag{3.51}$$

where y^c_{v+1} and ϑ^c_{v+1} represent the optimal primary problem solutions calculated in the $(v+1)th$ iteration.

There are two purposes for the secondary problem, one is to identify the worst-case condition that will maximize the regret of the primary problem decisions, and the other is to determine the optimal recourse actions under the worst-case scenario. Using the results obtained from the primary problem, the secondary problem can be formulated as:

$$\max_{\xi} \left\{ \min_{x} \left\{ f_2(x) - f_1(y^u) - f_2(x^u) \right\} \right\} \tag{3.52}$$

s.t.

$$(3.41) - (3.44) \tag{3.53}$$

$$A_2 y^c_{v+1} + A_3 x - A_4 u \leq q \tag{3.54}$$

The feasible domain of the secondary problem is more restricted, and the optimal objective value of the secondary problem is no less than that of the original problem. Thus, the upper bound can be obtained by solving the secondary problem:

$$UB = \min \left\{ UB, f_1(y^c_{v+1}) + f_2(x^c_{v+1}) - f_1(y^{u,c}_{v+1}) - f_2(x^{u,c}_{v+1}) \right\} \tag{3.55}$$

where $x^c_{v+1}, y^{u,c}_{v+1}$, and $x^{u,c}_{v+1}$ are optimized values of the secondary problem. The convergence of the problem can be declared once the following criterion is satisfied:

$$UB - LB \leq \varepsilon_{ccg} \tag{3.56}$$

where the convergence threshold of the C&CG algorithm is given by ε_{ccg}. The complete solution algorithm is provided in algorithm 3-1.

Algorithm 3-1 C&CG solution algorithm

1: **Initialization** $v = 0$, $UB = \infty$, $LB = -\infty$, $\varepsilon_{ccg} = 0.001$

2: **While** (3.56) is **False**, $v \leftarrow v + 1$ **do**

3: **Solve** (3.45) - (3.50), **derive** $(y^c_{v+1}, \vartheta^c_{v+1})$ and update the lower bound using (3.51).

4: **Solve** (3.52) – (3.54), **derive** $(x^c_{v+1}, y^{u,c}_{v+1}, x^{u,c}_{v+1})$ and update the upper bound using (3.55).

5: Create x_{v+2}, add (3.48), (3.49), and (3.50) to the primary problem.

6: **End While**

7: **Return** y^c_{v+1}

As referred to (Zeng and Zhao 2013), the developed C&CG framework will converge in $O(Q)$ iterations, where Q is the number of extreme points of the renewable generation uncertainty set.

3.4.3 Self-Adaptive Algorithm

Due to the minimax nature of the MMR approach in the real-time stage, the dispatch solutions will inevitably be conservative if the uncertainty intervals are too big. To obtain dispatch solutions that are more economic, this section proposes an effective look-back-and-adjust self-adaptive algorithm that can reduce the size of the uncertainty intervals. By observing the past wind uncertainty realizations, the optimal uncertainty coefficient that minimizes the total profit loss of the n previous time windows will be identified and used at the current decision period.

Based on the revealed uncertainty information (i.e., the real renewable production value rv^r), the optimal uncertainty coefficient σ that minimizes the total profit loss of the n previous decision periods can be obtained by solving the consensus optimization problem under the ADMM framework. In this framework, the primary problem is meant to address the conflicts between different time windows, and the secondary problems are designed to locate their own optimal uncertainty coefficient σ. The self-adaptive process is summarized as follows:

(1) Select proper values for ρ and ξ^0, set $v = 0$, and $\varepsilon_{coef} = 0.001$.

(2) Identify such an overall uncertainty coefficient σ that will coordinate the optimal uncertainty coefficients σ_τ for the n previous time windows:

$$\sigma^{v+1} = arg \min_{\sigma^{v+1}} \left[\sum_{\tau=t-n}^{t-1} (\sigma^{v+1} - \sigma_\tau^v)^2 + \frac{\rho}{2} \sum_{\tau=t-n}^{t-1} (\sigma^{v+1} - \sigma_\tau^v - \xi^v)^2 \right] \tag{3.57}$$

paragraph(3) For each past time window, using the revealed uncertainty information and the calculated optimal overall uncertainty coefficient σ^{v+1} to concurrently minimize the energy imbalance cost and the difference between the optimal single window σ_τ^{v+1} and the overall optimal σ^{v+1}:

$$\sigma_\tau^{v+1} = arg \min_{\sigma_\tau^{v+1}} \left[f^B(P_\tau^B) + \frac{\rho}{2} (\sigma^{v+1} - \sigma_\tau^{v+1} - \xi^v)^2 \right], P_\tau^B \propto f v_\tau^r \sigma_\tau^{v+1}, \forall \tau \in [t-n, t-1] \tag{3.58}$$

(4) Update the scaled dual variable ξ^{v+1} using the optimized solutions from problems (3.57) and (3.58):

$$\xi^{v+1} \leftarrow \xi^v - (\sigma^{v+1} - \sigma_\tau^{v+1}) \tag{3.59}$$

(5) Check the convergence by:

$$\sqrt{(\xi^{v+1} - \xi^v)^2} \leq \varepsilon_{coef} \tag{3.60}$$

(6) If the problem has converged, then the optimal overall uncertainty coefficient can be obtained as σ^{v+1}. Otherwise, update the iteration number to $v \leftarrow v+1$ and go back to step 2.

where the penalty factor, scaled dual variables, and convergence threshold in the ADMM method are given by ρ, ξ, and ε_{coef}, respectively. The process for selecting the optimal uncertainty coefficient is illustrated in Algorithm 3-2.

Algorithm 3-2 Self-adaptive algorithm for adjusting σ

Initialization $v=0$, $\xi^0=0$, $\rho=100$, $\varepsilon_{coef}=0.001$,$\sigma_\tau^0=\frac{|rv_\tau^r - fv_\tau^r|}{fv_\tau^r}$

While (3.60) is **False**, $v \leftarrow v+1$ **do**

Solve (3.57) to obtain σ^{v+1}

Solve (3.58) for each past time window parallelly with (σ^{v+1}, ξ^v) to obtain σ_τ^{v+1}.

Update $\xi^{v+1} \leftarrow \xi^v - (\sigma^{v+1} - \sigma_\tau^{v+1})$

End While

Return σ^{v+1}

3.5 Case Study

This section provides the numerical results to demonstrate the superiority of the proposed operation regime for VPPs.

3.5.1 Experiment Setup

The VPP under study is composed of two thermal generators and one wind generator. Battery is not considered in the case study due to its high investment costs. The generator characteristics are presented in Table 3.2. The Finland day-ahead market price and called reserve volume data from the NORDPOOL market (*Day Ahead Auction Prices* 2019) are used. The renewable generation data is the scaled wind generation from Finland (*Wind Generation Data* 2019). The penalty coefficients ψ^+ and ψ^- are set to be 1.5 and 0.5, respectively. At the day-ahead and real-time stages, the empirical worst-case uncertainty coefficients are set to be 0.7 and 0.4, respectively. In the real-time stage, three look-back time windows are considered.

Table 3.2: Generator Characteristics

Generator	P_{max} [MW]	$EcoP_{min}$ [MW]	RU [MW/h]	RD [MW/h]	$a[\$/h]$	$b[\$/MWh]$	$c[(\$/MWh)^2]$
Diesel	45	5	25	15	708	30.7	0.77
Gas	55	5	35	25	531	34.2	0.83
Wind	65	0	/	/	/	/	/

Fig.3.3a gives the day-ahead wind forecast data, where the uncertainty coefficient is constant; Fig.3.3b shows the real-time wind forecast data, where the uncertainty coefficient is continuously modified.

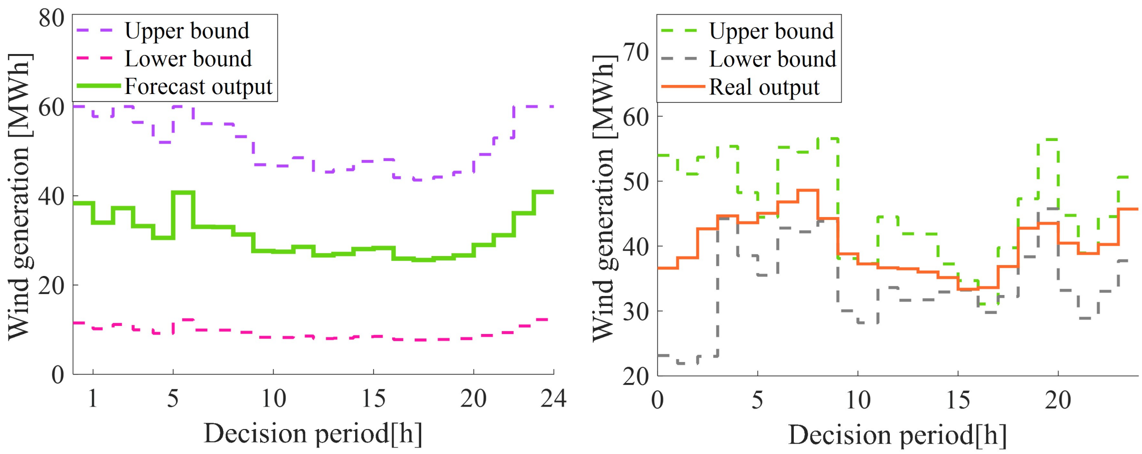

(a) (b)

Figure 3.3: (a) the forecast data and the day-ahead forecast intervals (b) the real-time wind forecast intervals

The market accepts bidding curves with at most five steps. Hence, five price-quantity pairs are required in each market-clearing period to construct the bidding curve. Because each bidding step is obtained by a price scenario and its corresponding bidding quantity, five price scenarios are generated for each market-clearing hour to yield five price-quantity pairs. The actual price and generated price scenarios are presented in Fig.3.4.

3.5.2 Results and Discussions

The computation platform is AMD Ryzen 8-3700X 3.60 GHz with 16G RAM. The average total computation time is 1,424s, which is acceptable under the time scales of day-ahead bidding (i.e., multiple hours) and real-time dispatching (i.e., within one hour).

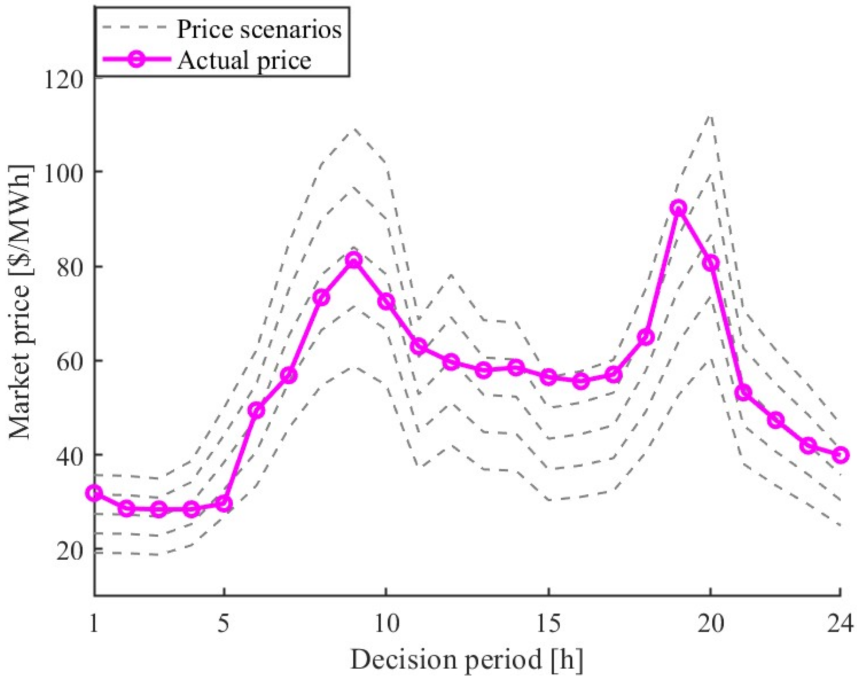

Figure 3.4: Generated price scenarios and the actual price.

The stepwise energy offers of the VPP in several representative hours are depicted in Fig.3.5. In hour 3, the forecast price is low and the VPP is only willing to offer the energy from the wind generator for the first 3 price scenarios. As the price increases, the VPP starts to offer energy generated by the thermal generators for the fourth and fifth price scenarios. Therefore, three bidding steps are constructed for hour 3. In hour 15, the forecast price is medium and for each price scenario, the VPP has a different bidding volume. In hour 21, the forecast price is high and the VPP is willing to offer its maximum capacity at the fourth price scenario. Though the fifth price scenario is higher than the fourth scenario, the VPP cannot offer more energy to the market, thus, only four steps in hour 21 can be observed.

According to the market-clearing prices, the accepted VPP energy offers together with the called reserve are presented in Fig.3.6. The required energy is the sum of the market-allocated energy and the reserve volume called by the system operator.

Fig.3.7 shows the dispatching decisions of the thermal generators over the day. In Fig.3.7, the VPP does not turn on the thermal generators in hours 1 to 5 and 24 because the market prices are very low. In hours 13, 21 to 23, only the diesel generator remains online, the gas generator is turned off due to its higher variable cost. In hours 12 and 14, both the diesel and gas generators are not generating at their optimal power because of the minimum economic power restriction.

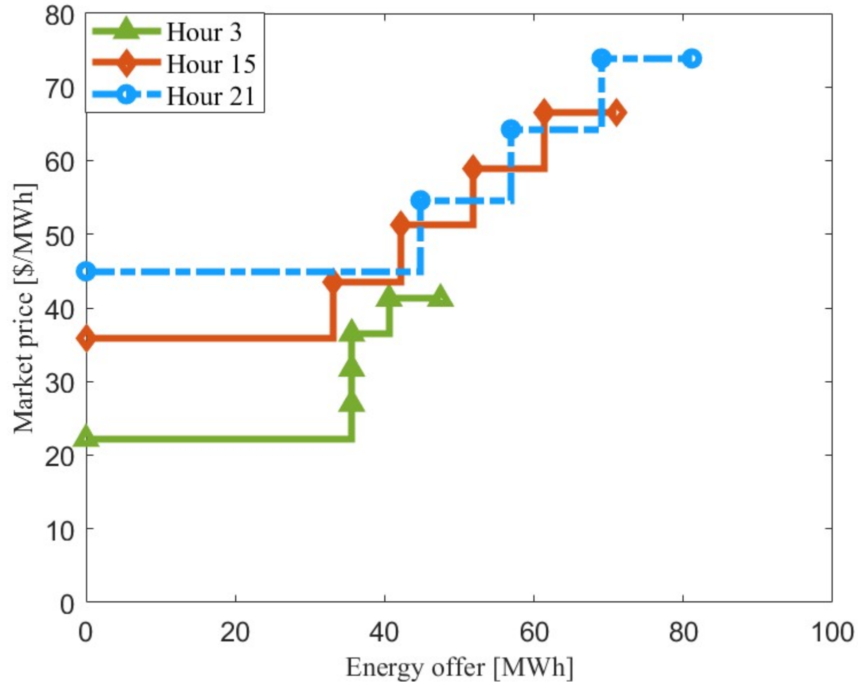

Figure 3.5: Bidding curves for hours 3, 15, and 21

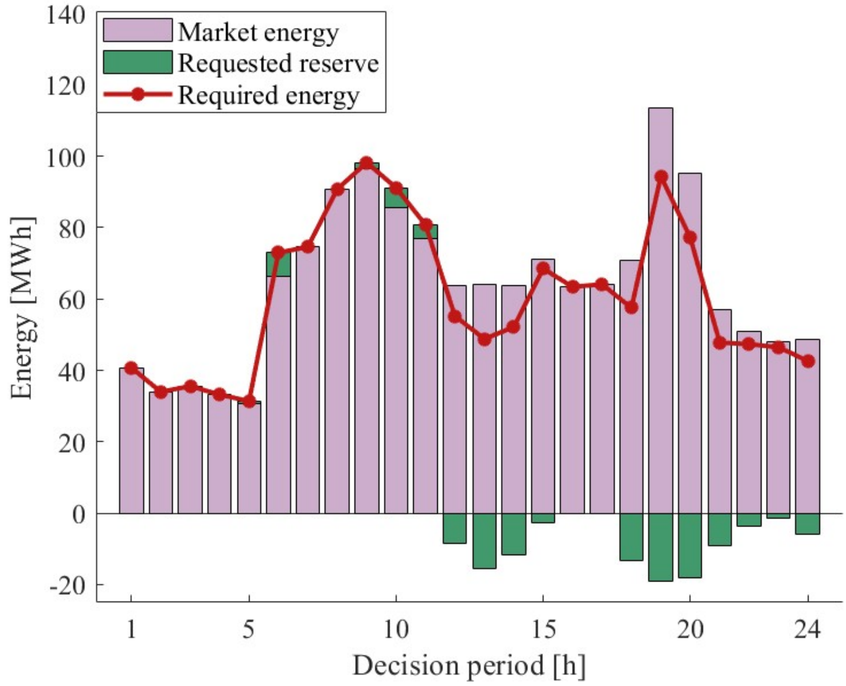

Figure 3.6: The market allocated energy, called reserve, and required energy

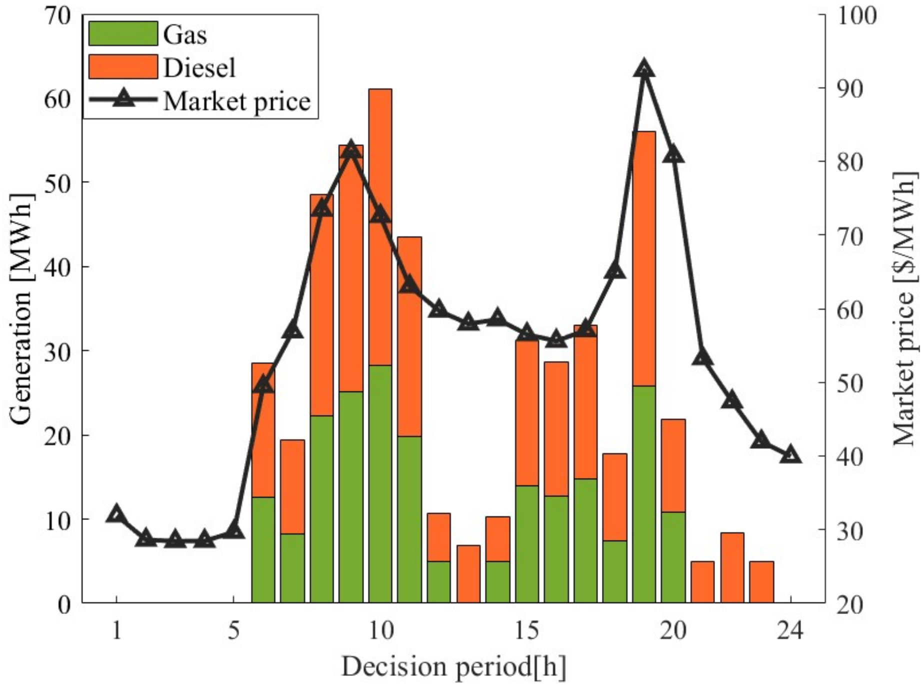

Figure 3.7: The dispatching results of the thermal generators

It should be noted that in Fig.3.7, the scheduled generation levels do not exactly match the market price levels. For example, the market price at hour 19 is the highest over the day, while the production at hour 19 is not the highest. This violation is due to the VPP's need to respond to the system operator's call for reserve deployments. Therefore, the VPP may curtail its production even at high price hours as shown in Fig.3.14.

The hourly net profit and the details of the profit components of the VPP are shown in Fig.3.8. The question of how to participate in the forward reserve market is out of the scope of this chapter; thus, the revenue in the forward reserve market is not presented here. Due to the existence of the reserve contract, the VPP must respond to the reserve calls from the system operator, which induced $6,156 of revenue loss. The most important revenue is from selling energy to the day-ahead market ($92,875), and the major cost comes from the thermal generator fuel costs ($45,179). The total cost in the balancing market is $3,444, and the overall operating profit from the proposed operation regime is $38,096.

To evaluate the economic performance of the proposed operation regime (Case 1), multiple strategies and optimization models are also tested for the VPP under study. The results from the price-dependent bidding using the stochastic robust optimization model (Case 2), the price-dependent bidding using the multistage stochastic programming model (Case 3), the price-

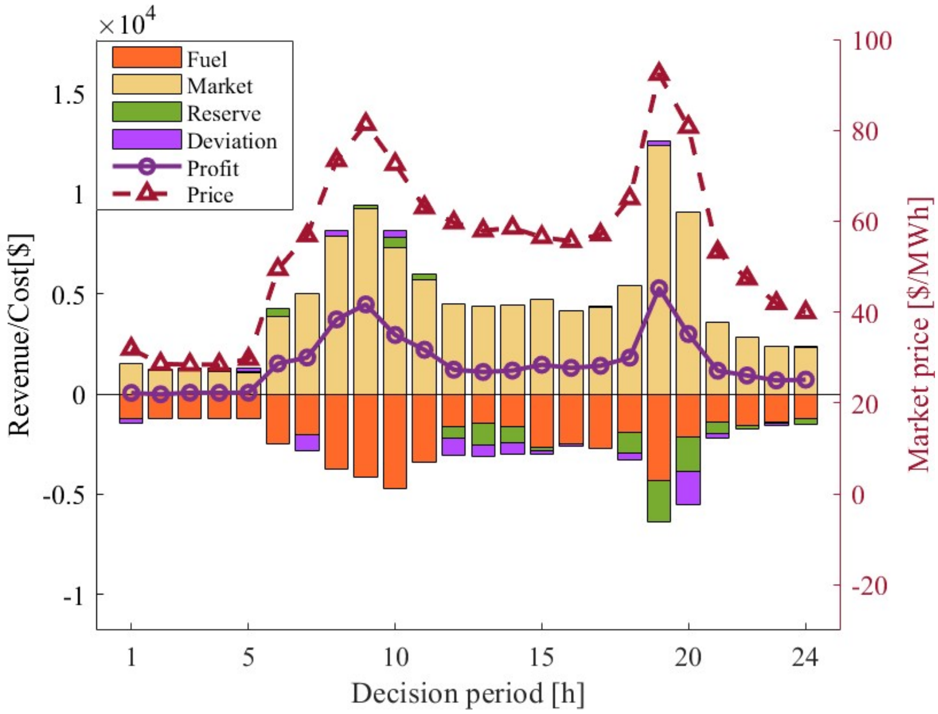

Figure 3.8: The VPP's profit using the proposed methods (case 1)

independent bidding using the stochastic MMR model (Case 4), and the price-dependent bidding using the stochastic MMR model without performing real-time dispatch (Case 5) are provided in Fig.3.9 to Fig.3.12. The daily profit results of the discussed strategies are summarized in Table 3.3.

To compare the stochastic MMR model with the stochastic robust optimization model, the stochastic MMR optimization model is replaced with the stochastic robust optimization model while maintaining everything else unchanged. Since the bidding decisions of different hours are independent of each other, the considered budget of uncertainty in the stochastic robust optimization model is set to be 1.

The VPP's revenue from the energy market is \$65,765. Compared to the revenue (\$92,875) obtained when using the stochastic MMR model, one can see that the stochastic robust optimization model offers less energy in the electricity market for the same price levels. The overall profit obtained from the stochastic robust optimization model is \$29,314, which is only 76.95% of the profit when the stochastic MMR model is used. Therefore, one can conclude that, compared to the stochastic robust optimization model, the proposed stochastic MMR model can significantly improve the economic performance of the VPP. Also, it can be observed that the deviation cost is negative, which means that the revenue in the balancing market is larger than

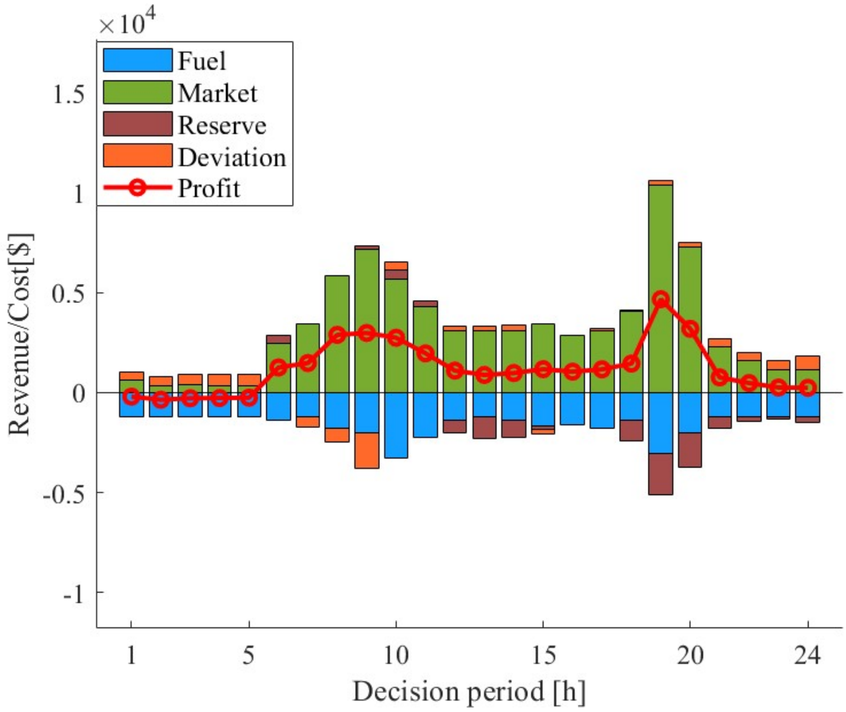

Figure 3.9: The VPP's profit using the stochastic robust optimization model under the price-dependent framework (case 2)

the cost. This result confirms the conclusion that the performance of the stochastic robust optimization model is very conservative and leads to significant positive energy deviations.

In Fig. 3.9, the bars located above the x-axis represent the revenues earned by the VPP, while the bars below the x-axis indicate the costs incurred by the VPP. It is important to note that the day-ahead market payments always count towards the VPP's revenues, which is why the green bars are always located above the x-axis. Conversely, the fuel cost is an expense that reduces the VPP's net profit, and as such, the blue bars are always negative. Furthermore, the bars that represent energy deviations and reserve calls can be either positive or negative. In the case of positive energy deviations (energy surplus) and up-reserve calls (energy increment requests), the VPP can generate additional revenues, while negative energy deviations (energy deficiency) and down-reserve calls (energy reduction requests) can result in additional costs for the VPP. Therefore, the bars representing energy deviations and reserve calls can be either positive or negative, depending on the specific circumstances.

To further demonstrate that the proposed method can provide economic solutions without the accurate probability distribution of wind uncertainty, the multistage stochastic programming approach is applied to the VPP under study. In stochastic programming, the restriction that

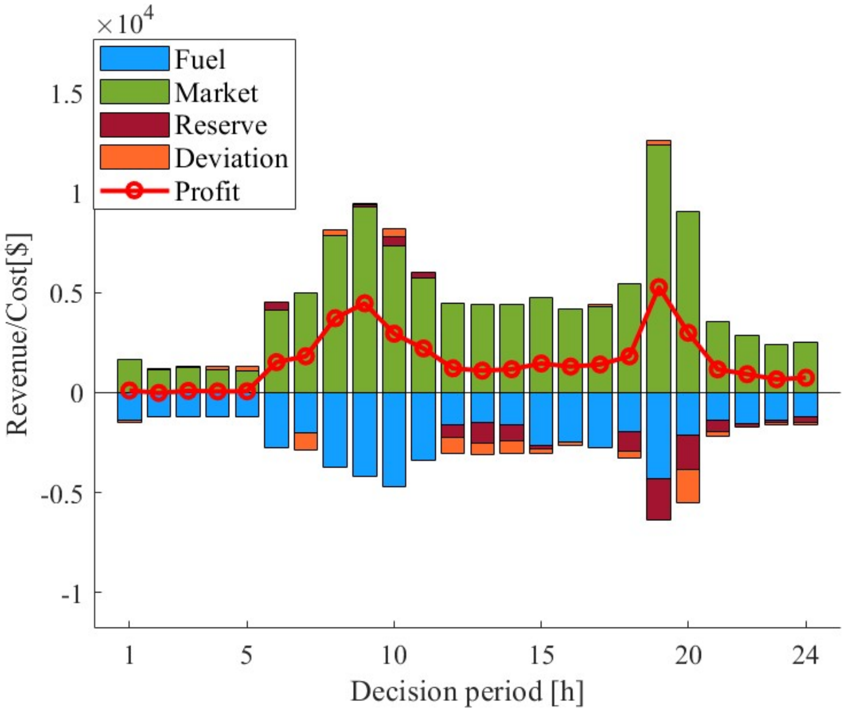

Figure 3.10: The VPP's profit using the multistage stochastic programming approach (case 3)

the accurate probability distribution of wind uncertainty is not available is removed, and wind uncertainty is modeled by using scenarios instead of uncertainty intervals. From the result in Table 3.3, one can see that our method performs very closely to the stochastic programming approach. The overall profit by using the proposed method has been merely reduced by 0.25% compared to the multistage stochastic programming approach. The major reason for this difference is that the stochastic programming approach has more precise information that enables it to handle the wind uncertainty by using expected values as the objective, whereas the proposed method only has less-precise information and needs to deal with wind uncertainty based on the minimax criterion. As a result, the conservativeness in the bidding and dispatching solutions of the proposed method has increased slightly compared with the multi-stage stochastic optimization approach.

Then, to evaluate the difference between price-dependent and price-independent bidding strategies, in the price-independent bidding using the stochastic MMR model, a single bidding profile is generated by using the expected market price. Compared to the price-dependent bidding strategy, the price-independent bidding strategy is less capable of capturing arbitraging opportunities due to insufficient flexibility. This effect is obvious when the market price significantly deviates from the expected price, such as in hours 15, 16, and 19, the ratios of the

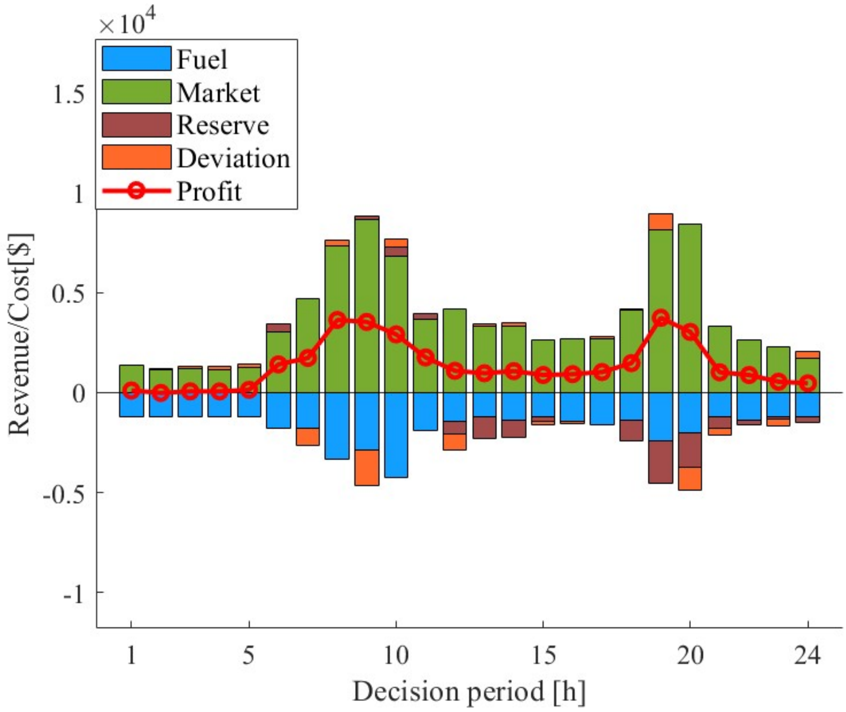

Figure 3.11: The VPP's profit using the proposed stochastic MMR model under the price-independent framework (case 4)

price-independent strategy profit to the price-dependent strategy profit are 60.28%, 70.85%, and 70.89%, respectively. As a result, the overall profit using the price-independent strategy ($32,440) only takes up 85.15% of the price-dependent strategy profit.

The impact of performing the real-time dispatch is illustrated by comparing Fig.3.12 with Fig.3.8. It is easy to notice that the generation cost has been increased when real-time dispatch is not considered. This is because, with less accurate wind power production prediction, the day-ahead dispatching result is more conservative, which leads to overproduction of the thermal generators. The overproduced energy can only be sold at penalty prices and cause losses in the overall VPP profit.

To illustrate the effectiveness of the proposed self-adaptive algorithm, the same dispatching problem is solved using both the adjusted and unadjusted uncertainty coefficients. Fig.3.13 shows the hourly profit loss using both uncertainty coefficients. The profit losses are obtained by subtracting the profits of the dispatching solutions obtained with incomplete information from the profits of the perfect information approach (Jia et al. 2019). Most of the time, the profit loss from using the adjusted uncertainty coefficient is significantly lower than using the constant worst-case uncertainty coefficient. However, in hour 20, the VPP's profit loss using the

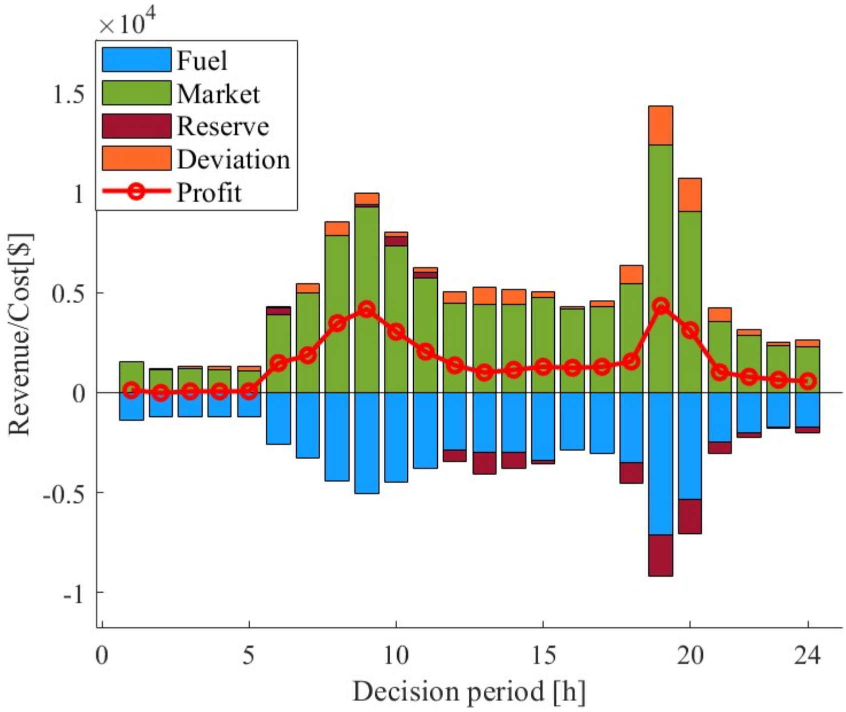

Figure 3.12: The VPP's profit using the proposed price-dependent stochastic MMR model without performing real-time dispatch (case 5)

Table 3.3: Profit Results Using Different Strategies and Models

Operating strategy	Energy market revenue [$]	Fuel cost [$]	Deviation cost [$]	Net profit [$]
Proposed methods	92,875	45,179	3,444	38,096
Stochastic robust optimization	65,765	32,809	-2,514	29,314
Multistage stochastic	93,450	45,547	3,556	38,191
Price independent	76,121	35,187	2,338	32,440
Day-ahead only	92,875	60,982	-9,986	35,723

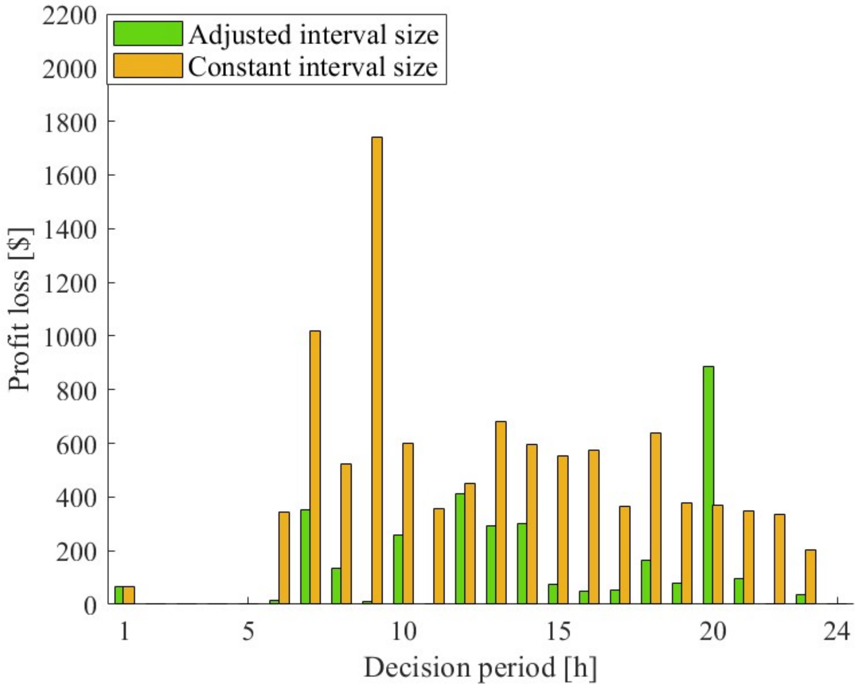

Figure 3.13: Profit loss in the dispatching stage using the adjusted and constant uncertainty coefficients

adjusted σ is larger than using the worst-case σ, this is because the adjusted confidence bounds failed to contain the real wind generation scenario, as shown in Fig.3.4b. This failure is due to the tradeoff that is made between robustness and economic performance. Though larger profit loss may be induced in some hours, the overall profit loss in the dispatching stage using the adjusted σ is \$3,280, which is only 32.34% of the profit loss when using the constant worst-case σ (\$10,143).

The reserve response result is presented in Fig.3.14 which shows that for most of the time, the VPP can exactly complete the reserve requests from the system operator. However, the VPP's capability for reserve deployment is also limited at some hours. When the price is very low, the thermal generators are either offline or producing at minimum economic power. Hence, the VPP cannot flexibly change its power output to complete the reserve calls, such as hours 5, 23, and 24. Similar limitations can also happen when the market price is exceptionally high. Another situation that can limit the VPP's reserve provision capability is large price differences between adjacent hours, which happened at hours 20 and 21. Because most of the ramping capability is used to fulfill the market-clearing results, the flexibility left for responding to reserve calls is not enough to complete the task. The frequency of observing such limitations depends on how often the aforementioned extreme scenarios will happen in the energy market. In total, the

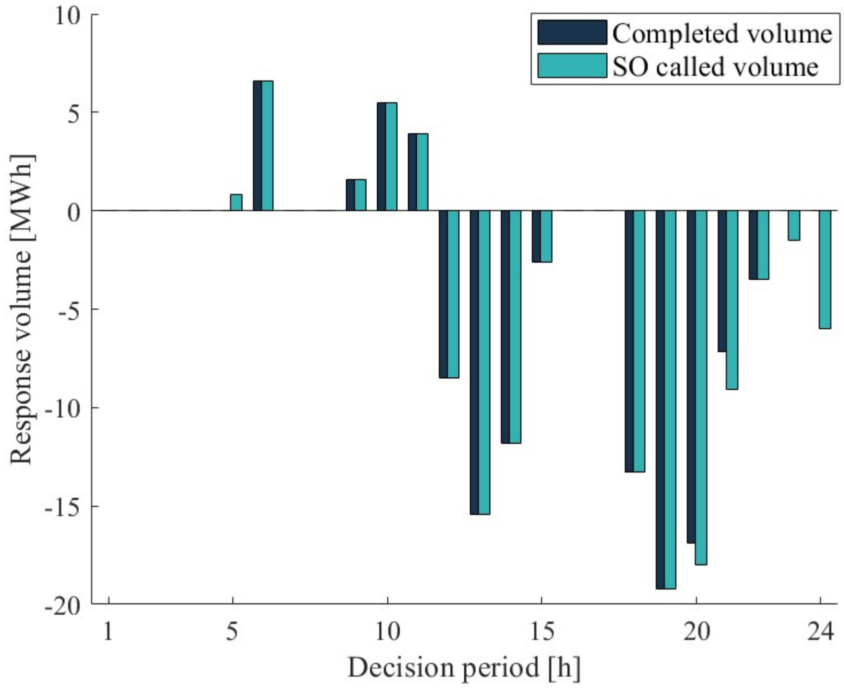

Figure 3.14: Reserve response results of the VPP

VPP complete 91.29% of the requested reserve volume

It should be noted that such limitations in the VPP's reserve response capability are acceptable in this case study because system security is not involved. If extreme operational scenarios that can severely threaten the system security must be considered, some economically unfavorable approaches such as cutting down the renewable generation and investing in expensive energy storage systems can be adopted to eliminate such limitations.

Although a small-scale VPP is investigated in the case study, the proposed operation regime can be effectively extended for larger VPPs consisting of more generators without significantly increasing the computational burden. Table 3.4 gives the average total computation time for VPPs managing different numbers of generators. As the number of generators is increased from 3 (2 thermal generators and 1 renewable generator) to 40 (20 thermal generators and 20 renewable generators), the total computation time only increases from 1,424s to 1,625s. The reason for this result is two-fold. Firstly, calculating the optimal power generation of the thermal generators does not take too much time. Secondly, increasing the number of renewable generators will not substantially affect the convergence rate of the C&CG algorithm because the number of extreme scenarios for renewable energy production is not changed. Hence, the computational burden increment due to the increased number of generators is not significant

Table 3.4: Computation time analysis

Number of generators	2T / 1R	5T / 5R	10T / 10R	20T / 20R
Computation time	1,424s	1,497s	1,554s	1,652s

TP: thermal power plant; RP: renewable power plant

compared with the time required to solve the stochastic MMR model.

3.6 Chapter Summary

This chapter proposes an optimal VPP operation regime under reserve uncertainty. In the day-ahead bidding stage, the developed price-dependent bidding strategy improves the bidding flexibility of the VPP in the energy market. Also, the proposed stochastic MMR optimization model utilizes a combination of scenarios and uncertainty intervals to describe the uncertainties, making it advantageous for problems where some uncertainties have accurate probability distributions while others do not. In the real-time dispatching stage, the proposed self-adaptive algorithm can optimally determine the size of the uncertainty intervals in a look-back-and-adjust manner. The proposed regime was assessed using the typical day data.

The results suggest that the price-dependent bidding strategy can increase the VPP profitability in contrast with the price-independent strategy, this effect is most obvious when the real price deviates a lot from the price forecast. Also, the proposed stochastic MMR model can provide bidding decisions that are less conservative compared with the stochastic robust optimization model. Furthermore, by properly determining the size of the uncertainty intervals, the proposed self-adaptive algorithm significantly reduces the profit loss due to incomplete information in the dispatching stage.

Though all the above conclusions are based on offline analysis, the proposed method is of high potential to be implemented in the future because joint participation in multiple markets and price-dependent bidding strategy are widely adopted in existing electricity markets. Besides, methods that can improve the economic performance of VPPs will be more favorable in practical applications because profitability is the major concern for VPPs.

In this chapter, the DERs considered in the VPP operation only include renewable and thermal generators. The results show that the uncertainty in renewable generation and electricity markets can bring negative impacts on the VPP operation in terms of its profit. Such negative impacts can be partially reduced by using the energy flexibility of thermal generators. EVs are not considered in this chapter, but they can also offer energy flexibility to mitigate the negative impacts of operational uncertainties. Hence, to further enhance the energy flexibility of the VPP, integrating EVs into the VPP operation is a promising topic due to the energy storage nature of EV batteries. In the next chapter, energy management methods for EV fleets through EV charging stations will be developed to control the EV charging load and make use of EV energy flexibility.

Chapter 4

EV Charging Station Energy Management

EVs are important components in this thesis to maximize the utility of DERs. Due to the heavy capital cost of energy storage devices (Rahman et al. 2020), building energy storage systems to mitigate the negative impacts of operation uncertainties can be economically unfavorable. Fortunately, EVs are natural energy buffers that can perform similar functionalities as traditional energy storage systems thanks to their rapidly increasing stock (*Global electric car stock* 2022) and energy flexibility (Heinisch et al. 2021). However, exploiting EV energy flexibility is hindered by many factors such as insufficient EV user cooperation and the complexity of EV charging scheduling problems. To fully make use of EV energy flexibility, an EV user incentive program is proposed in this chapter as the main focus to encourage the proactive participation of EV users in the smart charging process. Based on the incentive method proposed in this chapter, an EV charging station energy management strategy under volatile electricity prices can be developed as optimization problems.

4.1 Chapter Introduction

Transportation is one of the largest emitting sectors of greenhouse gas emissions largely due to internal combustion engine vehicles (Koufakis et al. 2019). Hence, shifting from internal combustion engine vehicles to EVs has been widely recognized as one of the most effective means to decarbonize the transportation sector because EVs can be powered by electricity generated from renewable sources.

The EV charging demand has grown dramatically over the past few years (Injeti and Thunuguntla 2020). This is contributed by the mass roll-out of EVs in many countries and regions, and the advances in EV battery technology. The increased charging demand can impose significant challenges to the power network operation if the EV charging behavior is unscheduled and unregulated (Shi et al. 2018). Previous research reveals that the EV parking time is often longer than that is required for charging in many scenarios (Heinisch et al. 2021), which leads to charging flexibility that can support economic and secured power system operations in the future (Richardson 2013).

Due to the distributed nature and large quantities of EVs, direct control of EV charging by the system operator is computationally challenging. Hence, EV charging coordination is often accomplished by intermediary agents including EV aggregators, charging stations, VPP operators, and microgrid operators. For these intermediary agents, the EVs under their control can act as flexible demand response resources to generate revenues and benefits in many ways, such as participating in the energy market to reduce the energy procurement cost (Zheng et al. 2020; Rassaei, Soh, and Chua 2015; Hajebrahimi et al. 2020), providing ancillary services to generate income (Duan, Hu, and Song 2020; Sarker, Dvorkin, and Ortega-Vazquez 2015; Vayá and Andersson 2015), and gaining remunerations by responding to the demand response signals (Shafie-Khah et al. 2015; Yao, Lim, and Tsai 2016). The underlying assumption in these works is that the intermediary agents can utilize EV charging flexibility without incentivizing EV users, which is bluntly unrealistic as scheduled charging may bring considerable inconvenience to EV users, and convenience is the primary motivation for personal ownership of vehicles. Hence, the design of incentives for EV users is vital for the intermediary agents to acquire their expected EV charging flexibility.

Since EV users tend to charge their EVs as quickly as possible (Chung et al. 2018), incentive programs are needed to remunerate EV users for acquiring their charging flexibility and reshaping EV charging load. Otherwise, EV users will not be motivated to participate in the demand response programs. In a demand response incentive program, the demand response program operator should specify what kinds of EV users' actions will be rewarded and how much will be paid for these actions. Hence, this chapter is specifically focused on the design of EV users' remunerative actions and the pricing methods for these actions.

In the literature, a variety of incentive programs have been proposed for inspiring EV users to participate in demand response programs managed by intermediary agents. These incentive programs, though varying from one to another, can be categorically classified as static programs and dynamic programs from the incentive signal update frequency angle.

The incentive signal update frequency of static incentive programs is relatively low, which keeps the incentive programs unchanged over a relatively long period. The advantages of such programs are that they are consistent and simple for implement, EV users can easily use them as a reference for scheduling their charging plans.

Practices of static incentive programs include time-of-use pricing and critical peak pricing. In (Su, Lie, and Zamora 2020), an optimal time-of-use tariff plan decision model is proposed to shift the EV charging load from high-price hours to low-price hours. In (Dubey et al. 2015), an optimal time-of-use tariff plan is proposed by evaluating various aspects of EV charging behavior under the time-of-use tariff. In (Muñoz et al. 2016), several strategies including time-of-use tariff is applied to EV charging load to mitigate the transformer burden imposed by the high penetration level of EVs. In (Song, Shangguan, and Li 2021), a time-of-use charging price program with a price reduction strategy is applied to reduce the energy procurement costs and distribute the benefits between EV users and charging infrastructure operators. In (Sheidaei and Ahmarinejad 2020), both time-of-use and critical-peak-pricing mechanisms are applied to the EVs to improve the VPP's profitability. Similarly, both time-of-use and critical-peak-pricing programs are used in (Sadati et al. 2019) to increase the profit of a distribution company. In static incentive programs, consumers are allowed to sacrifice a certain degree of convenience in return for reduced charging fees in a simple way. However, existing static programs do not offer the intermediary agents the controllability to maximize their gain from short-term market and system fluctuations.

Compared with static programs, dynamic programs update incentive signals more frequently in response to short-term market and system information, which enables more controllable actions to handle short-term market and system fluctuations, hence encouraging more proactive participation of EV users in offering flexibility services to the power grid through intermediary agents.

The most popular dynamic programs are dynamic pricing and transactive control programs. In (Zhao et al. 2017), a charging station uses real-time energy and reserve price signals to incentivize EV users for altering their charging schedules. In (Liu et al. 2021), an EV aggregator sends dynamic price signals to encourage EV users to change their charging plan or authorize the battery access right to the aggregator. In (Moghaddam et al. 2019), a dynamic pricing model is proposed for multiple charging stations to coordinately shift EV charging load from residential load peaks. A dynamic pricing framework for charging stations is proposed in (Limmer and Rodemann 2019) to concurrently maximize the profit of charging stations and reduce the peak load. In (Liu et al. 2018), the EV aggregator manages the charging load by clearing the transactive market according to the day-ahead energy procurement and real-time requests of EV users. The charging load in (Wu et al. 2018) is controlled through a transactive market to which EV users need to submit their real-time charging requirements and preference setting of demand response. A sensitivity-based real-time transactive control framework is proposed in (Hoque et al. 2021) to coordinate the EV charging behavior through a local energy market.

Although dynamic programs are more controllable, they lack simplicity and consistency compared to static programs. Besides, dynamic incentive programs assume that EV users can actively respond to the price signals and alter their charging behavior responsively (Zhou et al. 2019), which is too optimistic as it takes effort and specific knowledge to complete such tasks. Furthermore, in order to make the optimal decisions to maximize the benefit, EV users have to be constantly updated with the latest market information, which demands extra effort from the EV users.

Considering the pros and cons of existing EV incentive programs, a hybrid incentive program is proposed for a charging station that aims to offer incentives to the EV users to share their charging flexibility. The proposed hybrid incentive program combines static incentives with dynamic control. Under the proposed hybrid incentive program, the consistency and simplicity of static programs are retained, while the controllability of dynamic programs can be achieved. Table 4.1 compares the key features of the proposed incentive program with both static incentive programs and dynamic incentive programs.

In Table 4.1, the properties of different incentive programs are ranked by comparing them with each other. The simplicity of dynamic programs is the lowest because EV users are required to regularly react to incentive signals. Besides, the proposed programs are ranked higher in simplicity than static programs as the proposed programs eliminate the need for EV users to wait for low-price hours for recharging. Hence, the simplicity property for static, dynamic,

Table 4.1: Key properties of different types of incentive programs

	Simplicity	Consistency	Controllability
Static programs	Medium	High	Low
Dynamic programs	Low	Low	High
Proposed program	High	High	Medium

and the proposed programs are listed as medium, low, and high. In terms of consistency, it is assumed that the incentive signals for both static and proposed incentive programs will remain effective for a relatively long period. On the other hand, dynamic programs regularly change the incentive signals to deal with short-term variations. Hence, the consistency property is listed as high for static and proposed programs and low for dynamic programs. The ranking of controllability is based on the calculated results of the controllability index, which will be presented in the case study later.

The considered charging station faces volatile day-ahead wholesale market-clearing prices and variability of EV users' willingness to sell their charging flexibility. For the charging station, the incentive prices can affect both the incentive payment and the amount of charging flexibility that can be acquired to reduce energy bills. Therefore, the selection of incentive prices is crucial for the performance of the proposed hybrid incentive program. To maximize the charging station's benefit while encouraging proactive participation of the EV users, an optimal incentive price selection model is developed in this chapter to determine the incentive prices for EV charging flexibility.

As the proposed hybrid incentive program needs to retain consistency for a relatively long period, market price patterns at different times should be considered in the optimization model to ensure unbiased incentive price selection. Increasing the number of price scenarios leads to a larger number of EVs under consideration, which makes the solution process computationally challenging. In confronting the dimensional problem for large EV fleets, distributed and meta-heuristic methods are the most popular approaches in the literature (Solanke et al. 2020). Compared with meta-heuristic approaches, distributed methods are more specific and take less time to converge (Zheng et al. 2019). Hence, a distributed solution process based on the ADMM method is developed in this chapter to guarantee computational efficiency in solving the optimal incentive price selection problem.

The major contributions of this chapter are as follows:

- A novel hybrid incentive program is proposed to encourage EV users to sell their charging flexibility to the charging station. The proposed hybrid incentive program combines the advantages of both static and dynamic incentive programs, namely, it has the features of simplicity, consistency, and controllability.
- An optimal incentive price selection model is developed to maximize the charging station's profit from the electricity market and the demand response program. The optimization results of the proposed model can serve as a reference for policymakers who adopt the proposed hybrid incentive program.
- An ADMM with adaptive penalty (ADMM-AP) solution algorithm is presented to efficiently solve the problem in a distributed manner for large EV fleets.

The remainder of this chapter is organized as follows. Section 4.1 gives an overview of the charging station operation framework and provides the details of the proposed hybrid incentive program. Section 4.3 presents the optimal incentive price selection model. The proposed solution methodology is detailed in Section 4.4. Section 4.5 presents the numerical results and discussions. Section 4.6 concludes this chapter.

4.2 Problem and Model Description

This section first introduces the operation framework of the considered charging station, then presents the details of the proposed EV user incentive program.

4.2.1 Charging Station Operation Framework

The configuration of the charging station's operation framework is presented in Fig. 4.1. The charging station under consideration is a public charging station, which can directly control the charging rates of its charging piles. To acquire information about the EV users' demand response preferences, it is assumed that EV users can directly communicate with the charging station in advance before they choose to park and charge there. In the day-ahead wholesale market, the clearing resolution is one hour, and the charging station is a price-taker who purchases energy at the market-clearing price to satisfy EV energy requirements.

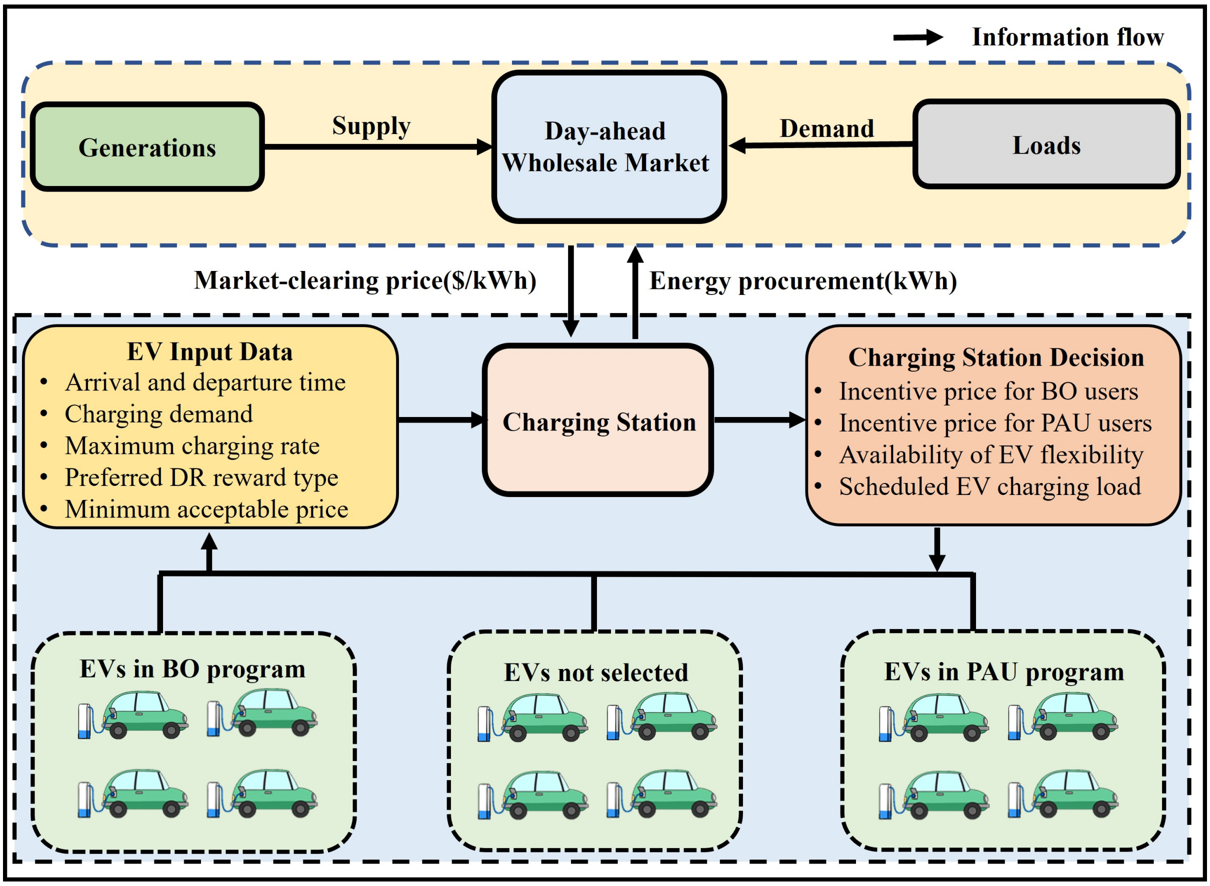

Figure 4.1: Operation framework of the charging station

Due to market entrance requirements, the considered charging station may not have access to the wholesale market and benefit from competitive wholesale prices. Hence, an intermediary agent that can integrate the charging station and access the wholesale market (e.g., virtual power plants that can integrate the charging stations) is needed in the energy procurement process. Since the charging station cannot affect the market price, it is motivated to shift the EV charging load from high-price hours to low-price hours to reduce energy bills.

Under the time-of-use pricing scheme, EV users who want to reduce their charging fee must wait for low-price hours to park and charge, which reduces the simplicity of the incentive program by significantly limiting EV users' convenience. Hence, to minimize the restrictions on EV users' traveling and parking plans, a flat charging price is applied to the charging station. The charging loads are shifted through the charging station's demand response program, which provides certain remuneration to EV users in exchange for access rights to EV batteries. The demand response program managed by the charging station includes the buy-out (BO) program and pay-as-use (PAU) program, which correspond to different incentive payment calculation methods in the proposed hybrid incentive program.

The charging station needs to set up proper incentive prices to encourage EV users to sell their charging flexibility. Also, the charging station is responsible for scheduling the charging flexibility to minimize the energy procurement cost. EV users only need to claim their charging demands and demand response preferences upon arrival. Besides the dwelling time, other battery information including the initial SOC, battery capacity, and maximum charging rate can be directly acquired from the battery management system of the EVs. The demand response preference information includes which incentive they want to receive and the minimum prices they can accept for authorizing the battery access rights.

There are several advantages of applying such a flat pricing and incentive demand response program operation framework. Firstly, EV users do not have to wait for low-price hours to park and charge. Secondly, EV users do not need to actively respond to the incentive signals during the charging duration. Instead, they only need to clarify their demand response preferences upon arrival. Thirdly, the negotiation process for real-time demand response is avoided since all the information needed to approach the optimal solution is pre-communicated.

4.2.2 Proposed EV User Incentive Program

This subsection first discusses the key properties of existing incentive programs for EV users. The strengths and drawbacks of different types of incentive programs are analyzed based on the discussed key properties. To combine the advantages of existing EV user incentive programs, two incentive programs, including the BO and the PAU incentive programs are proposed in this subsection.

(1) Discussion on Key Properties of Incentive Programs

In this chapter, an incentive program is considered to be simple if the required actions from the EV users are minimal. Consistency of an incentive program means that EV users' knowledge about the incentives does not have to be updated frequently. Besides, the controllability of incentive programs refers to the ability to match the charging load with short-term market price variations. Simplicity and consistency can be difficult to quantify because the criteria can vary from person to person. One example of simple and consistent incentive programs is time-of-use pricing, where prices for peak-flat-valley periods are stable for a relatively long period to allow decision-making simple and straightforward. An opposite example is the transactive control program, where EV users need to actively respond to the incentive signals that change in real-time. For controllability, a controllability index (CI) is defined in this chapter to quantitatively reflect how controllable a demand response incentive program is:

$$CI(\$/kWh) = \frac{Energy\_Bill\_Reduction(\$)}{Effective\_Flexibility(kWh)} \tag{4.1}$$

where energy bill reduction is the reduced energy procurement cost (measured in \$) in the wholesale market, and effective flexibility (measured in kWh) is the flexibility that is utilized. A larger CI implies more efficient utilization of each unit of effective flexibility, which can be achieved by more exactly matching the charging load with the variable market price.

For EV users, simplicity and consistency are favorable properties of an incentive program. From the charging station's point of view, controllability is a desirable property as it can achieve more benefits. However, achieving controllability may contradict the simplicity and consistency if EV users have to actively respond to incentive signals. To address this contradiction, a hybrid incentive program is proposed for the charging station, which consists of the BO incentive and the PAU incentive. The prices for both the BO and PAU incentives will remain unchanged for a relatively long period. Under the proposed hybrid incentive program, if EV users accept the charging station's offer, they would receive payments for the access right of their EV batteries. With access rights to the batteries, the charging station can achieve accurate EV charging load control under the constraint of satisfying EV charging demand. Specifically, by directly controlling the operation of its charging piles, the charging station can determine the charging time and charging rates of EVs that chose to participate in the demand response programs.

To this end, the proposed hybrid incentive program features simplicity in terms of EV users' participation, while consistency is retained regarding the incentive price update frequency. Moreover, controllability can be achieved by the dynamic charging control of the charging station.

(2) Buy-Out Incentive Program

For EV users who accept the offers from the BO program, they will receive a payment to buy out all the potential charging flexibility (measured in kWh), which may or may not be used in the charging scheduling. Since the battery charging rates are assumed to be continuously controllable (Jin and Xu 2020), the potential flexibility pf_n of the nth EV can be calculated as:

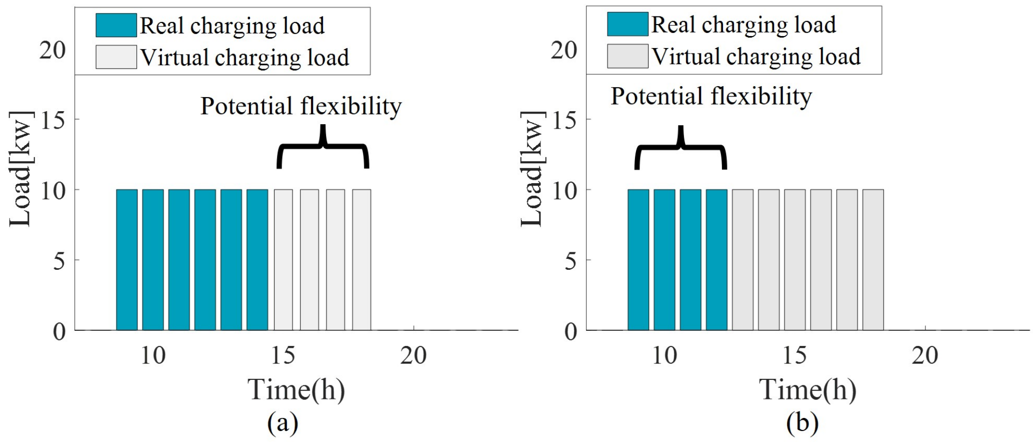

Figure 4.2: EV Flexibility in the BO program

$$t_n^{dwell} = t_n^{out} - t_n^{in} \tag{4.2}$$

$$E_n^{ev} = (SOC_n^{max} - iSOC_n)Cap_n^{ev} \tag{4.3}$$

$$pf_n = \min\left\{E_n^{ev}, t_n^{dwell} P_n^{max} - E_n^{ev}\right\} \tag{4.4}$$

where n is the index for EVs in the BO program. The plug-in and plug-out times are represented by t_n^{in} and t_n^{out}, respectively. Term t_n^{dwell} denotes the total parking time. The energy requirement E_n^{ev} is calculated using the initial SOC (iSOC) and battery capacity Cap_n^{ev} through Eq (4.3), in which SOC_n^{max} represents the maximum SOC. The potential charging flexibility pf_n is given by Eq (4.4), which states that pf_n is the maximum shiftable load. The calculation of pf_n is schematically illustrated in Fig. 4.2.

Fig. 4.2 illustrates two possible charging scenarios for a typical EV whose parking time is longer than the time required for charging. Real charging load represents the energy that the EV consumes when parking; virtual charging load is the energy that the EV is parking but not consuming because the battery is already fully charged. In both scenarios, the real charging load can be shifted to the virtual charging load, which yields potential EV charging flexibility. In Fig. 4.2a, only part of the real charging load can be shifted to the virtual charging load, whereas all real charging load can be shifted to virtual charging load in scenarios illustrated in Fig. 4.2b. When only part of the real charging load can be shifted to the virtual charging load, the potential charging flexibility is given by the totality of the virtual charging load. Otherwise, the potential flexibility is restricted by the real charging load. For EVs with the required charging time less than the parking time, their potential charging flexibility is 0.

(3) Pay-as-Use Incentive Program

Unlike paying for all the potential flexibility in the BO program, the remuneration in the PAU program depends on effective flexibility. Hence, to calculate the payment in the PAU program, the unscheduled load profile for each EV must be identified. In the unscheduled charging scenario, the EV will charge at the maximum rate before reaching the battery capacity Cap_n^{ev} of EV m:

$$P_{m,t}^{us} = P_m^{max}, \left(SOC_{m,t-1} + \frac{P_m^{max} \Delta t}{Cap_m^{ev}} \right) \leq SOC_m^{max} \tag{4.5}$$

where m is the index for EVs in the PAU program. The unscheduled charging rate of the mth EV at time t is given by $P_{m,t}^{us}$, whose upper bound is P_m^{max}. The scheduling interval is given by Δt. $P_{m,t}^{us}$ with superscript 'us' refers to the charging power in the unscheduled charging scenario.

When the EV is about to be fully charged, it will charge at a rate such that the EV just reaches the maximum SOC:

$$P_{m,t}^{us} = \frac{\left(SOC_m^{max} - SOC_{m,t-1}^{max} \right) Cap_m^{ev}}{\Delta t}, \frac{P_m^{max} \Delta t}{Cap_m^{ev}} \geq SOC_m^{max} - SOC_{m,t-1} \tag{4.6}$$

After the EV is fully charged, the charging rate becomes 0 because discharging is not considered:

$$P_{m,t}^{us} = 0, SOC_{m,t-1} = SOC_m^{max} \tag{4.7}$$

As Eqs (4.5) – (4.7) are derived for unscheduled EV charging of the PAU program, they also apply to the BO program. After acquiring the unscheduled charging profile, the change in charging power can be obtained as the difference between the unscheduled charging power $P^{us}_{m,t}$ and the scheduled charging power $P^{s}_{m,t}$:

$$\Delta P_{m,t} = P^{s}_{m,t} - P^{us}_{m,t} \tag{4.8}$$

To avoid double remuneration, only the downward power change will be accounted for when calculating the incentive payment. Hence, the power change in the PAU program is divided into downward $\Delta P^{d}_{m,t}$ and upward$\Delta P^{u}_{m,t}$ changes:

$$\Delta P_{m,t} = \Delta P^{u}_{m,t} - \Delta P^{d}_{m,t} \tag{4.9}$$

$$\left[\Delta P^{u}_{m,t}, \Delta P^{d}_{m,t}\right] \geq 0 \tag{4.10}$$

Thus, the power changes are obtained as:

$$\Delta P^{u}_{m,t} - \Delta P^{d}_{m,t} = P^{s}_{m,t} - P^{us}_{m,t} \tag{4.11}$$

The flexibility calculation for the PAU program is schematically depicted in Fig. 4.3.

Fig. 4.3a shows the unscheduled (left) and scheduled (right) charging load profiles for a typical EV. Comparing the unscheduled load with the scheduled load, it is observed that only the charging loads between hours 9 and 13 are shifted to hours between 17 and 21, whereas the loads at hours 14, 15 and 16 remain unchanged. The load change result from the unscheduled charging scenario to the scheduled charging scenario is summarized in Fig. 4.3b, which shows that only the reduced load is counted as remunerable effective flexibility.

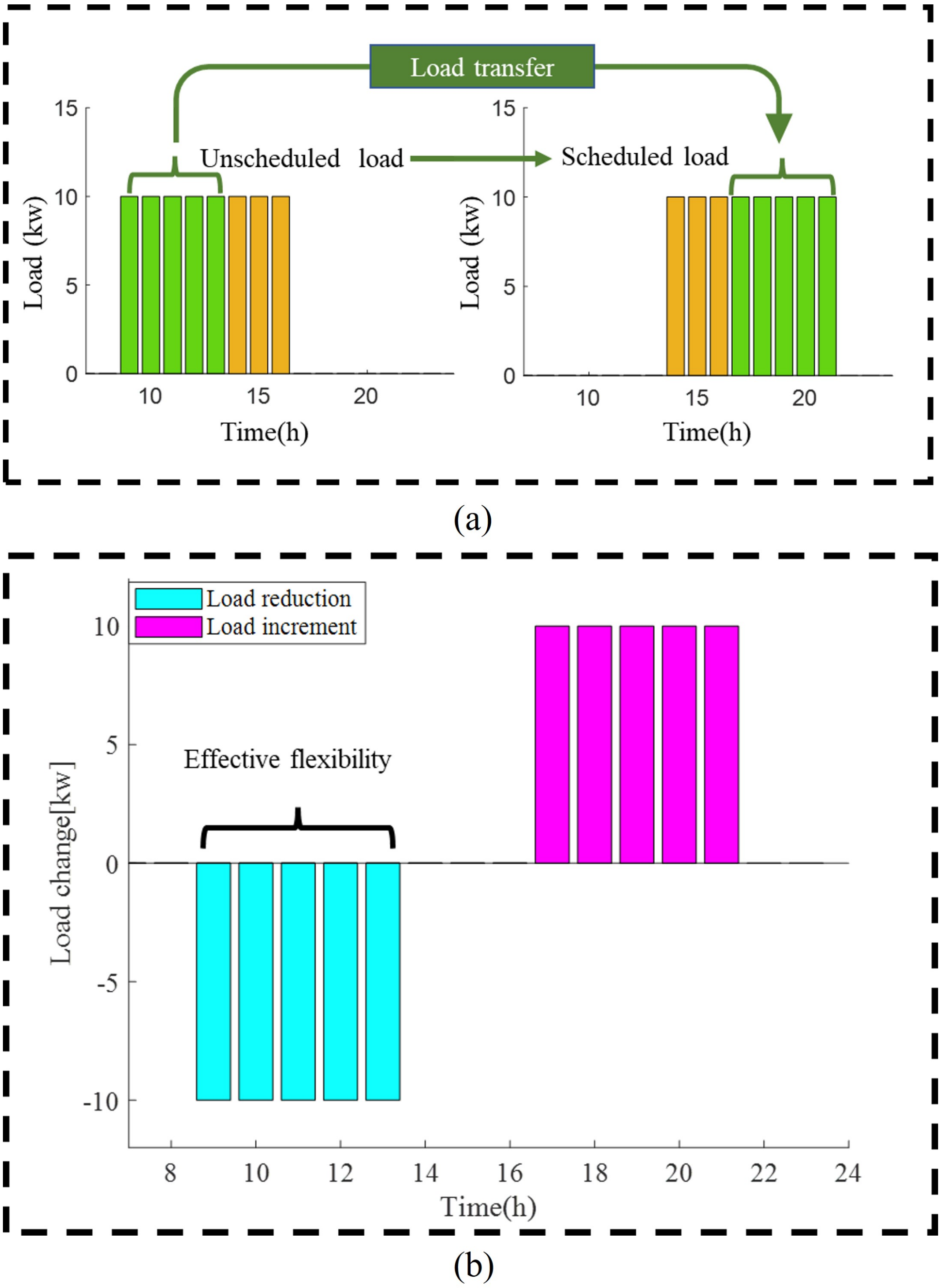

Figure 4.3: EV flexibility illustration in the pay-as-use program

(4) EV User Participation Status Decision

As the price threshold for authorizing the battery access right can vary among a large group of EV users, it is not likely that all the EVs will be involved in the demand response program. Instead, only EV users with minimum acceptable prices lower than the incentive prices are willing to sell their charging flexibility. Besides, the price for each unit of charging flexibility in each incentive program should be uniform to ensure fairness and consistency. Hence, the incentive prices must be determined before EV users can decide if they want to join the demand response program.

In the proposed hybrid incentive program, two prices need to be specified. In the BO program, the incentive price α represents the financial incentive paid to EV users for each unit of potential flexibility they can provide. In the PAU program, the incentive price β is the financial incentive paid to EV users for each unit of effective flexibility.

Once the incentive price information becomes available, the participation status of each EV can be determined through the following relationship:

$$y_n(\alpha - \gamma_n) \geq 0 \tag{4.12}$$

$$y_m(\beta - \gamma_m) \geq 0 \tag{4.13}$$

$$[y_n, y_m] \in (0, 1) \tag{4.14}$$

where γ_n and γ_m are the minimum acceptable prices for EV users to authorize their battery access right in the BO and PAU programs, respectively. Correspondingly, binary terms y_n and y_m are availability indicators for the battery access rights in the BO and PAU programs, respectively. As stated in (4.12) and (4.13), EV users will allow the charging station to control their EV charging rates only if the incentive price is higher than their minimum acceptable prices.

In real-life applications, the minimum acceptable prices of EV users depend on their specific features. Hence, the charging station needs to perform surveys of its consumers in order to determine the prices that would yield the best outcome.

4.3 Optimal Incentive Price Selection

From the charging station's perspective, higher incentive prices can encourage more EV users to share their charging flexibility, which allows the charging station to reduce the energy procurement cost. Meanwhile, the financial incentives paid to EV users will also increase due to uplifted incentive prices and a larger purchased flexibility volume. Hence, the selection of incentive prices α and β is of vital importance to the performance of the proposed hybrid incentive program.

To determine the optimal incentive price set (α, β) that will maximize the charging station's overall benefit, an optimal incentive price selection model is developed in this section. In the developed optimization model, the objective is to minimize the total cost from the wholesale energy market and the demand response program. Therefore, before presenting the optimal incentive price selection model, the incentive payment of EV users needs to be calculated. The payments of EV users are calculated as follows:

$$\omega_n^B = \alpha \cdot pf_n \tag{4.15}$$

$$\omega_m^P = \sum_t \frac{\beta \cdot \Delta P_{m,t}^d}{R} \tag{4.16}$$

where ω_n^B and ω_n^P are the incentive payments in the BO and PAU programs, respectively. The term R is the ratio between one hour and the scheduling resolution of the charging station.

After obtaining the incentive payments of EV users, the optimization problem can be formulated as:

$$\min_{\alpha,\beta,y_n,y_m,\Delta P_{n,t},\Delta P^u_{m,t},\Delta P^d_{m,t},P^M_t} \left\{ \sum_t \lambda_t P^M_t + \sum_n \omega^B_n y_n + \sum_m \omega^B_m y_m \right\} \tag{4.17}$$

s.t.

$$(4.2) - (4.7), (4.10) - (4.16) \tag{4.18}$$

$$\left(P^{us}_{n,t} + P^{us}_{m,t} + \Delta P_{n,t} + \Delta P^u_{m,t} - \Delta P^d_{m,t}\right) \Delta t = P^M_t \tag{4.19}$$

$$0 \leq P^{us}_{n,t} + \Delta P_{n,t} \leq P^{max}_n \tag{4.20}$$

$$-y_n P^{max}_n \leq \Delta P_{n,t} \leq y_n P^{max}_n \tag{4.21}$$

$$0 \leq P^{us}_{m,t} + \Delta P^u_{m,t} - \Delta P^d_{m,t} \leq P^{max}_m \tag{4.22}$$

$$\left[\Delta P^d_{m,t}, \Delta P^u_{m,t}\right] \leq y_m P^{max}_m \tag{4.23}$$

$$\sum_t \Delta P_{n,t} = 0 \tag{4.24}$$

$$\sum_t \left(\Delta P^u_{m,t} - \Delta P^d_{m,t}\right) = 0 \tag{4.25}$$

$$0 \leq \alpha \leq \overline{\alpha} \tag{4.26}$$

$$0 \leq \beta \leq \overline{\beta} \tag{4.27}$$

where λ_t and P^M_t represent the market-clearing price and energy purchased from the market at time t, respectively. The time interval for one charging scheduling period is given by Δt. The objective function contains the energy procurement cost and the incentive payments. Parameters $\overline{\alpha}$ and $\overline{\beta}$ are upper bounds for the incentive prices, which are selected as the highest minimum acceptable prices of EV users so as not to affect the optimality of the problem.

Constraint (4.19) is the power balance constraint. Constraints (4.20) – (4.23) represent the battery charging rate limitations under the EV participation status restrictions. Constraints (4.24) and (4.25) ensure that EV charging demands are satisfied across the scheduling horizon. Constraints (4.26) and (4.27) provide reasonable ranges for the incentive prices to reduce the searching domain and ensure problem convergence.

4.4 Proposed Solution Methodology

This section first provides a linearized form of the original problem by transforming the bilinear terms. Then, a distributed solution approach is developed based on the ADMM solution algorithm. To accelerate the convergence of the distributed solution approach, a penalty factor adaptive process is further proposed.

4.4.1 Problem Linearization

The proposed optimization model has bilinear terms $\beta \cdot \Delta P^{d}_{m,t}$ from the PAU program and $\alpha \cdot y_n$ from the BO program. Besides, the solution process for EV charging scheduling under large EV fleets is challenged by the curse of dimensionality issue. Hence, in this section, a linear reformulation of the original problem is provided first, then an ADMM-AP algorithm is developed to efficiently solve the reformulated problem for large EV fleets.

The bilinear term $\alpha \cdot y_n$ is the product of a bounded continuous variable α and a binary variable y_n. According to the method proposed in (Shabanzadeh, Sheikh-El-Eslami, and Haghifam 2017), this term can be modeled by introducing a new continuous variable ϑ^{B}_{n} and the following constraints:

$$\alpha \cdot y_n = \vartheta^{B}_{n} \tag{4.28}$$

$$\alpha - (1 - y_n)M \leq \vartheta^{B}_{n} \leq \alpha + (1 - y_n)M \tag{4.29}$$

$$-y_n M \leq \vartheta^{B}_{n} \leq y_n M \tag{4.30}$$

where M is a large enough positive constant.

Another bilinear term $\beta \cdot \Delta P^{d}_{m,t}$ is the product of two bounded continuous variables β and $\Delta P^{d}_{m,t}$. This term can be transformed into the product of a binary variable $y^{d}_{m,t}$, a continuous variable β, and a constant $P^{us}_{m,t}$ derived in (4.5) – (4.7). The transformation process is provided in Appendix 2. After the transformation, the original bilinear term $\beta \cdot \Delta P^{d}_{m,t}$ is equivalent to $\beta y^{d}_{m,t} P^{us}_{m,t}$. This new term $\beta y^{d}_{m,t} P^{us}_{m,t}$ can be modeled by using the same method as in (Shabanzadeh, Sheikh-El-Eslami, and Haghifam 2017).

The new term $\beta y^{d}_{m,t} P^{us}_{m,t}$ is the bilinear product of a bounded continuous variable β, a binary variable $y^d_{m,t}$, and a constant $P^{us}_{m,t}$. Similarly, the term $\beta y^d_{m,t} P^{us}_{m,t}$ can be modeled by introducing a new continuous variable $\vartheta^P_{m,t}$ and the following constraints:

$$\beta y^d_{m,t} P^{us}_{m,t} = \vartheta^P_{m,t} P^{us}_{m,t} \tag{4.31}$$

$$\beta - \left(1 - y^d_{m,t}\right) M \leq \vartheta^P_{m,t} \leq \beta + \left(1 + y^d_{m,t}\right) M \tag{4.32}$$

$$-y^d_{m,t} M \leq \vartheta^P_{m,t} \leq y^d_{m,t} M \tag{4.33}$$

where the bilinear term $\beta y^d_{m,t}$ is replaced by the auxiliary variable $\vartheta^P_{m,t}$ bounded by constraints (4.32) and (4.33).

Hence, the original problem can be reformulated as:

$$\min_{\alpha,\beta,y_n,y_m,\Delta P_{n,t},\Delta P^u_{m,t},\Delta P^d_{m,t},P^M_t,\vartheta^B_n,\vartheta^P_{m,t}} \left\{ \sum_n \vartheta^B_n \cdot pf_n + \sum_t \left[\frac{\sum_m \vartheta^P_{m,t} P^{us}_{m,t}}{R} + \lambda_t P^M_t \right] \right\} \tag{4.34}$$

s.t.

$$(4.18) - (4.33) \tag{4.35}$$

4.4.2 Distributed Solution Approach

As the numbers of price scenarios, as well as EVs, need to be large enough to obtain statistically significant results, the dimensional disaster in EV charging scheduling problem is hardly avoidable. To address this challenge, the original problem (4.34) – (4.35) is decomposed into a distributed form based on the ADMM algorithm. In the distributed problem, EVs are divided into different groups according to the date they park in the charging station. Specifically, EVs that are parked on the same day will be clustered within the same group. In the ADMM method, the primary problem is responsible for coordinating the optimal incentive prices from different groups. By using the scaled form of the ADMM method, the primary problem in the $(v+1)th$ iteration can be written as:

$$\min_{\alpha,\beta,y_n,y_m} \left\{ \begin{array}{c} \sum_n y_n \left(\alpha \cdot pf_n - CR_{n,v}\right) + \sum_m y_m \left(\beta \Delta P^d_{m,v} - CR_{m,v}\right) \\ + \sum_g \left[\left(\alpha - \alpha_{g,v}\right)^2 + \left(\beta - \beta_{g,v}\right)^2 \right] + \frac{\rho_{g,v}}{2} \left(\left\| \alpha - \alpha_{g,v} - A_{g,v} \right\|_2^2 + \left\| \beta - \beta_{g,v} - B_{g,v} \right\|_2^2 \right) \end{array} \right\} \tag{4.36}$$

s,t.

$$(4.2) - (4.4), (4.12) - (4.14) \tag{4.37}$$

$$\Delta P^d_{m,v} = \frac{1}{R} \sum_t \Delta P^d_{m,t,v} \tag{4.38}$$

$$CR_{n,v} = -\frac{1}{R} \sum_t \left(\Delta P_{n,t,v} \lambda_t\right) \tag{4.39}$$

$$CR_{m,v} = -\frac{1}{R} \sum_t \left(\Delta P^d_{m,t,v} - \Delta P^u_{m,t,v}\right) \lambda_t \tag{4.40}$$

$$\min\left\{\alpha_{g,v}\right\} \le \alpha \le \max\left\{\alpha_{g,v}\right\} \tag{4.41}$$

$$\min\{\beta_{g,v}\} \leq \beta \leq \max\{\beta_{g,v}\} \tag{4.42}$$

where $\Delta P^d_{m,v}$ is the total power reduction of the mth EV calculated in the vth iteration. The cost reductions $CR_{n,v}$ in the BO program and $CR_{m,v}$ in the PAU program are also calculated values obtained from the scheduling results of the secondary problems by using Eqs (4.39) and (4.40). The optimal incentive price set to be coordinated is represented by (α, β). Incentive price set $(\alpha_{g,v}, \beta_{g,v})$ gives the optimal values of the gth group obtained in the vth iteration. The term $\rho_{g,v}$ is the penalty for the gth group in the vth iteration. Terms $A_{g,v}$ and $B_{g,v}$ are scaled dual variables in the ADMM method. The ranges of the coordinated optimal incentive prices are given by Eqs (4.41) and (4.42). The bilinear terms in (4.36) are handled in a similar way as (4.28) - (4.30).

Upon receiving the optimized values of $\alpha_{v+1}, \beta_{v+1}$ from the primary problem, each group re-calculates the incentive prices using the secondary problem that considers the deviation penalty from the coordinated optimal incentive prices:

$$\min_{\alpha,\beta,y_n,y_m} \left\{ \begin{array}{c} \sum_n \vartheta^B_n \cdot pf_n + \sum_t \left[\frac{\sum_m \vartheta^P_{m,t} P^{us}_{m,t}}{R} + \lambda_t P^M_t \right] + \sum_g \left[(\alpha - \alpha_{g,v})^2 + (\beta - \beta_{g,v})^2 \right] \\ + \frac{\rho_{g,v}}{2} \left(\|\alpha - \alpha_{g,v} - A_{g,v}\|_2^2 + \|\beta - \beta_{g,v} - B_{g,v}\|_2^2 \right) \end{array} \right\} \tag{4.43}$$

s.t.

$$(4.18) - (4.33) \tag{4.44}$$

where α_g and β_g are incentive prices to be optimized by group g. Notably, the penalty terms are not included in the secondary problems in the first iteration.

By solving the primary and secondary problems, the scaled dual variables (A_{v+1}, B_{v+1}) are updated:

$$A_{g,v+1} = A_{g,v} + \alpha_{v+1} - \alpha_{g,v+1} \tag{4.45}$$

$$B_{g,v+1} = B_{g,v} + \beta_{v+1} - \beta_{g,v+1} \tag{4.46}$$

The convergence of the problem is declared when the change in scaled dual variables falls below a certain criterion:

$$\sqrt{\|A_{v+1} - A_v\|_2^2 + \|B_{v+1} - B_v\|_2^2} \leq \varepsilon_{admm} \tag{4.47}$$

4.4.3 Adaptive Penalty Factors

The conventional ADMM method applies the same penalty factors to all groups, which cannot reflect different qualities of the obtained incentive price sets. To accelerate the convergence of the solution process, an adaptive algorithm is proposed in this chapter to adjust the penalty factors at the early stages of the consensus optimization problem. The proposed adaptive algorithm assigns heavier penalties to price sets with better qualities to increase their significance in the coordination process. The quality of each price set is evaluated by calculating the charging station's final gain $FG_{g,v}$ using that price set:

$$FG_{g,v} = \sum_n y_n \left(\alpha_{g,v} \cdot pf_n - CR_{n,v}\right) + \sum_m y_m \left(\beta_{g,v} \Delta P_{m,v}^d - CR_{m,v}\right) \tag{4.48}$$

The first and second terms represent the charging station's gains from the BO and PAU programs, respectively. In (4.48), the values of $\left\{\alpha_{g,v}, \beta_{g,v}, pf_n, \Delta P_{m,v}^d, CR_{n,v}, CR_{m,v}\right\}$ are optimized results of the secondary problems for each group. Besides, the participation status (y_n, y_m) in the BO and PAU programs can be determined through equations (4.12) – (4.14). Hence, the charging station's gain under each group incentive price set can be obtained from a simple calculation process that only takes negligible computation time.

After obtaining the qualities of the price sets, the adaptive weight $\varphi_{g,v}$ of each group is acquired from (4.49) – (4.51):

$$FG_v^{max} = \max \{FG_{g,v}, g \in G\} \tag{4.49}$$

$$FG_v^{min} = \min \{FG_{g,v}, g \in G\} \tag{4.50}$$

$$\varphi_{g,v} = \frac{FG_{g,v} - FG_v^{min}}{FG_{g,v}^{max} - FG_v^{min}} \tag{4.51}$$

where FG_v^{max} and FG_v^{min} denote the charging station's maximum and minimum gains under different price sets in the vth iteration. The adaptive weight $\varphi_{g,v}$ is calculated based on the quality of each group by using (4.51).

Denote ρ_0 as the initial penalty factor, the penalty factors for different groups in each iteration can be acquired by:

$$\begin{cases} \rho_{g,v+1} = \rho_0 \left(1 + \varphi_{g,v}\right), & \forall v \leq v_{max} \\ \rho_{g,v+1} = \rho_0, & \forall v > v_{max} \end{cases} \tag{4.52}$$

where v_{max} is the iteration threshold, after which the adaptive update of the penalty factors is terminated

4.4.4 Convergence Discussion

In the early stages of the consensus optimization problem, the optimized incentive prices among different groups deviate hugely from each other, resulting in large quality variations. By using the adaptive algorithm, the qualities of different price sets are accounted for to accelerate the convergence. After some iterations, such quality differences become insignificant. Hence, the adaptive update of penalty factors is not needed, and the subsequent iterations work as the standard ADMM method to guarantee the convergence of the solution process.

In this chapter, an event-triggered mechanism is proposed to determine the timing v_{max} for switching from the pre-event stage to the post-event stage without requiring pre-knowledge on the problem convergence speed. The switch between stages occurs when the maximum quality difference among the price sets falls below a given threshold:

$$\frac{FG_v^{max} - FG_v^{min}}{FG_v^{min}} \leq \varepsilon_{adaptive} \tag{4.53}$$

After the switch of stage, the adaptive update of penalty factors is terminated, and the solution process enters the post-event stage for convergence. To this end, the ADMM-AP algorithm can be summarized as follows:

Algorithm 4-1 Solution algorithm based on ADMM-AP

1: **Initialization** $\varepsilon_{admm} = 0.00001$, $\rho_0 = 100$, $\varepsilon_{adaptive} = 0.01$

2: **While** (4.47) is **False**, $v \leftarrow v + 1$ **do**

3: **Obtain** $\rho_{g,v+1}$ for each group from (4.48) – (4.53)

4: **Solve** (4.36) – (4.42) and **Derive** $(\alpha_{v+1}, \beta_{v+1})$

5: **Solve** Problem (4.43) – (4.44) for each group and **Derive** $(\alpha_{g,v+1}, \beta_{g,v+1})$.

6: **Update** A_{v+1} and B_{v+1} using (4.45) – (4.46)

7: **End While**

8: **Return** $(\alpha_{v+1}, \beta_{v+1})$

4.5 Case Study

This section provides the simulation results and discussions about the proposed EV energy management methods for an EV charging station.

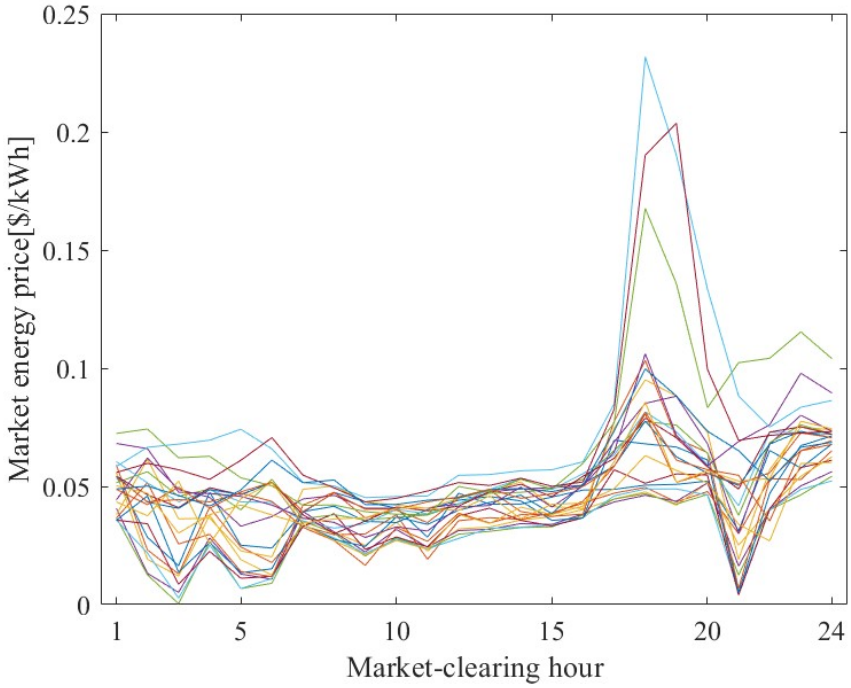

Figure 4.4: Selected market energy price scenarios for 24 operating days.

4.5.1 Experiment Setup

The case study considers 24 operating days that are uniformly distributed over the year 2020. The price data for 24 days from the Nord Pool UK day-ahead market (*Day Ahead Auction Prices* 2019) is shown in Fig. 4.4.

Four typical EV models provided in Table 4.2 are selected to generate EV charging scenarios through the Monte-Carlo-Simulation method introduced in (Su, Lie, and Zamora 2019). For each EV, the charging efficiency is assumed to be 0.95 and the maximum SOC is 0.95 (Wang et al. 2022c). A total of 2,400 EV charging scenarios are generated and evenly distributed to the selected 24 operating days. Among the 2,400 EV charging scenarios, it is assumed that half of the EV users prefer the BO program and the rest prefer the PAU program. In the BO program, EV users' minimum acceptable prices are assumed to follow the normal distribution with mean and variance equal to 25% of the average energy market price. Since the PAU incentive is risker than the BO incentive, the minimum acceptable prices for EV users in the PAU program are assumed to be 50% higher than the BO programs. The scheduling resolution of the charging station is set to be 15 minutes (Saner, Trivedi, and Srinivasan 2022).

Table 4.2: EV model parameters

Model	Tesla model Y	Tesla Model 3	BYD Qin plus	Volkswagen ID.4
Capacity	66kWh	62kWh	57kWh	62kWh
Maximum charging rate	11.5kW	11.5kW	11kW	11kW

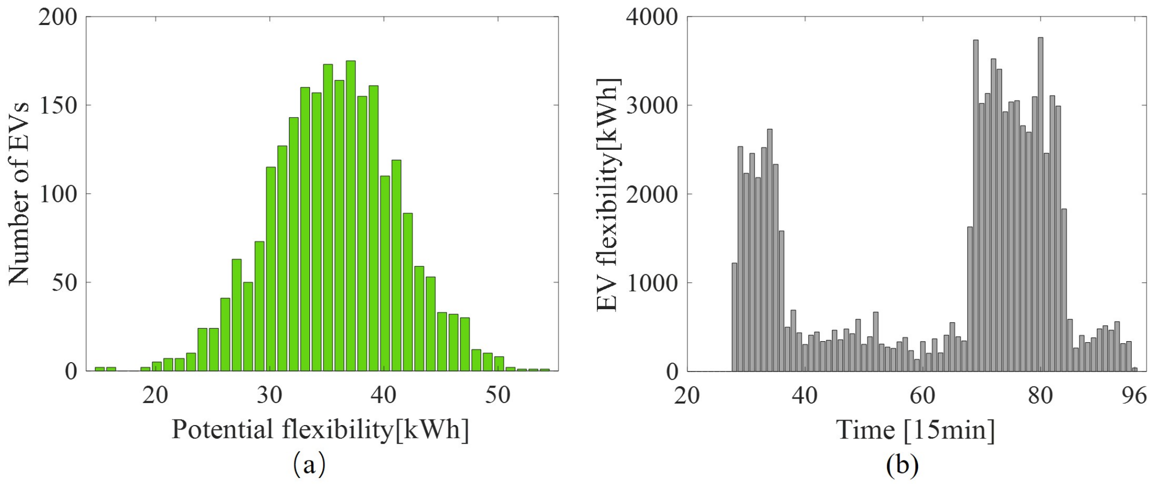

Figure 4.5: Flexibility distributions for (a) different flexibility amounts and (b) different EV arrival time.

4.5.2 Results and Discussions

The potential flexibility distributions of the generated EV charging scenarios are presented in Fig. 4.5 regarding different flexibility amounts and EV arrival times. The distribution of EV charging flexibility amount is provided in Fig. 4.5a, which shows that most EVs can provide an amount of charging energy flexibility between 30 kWh and 45 kWh. Given the battery capacities shown in Table 4.2, it can be concluded that a considerable amount of the EV charging demand in this chapter can be treated as flexible loads. The potential flexibility distribution regarding different EV arrival times is shown in Fig. 4.5b. The peaks in Fig. 4.5b correspond to the time windows when most EVs come and charge, one is from hour 8 to hour 9, and the other is between hours 18 and 21. Especially, the second peak covers the price spikes shown in Fig. 4.4, which makes this part of flexibility highly valuable. Hence, the amount and value of EV charging flexibility make it promising for supporting the economic operation of the charging station.

Fig. 4.6a presents the optimal incentive price selection results together with the minimum acceptable price distributions. By considering the typical price scenarios over a year, the incentive

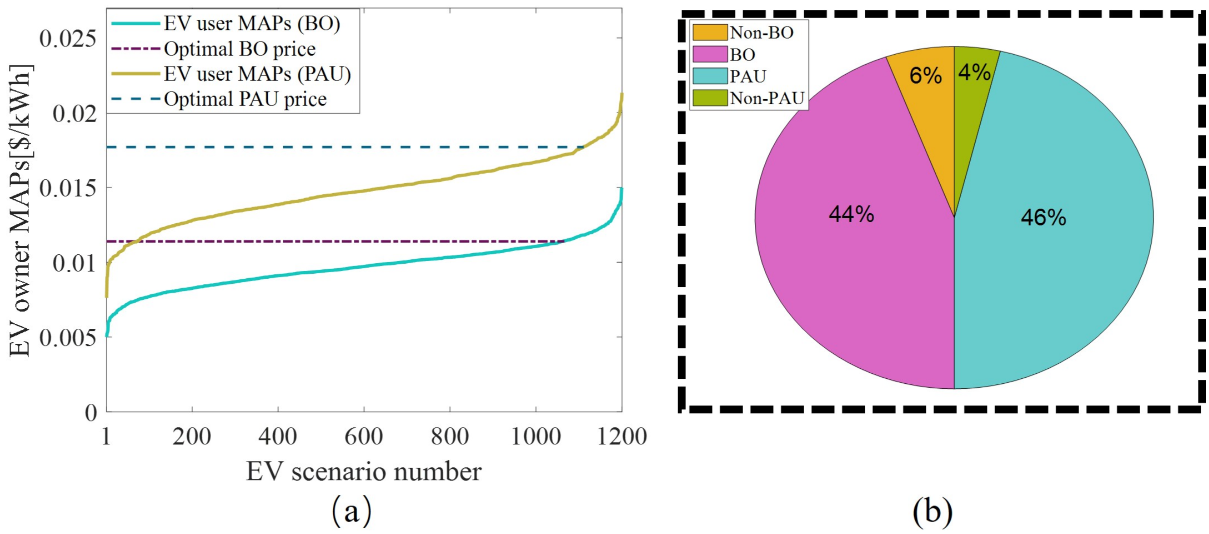

Figure 4.6: (a) EV user minimum acceptable prices and optimized incentive prices, (b) participation results

prices that can maximize the charging station's benefit are selected to be 0.0114 $\$/kWh$ and 0.0177 $\$/kWh$ in the BO and PAU programs, respectively. In the PAU program, all the remunerated charging flexibility is effective for reducing the energy procurement cost of the charging station. However, in the BO program, the charging station must pay for potential charging flexibility that may not be useful. Hence, the BO incentive price is lower than the PAU incentive price. Fig. 4.6b shows the participation status of EV users. Under the selected incentive prices, 44% and 46% of EV users are involved in the BO and PAU programs, respectively. In total, 90% of EV users are incentivized to offer their EV charging energy flexibility.

In the case study, 1,066 EV users are participating in the BO program. Because the BO program remunerates EV users based on their potential charging flexibility, all the participating users are paid even if their charging flexibility is not utilized during the charging scheduling. Thus, the average incentive payment is \$0.42 per EV user in the BO program. On the other hand, 1,113 EV users are participating in the PAU program. However, since the PAU program only considers effective charging flexibility, some EV users are not rewarded because their charging flexibility is not used during the charging scheduling. Consequently, only 762 EV users are paid in the PAU program with an average incentive payment of \$0.57 per EV user, and a total of 351 EV users participating in the PAU program are not rewarded at all. From the EV users' perspective, this result implies that the PAU program is a more risky program but with a higher average return. Hence, for conservative EV users, the BO program can be a better

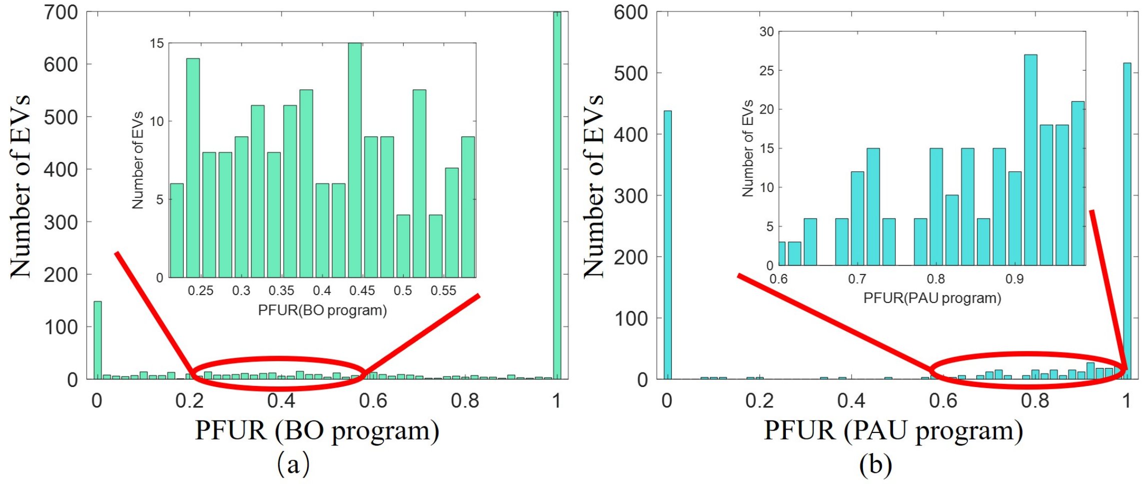

Figure 4.7: PFUR distribution for individual EV users in (a) the BO program and (b) the PAU program.

choice because it offers a stable return. For risk-seeking EV users, the PAU program may be preferable because it has a higher average return.

An important criterion to assess the incentive programs is the potential flexibility utilization ratio (PFUR), which can reflect the effectiveness of incentive programs in motivating the utilization of potential charging flexibility:

$$PFUR = \frac{Effective\_Flexibility(kWh)}{Potential\_Flexibility(kWh)} \tag{4.54}$$

In the optimization result, the PFUR for individual EVs in both the BO and PAU programs are presented in Fig. 4.7. The PFUR distribution for EVs in the BO program is shown in Fig. 4.7a. The number of EVs whose potential flexibility is not utilized at all is 134, which is in line with the participation status presented in Fig. 4.6b. In the BO program, the PFUR for 699 EVs reaches 100%, which implies that all their potential charging flexibility is utilized to reduce the energy procurement cost. It is also shown that the PFURs for some EVs are distributed between 0% and 100%, indicating that their potential flexibility is not fully utilized. Since utilizing the purchased potential flexibility will not induce extra costs to the charging station, the only reason for this result is that some potential flexibility is useless in terms of reducing the charging station's energy procurement cost. In total, 71.05% (31,328 kWh out of 44,091 kWh) of the potential flexibility is used by the charging station through the BO incentive program.

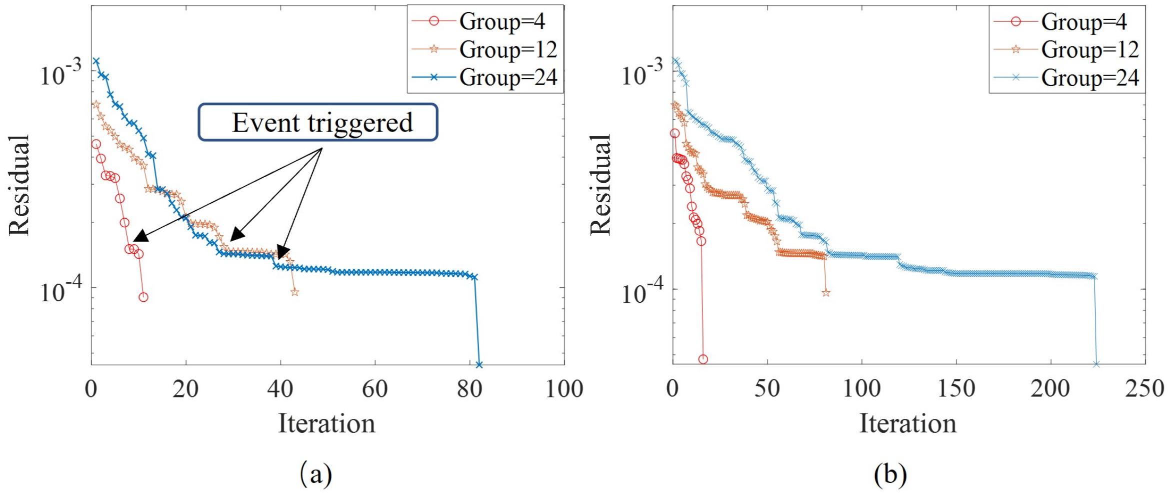

Figure 4.8: Convergence rates of (a) the proposed ADMM-AP algorithm and (b) the conventional ADMM algorithm

Fig. 4.7b illustrates the PFUR distribution for EVs in the PAU program. Similar to the BO program, two peaks are observed at PFUR equals to 0% and 100%, respectively. However, the number of EVs whose potential flexibility is not utilized is 438, which exceeds the number of EVs that are not selected in the PAU program (87 EVs). This is because the utilization of charging flexibility in the PAU program will lead to extra costs. The utilization of charging flexibility depends on the competing result of the flexibility price and energy bill reduction. Hence, though some EVs are involved in the PAU program, their flexibility is not utilized because the reduced energy procurement cost cannot cover the incentive payment. In the PAU program, there are also some EVs with PFUR distributed between 0% and 100%. The reason for this situation is twofold, one is that some flexibility cannot be used to reduce the energy cost, and the other is that the cost of utilizing some flexibility is larger than the benefit. Overall, 59.06% (25,072 kWh out of 42,452 kWh) of the potential EV charging flexibility is deployed through the PAU incentive program.

The convergence rates of the proposed ADMM-AP and the conventional ADMM approaches using different numbers of groups are shown in Fig. 4.8. It can be seen that the convergence speed of the proposed ADMM-AP algorithm becomes more accelerated as the number of groups increases. This is due to the fact that a larger number of groups leads to larger variations of EV charging information and market price data among different groups, and hence reflecting the quality of different price sets becomes more important in the algorithm design.

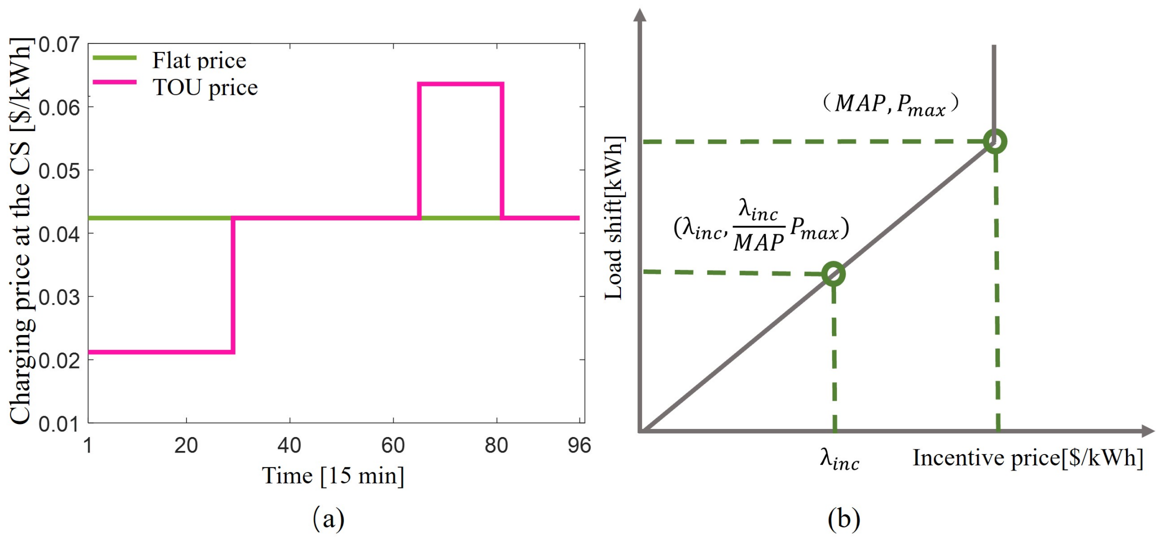

Figure 4.9: (a) Charging prices at the charging station. (b) EV response curve in the transactive control program.

4.5.3 Comparative Case Study

To demonstrate the performance of the proposed hybrid incentive program, it is compared with the time-of-use program and transactive control program in this subsection. In the comparative case studies, typical day price data from the Nord Pool market is used to evaluate these incentive programs. The flat and time-of-use prices (*TIDE: Take control of your energy bills the smart way* 2022) at the charging station are presented in Fig. 4.9a. In the proposed hybrid incentive program, EV users with minimum acceptable prices lower than the incentive prices (i.e., 0.0114 $\$/kWh$ in the BO program and 0.0177 $\$/kWh$ in the PAU program) will be involved in the demand response program. In the time-of-use program, EV users with minimum acceptable prices lower than the peak-flat-valley price differences will participate in the demand response program. In the transactive control program, the charging station determines the price signals to shift EV charging load based on the relationship between the load change and incentive price signal λ_{inc}, which is illustrated in Fig. 4.9b (Liu et al. 2018). The comparative cases are tested using 200 EV charging scenarios shown in Fig. 4.10.

The energy market price and net load change in the time-of-use program are provided in Fig. 4.11, in which one can observe that the load is only shifted from hours between 16 and 24 to hours between 1 to 4 of the next day. No load shift is observed in other periods of the day because EV users shift their charging load based on the fixed time-of-use price, which cannot accurately reflect the short-term market price fluctuations. Notably, in some periods, there are

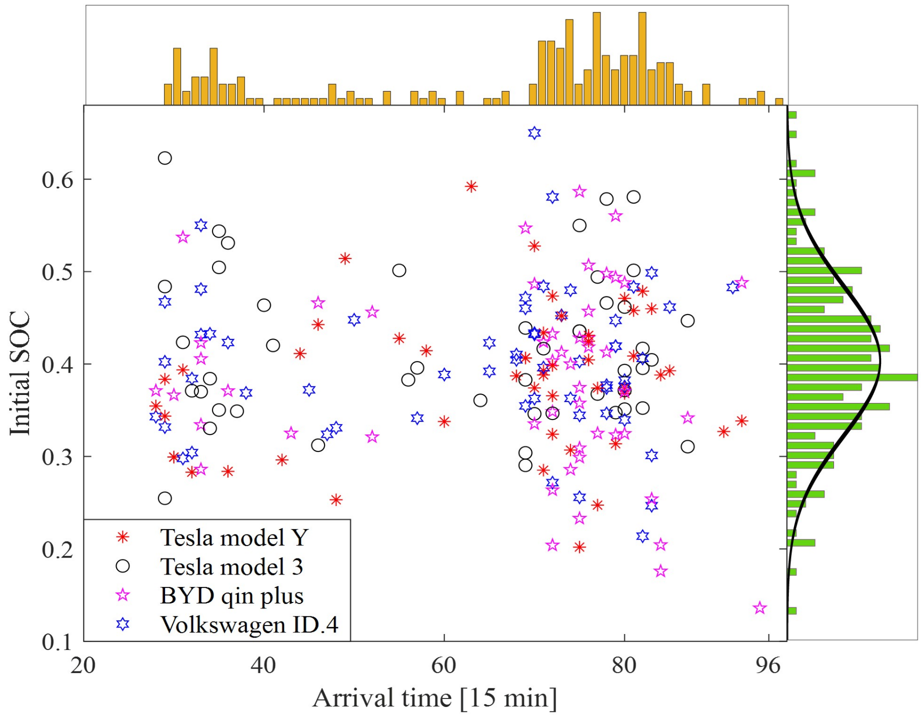

Figure 4.10: 200 EV charging scenarios.

both loads shifted in from higher price hours and loads shifted out to lower price hours, which cancel each other in the net load change result. Hence, the net load change is less than the total utilized charging flexibility.

In the time-of-use program, the charging station's revenue and energy bill for charging the EVs are \$260.90 and \$227.46, respectively. Compared to the unscheduled charging scenario, the charging station's revenue and energy procurement cost have been reduced by \$44.95 and \$65.84, respectively. In total, the charging station's profit is increased by \$20.89 (from \$12.55 to \$33.44). Meanwhile, by shifting the charging load in the time-of-use program, EV users' cost is reduced by \$44.95.

The net load change and optimized incentive price signals in the transactive control program are shown in Fig. 4.12. Compared to the load shift in the time-of-use program, the load change in the transactive control program can more accurately capture the market price variations. For instance, in the transactive control program, the load increment is more concentrated at hours 2 and 3, which have lower energy prices. Also, the transactive control program shifts loads from high-price hours (10 to 14) to low-price hours (15 to 17), whereas the time-of-use program does not react to the price differences during this period.

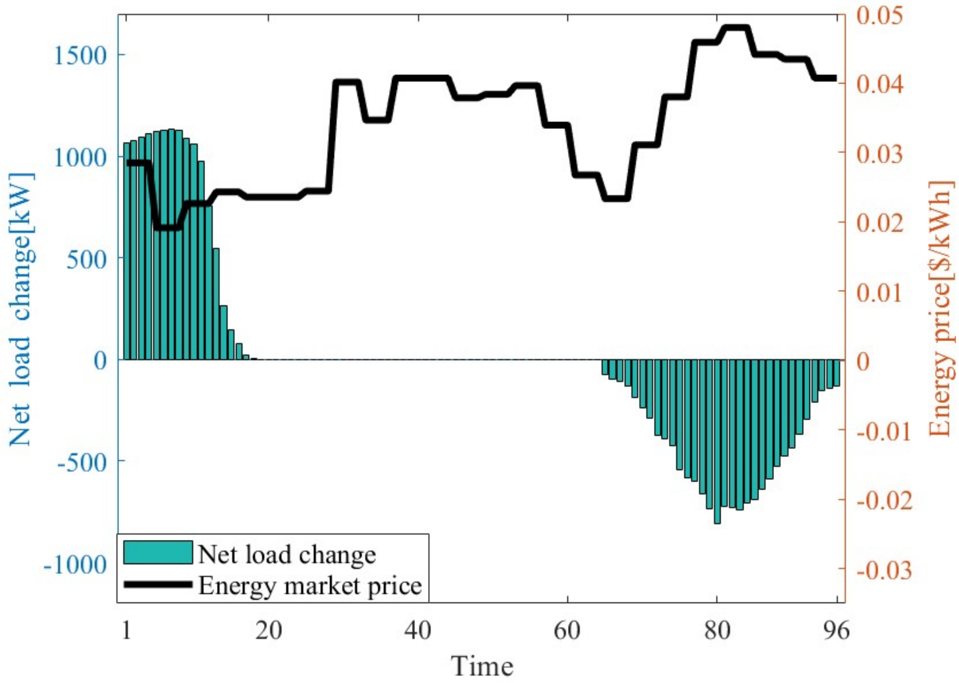

Figure 4.11: Load shift results in the time-of-use pricing program

When the market price is high, the charging station uses high incentive prices to shift the EV charging load. At low-price hours, to motivate EV users to charge at full power, the incentive prices can be very low or even zero, such as hours 2 to 7.

In the transactive control program, the charging station pays $25.06 for utilizing the charging flexibility, which reduces the energy procurement cost by $57.15. In total, the charging station's profit is increased by $32.09 (from $12.55 to $44.64) compared to the unscheduled charging scenario. For EV users, their charging fee is reduced by $25.06 due to the incentive payment.

The net load shift result in the proposed hybrid incentive program is presented in Fig. 4.13. In the BO program, the charging load is shifted from high-price hours to low-price hours even if the price differences are small, which can maximize the charging station's gain because utilizing the charging flexibility in the BO program will not induce extra costs. In the PAU program, because shifting the load can bring extra incentive costs, the charging load is only shifted between hours with large price differences (e.g., price differences between hours 18 to 24 and hours 2 to 3) to be profitable.

By applying the proposed hybrid incentive program, the charging station's electricity bill is reduced by $91.45. The incentive payments in the BO and PAU programs are $37.75 and $31.11, respectively. Overall, the charging station's profit is increased by $22.59 compared to

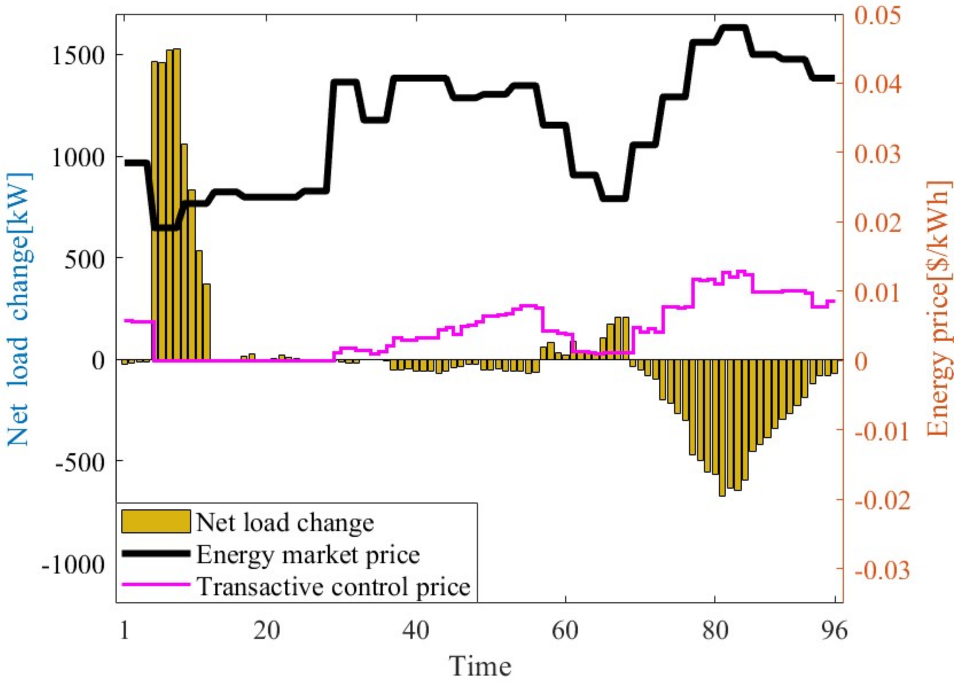

Figure 4.12: Load shift results in the transactive control program

the unscheduled charging scenario. For EV users, their charging fee is significantly reduced by $68.86 from the proposed hybrid incentive program.

The performances of the unscheduled charging scenario and investigated incentive programs are all summarized in Table 4.3. Among the investigated programs, the proposed hybrid incentive program achieves the smallest EV users' cost, which is reduced by 22.51% compared to the unscheduled charging scenario (from $305.85 to $236.99). Hence, the proposed program is the most attractive program for EV users. It also reduces 31.18% of wholesale market energy procurement cost for the charging station (from $293.30 to $201.85), which is more than other programs. Among the investigated incentive programs, the proposed hybrid incentive program has the largest PFUR of EVs, which confirms that it is the most efficient program in encouraging the utilization of EV charging flexibility and makes it more attractive to the power system. As a simple and consistent incentive program, the controllability of the proposed hybrid incentive program is much better than the time-of-use program. Though the CI of the transactive control program is higher than the proposed hybrid incentive program, it has however sacrificed simplicity and consistency.

The charging station's profit obtained from the proposed hybrid incentive program is higher than the time-of-use program and lower than the transactive control program. The better

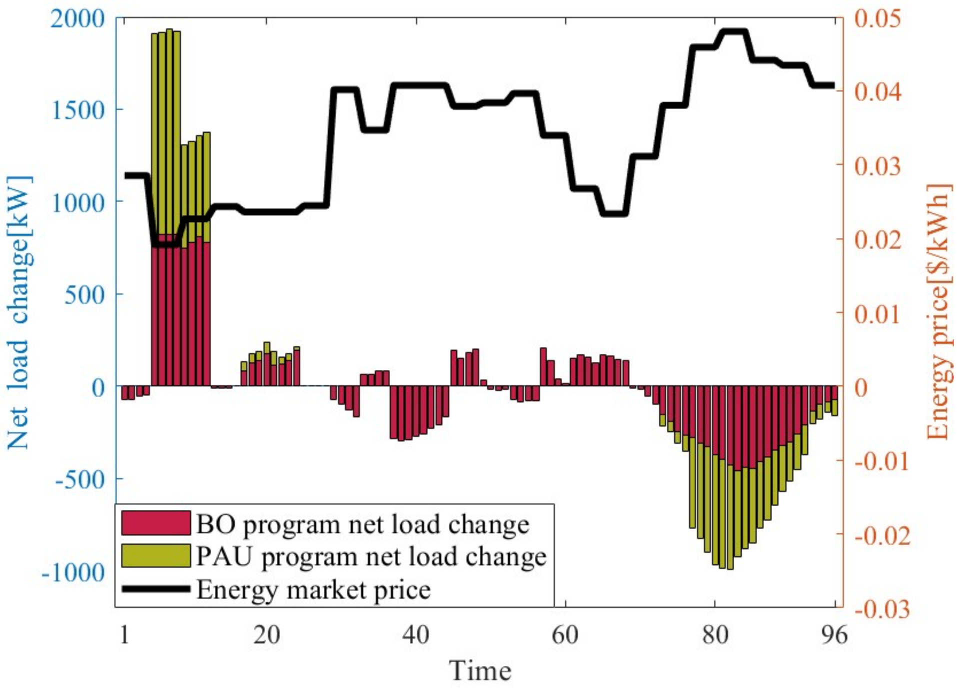

Figure 4.13: Load shift results in the proposed hybrid incentive program.

Table 4.3: Scheduling results

	Charging station profit [$]	EV user cost [$]	Market bill [$]	CI [$/$kWh$]	PFUR(%)
Unscheduled charging	12.55	305.85	293.30	0	0
Transactive control	44.64	280.79	236.15	0.0225	35.50
TOU program	33.44	260.90	227.46	0.0183	50.25
Proposed program	35.14	236.99	201.85	0.0200	64.13

profitability of the transactive control program comes from the adjustability of flexibility prices. Notably, the charging station's profits shown in Table 4.3 are obtained under the assumption that the numbers of EVs participating in the incentive programs are all the same. However, compared to the transactive control program, the proposed hybrid incentive program is simpler, more consistent, and less costly to EV users. Hence, it is very likely that a charging station adopting the proposed hybrid incentive program can attract more EVs than a charging station applying the transactive control program, which can potentially increase the charging station's profit.

In summary, the proposed hybrid incentive program is consistent and simple for EV users to participate. Meanwhile, the proposed hybrid incentive program can minimize the potential restrictions and impacts on EV users' daily plans and charging costs. Thus, the proposed hybrid incentive program can be a highly attractive and practical program for real-world EV users that are willing to participate in the demand response programs. Besides, the high potential profitability feature of the proposed hybrid incentive program makes it also attractive to the charging stations facing volatile electricity prices. Hence, the proposed hybrid incentive program has great potential for practical implementation.

Notably, to avoid disturbances of uncertain factors, deterministic price and EV charging scenarios are used in the case studies to compare the proposed hybrid incentive program with existing methods. However, uncertainties in the variable market price and the EV charging demand are inevitable in real-world applications. These uncertainties may have several impacts on charging station operations. Firstly, in the day-ahead scheduling stage, to consider the price and EV charging demand uncertainties, some uncertainty handling techniques such as stochastic and robust optimization approaches are required to determine the energy procurement in the wholesale market. Secondly, due to the information gap between the forecast and real EV charging demand, the real-time operational stage needs to simultaneously consider the deviation penalty and price differences. The uncertainty problem in EV charging demand and electricity prices will be comprehensively considered in Chapter 5, and the methodologies for handling the uncertainties will also be discussed.

4.6 Chapter Summary

This chapter has proposed a novel hybrid incentive program for motivating EV users to share their EV charging flexibility. The proposed hybrid incentive program combines the advantages of both the static and dynamic incentive programs, making it simple and consistent for EV users, as well as controllable for the charging station. To determine the incentive prices, an optimal incentive price selection model is developed in this chapter. Because large EV fleets are involved in the optimization model, an improved ADMM algorithm with adaptive penalties is proposed to efficiently solve the incentive price selection problem.

The proposed hybrid incentive program is compared with the time-of-use and transactive control programs using real-world price data. The numerical results confirm that the proposed hybrid incentive program is highly efficient in cutting down the charging station's energy market bill, reducing EV users' charging fees, and encouraging the utilization of EV charging flexibility. The proposed hybrid incentive program has superior controllability compared to the time-of-use program while maintaining simplicity and consistency. Though the transactive control program is more controllable than the proposed hybrid dynamic incentive program, it is more demanding for EV users in order to participate. The charging station's profit is also improved considerably by applying the proposed hybrid incentive program. Although the improvement is not as significant as the transactive control program, the proposed hybrid incentive program is more attractive to EV users, which may further increase the charging station's profit.

In this chapter, the energy management strategy of EVs is considered separately from other DERs (e.g., renewable energy resources and thermal generators), this can undermine the functionality of EVs in providing energy flexibility to handle uncertainties. To further unleash the potential of EV energy flexibility, the next chapter will integrate EVs into the VPP operation via EV charging stations. Besides, the EV charging station operation strategy is formulated as a deterministic optimization problem in this chapter. To make the proposed method more practical, uncertainties including EV charging demand and market prices will be comprehensively considered in the next chapter.

Chapter 5

VPP Operation Considering EV Charging Stations

In chapter 3, a VPP operation strategy for managing renewable generation resources and thermal generators to maximize the financial benefits in the electricity market environment is introduced. Then, chapter 4 provides an energy management method for EV charging stations to encourage EV users and optimally schedule EV energy. Based on the methods proposed in chapters 3 and 4, this chapter further proposes a mutually beneficial framework for a VPP and multiple EV charging stations to coordinate the energy scheduling of renewable energy resources, thermal generators, and EVs via the cooperative operation between the VPP and EV charging stations.

5.1 Chapter Introduction

The growing concerns about climate change are boosting the worldwide decarbonization trend (Zhang and Hredzak 2020). To achieve cleaner production and more efficient energy utilization, the VPP (Naval and Yusta 2021) research and EV (Wu et al. 2022) research have attracted much attention over the past years.

To further unleash the potential of VPPs and EVs in supporting sustainable developments, researchers have made pioneering efforts in integrating EV charging scheduling into the VPP operation (Yang and Zhang 2021). In the literature, EVs are normally used as energy storage that can be directly managed by the VPP operator to strengthen the VPP performance. For example, to enhance the VPP power quality, the energy flexibility of EVs is controlled by the VPP to smooth out the energy fluctuations of renewable generators in (Abbasi et al. 2019) and (Ju et al. 2016b). Besides, to improve the VPP profitability, the VPP operator can utilize the EV energy flexibility to compensate for energy deviations stemming from various uncertain factors, such as in (Shayegan-Rad, Badri, and Zangeneh 2017; Vasirani et al. 2013; Sheidaei and Ahmarinejad 2020; Alahyari, Ehsan, and Mousavizadeh 2019; Sadeghi et al. 2021; Yang et al. 2020a).

Existing research has made remarkable progress in integrating EVs into the VPP operation. However, most proposals assume the same ownership for both the VPP and EV charging facilities and little has been done on addressing the challenges when they are owned by different stakeholders. In real-world applications, public charging stations are the major EV charging facility owners (Ministry 2021). charging stations can also act as natural aggregators for EV energy scheduling because they can deal with a greater number of charging piles than individual household charger owners. Hence, some early attempts have been made to incorporate charging stations into the VPP operation.

In (Behi et al. 2021), a VPP comprising dwellings, renewables, energy storage systems, and a charging station is investigated. However, the VPP considered in (Behi et al. 2021) owns the charging station and gives direct dispatching signals to control the charging station operation. In (Zhou et al. 2020), a VPP composed of renewables and a charging station is considered. The work in (Zhou et al. 2020) also assumes that the VPP and charging station have the same interest and there is a central control unit to coordinate the charging station operation with other VPP components. In (Wang et al. 2022d), the authors considered a VPP with thermal generators, renewables, and energy storage. A self-interested charging station is also considered in (Wang et al. 2022d), and the interactions between the VPP and charging station are modeled by using a Stackelberg game framework. In (Fan et al. 2020), a VPP containing distributed generation and a self-interested charging station is investigated. The charging station operation in (Fan et al. 2020) is affected by the VPP price signals. Hence, the VPP in (Fan et al. 2020) can set different prices to indirectly adjust the charging load of the charging station in (Fan et al. 2020). Though (Wang et al. 2022d; Fan et al. 2020) considered VPP and charging stations with different ownerships, the charging stations in (Wang et al. 2022d; Fan et al. 2020) can only passively respond to VPP price signals instead of proactively interacting with the VPP operator, which can weaken the functionality of EVs as energy buffers. To address this issue and allow proactive interactions between the VPP and charging stations, this chapter proposes a mutually beneficial operation framework for VPP-Charging stations (VPP-CSs) systems consisting of a distributed generator-based VPP and multiple charging stations.

The proposed mutually beneficial VPP-CSs operation framework includes day-ahead offering and real-time balancing models. In the day-ahead stage, charging stations schedule their energy procurements to satisfy the expected EV charging demand under both the EV charging demand and market price uncertainties. After charging stations complete their energy scheduling, the VPP collects charging station energy procurement plans to generate the aggregated day-ahead energy market offering strategy considering the price and renewable uncertainties. In the real-time stage, the VPP and charging stations coordinately schedule the generator generations and EV charging plans to compensate for energy deviations stemming from forecast errors.

The day-ahead offering and real-time balancing models in the proposed operation framework are meant to maximize the total benefit of the VPP-CSs system. To maximize the total benefit of the VPP-CSs system, EV energy flexibility is a crucial solution to mitigate the negative impacts of forecast errors. A key enabler of utilizing EV energy flexibility is EV user cooperation, which directly affects the regulation capability of charging stations. When no incentives are provided to change the charging behaviors, EV users tend to recharge their EVs as quickly as possible to mitigate range anxieties (Chung et al. 2018), leaving no EV energy flexibility for the VPP-CSs system. Hence, the problem of how to encourage EV users to respond to control signals from charging stations awaits to be addressed.

As discussed in chapter 4, previous incentivizing methods can be roughly classified as static and dynamic methods. The static incentive programs have low incentive signal update frequency. That is, the incentive signals will remain effective for a relatively long time in static programs. Typical static incentive programs for EV users include time-of-use pricing and critical peak pricing. In (Su, Lie, and Zamora 2020; Dubey et al. 2015; Song, Shangguan, and Li 2021), the time-of-use pricing program is used to shift the EV charging load from high-price periods to low-price periods. In (Sadati et al. 2019; Sheidaei and Ahmarinejad 2020), the time-of-use and critical peak pricing programs are jointly applied to affect EV user charging behavior. As compared to static incentive programs, dynamic incentive programs update incentive signals more frequently to handle short-term system variations. Typical dynamic incentive programs include transactive control and dynamic pricing methods. In (Wu et al. 2018; Hoque et al. 2021; Liu et al. 2018), the transactive control method is applied to manage EV charging load through local transactive markets. In (Zhao et al. 2017; Liu et al. 2021; Moghaddam et al. 2019), the real-time dynamic pricing strategy is applied to instantly affect the EV charging load to maximize the charging station profit or reduce residential load peaks.

As a hybrid method that combines the advantages of both static and dynamic methods, the incentive method proposed in chapter 4 is proven effective in encouraging EV user cooperation. However, two factors can restrict the efficiency of the methods proposed in chapter 4. Firstly, the V2G operation is not considered. Also, the uniform pricing strategy in chapter 4 can discourage EV energy flexibility utilization on some occasions. Hence, on top of the methods proposed in chapter 4, an enhanced incentive program is proposed in this chapter to further encourage EV user cooperation.

After maximizing the total benefit of the VPP-CSs system by using both generator and EV energy flexibility, the conflicting interests between different stakeholders in the system need to be addressed to maintain the willingness of different stakeholders to cooperate. In power engineering, the Shapley Value method is the most popular approach for handling the cost allocation problem in cooperative games (Sharma and Abhyankar 2016; Li et al. 2018; Mei et al. 2019). However, the application of the Shapley Value method is hindered by its computational intractability, which makes it impractical for the considered cost allocation problem. To solve the cost allocation problem while keeping the computational burden under control, an estimated τ-value cost allocation method is proposed in this chapter. In the conventional τ-value method, all possible sub-coalitions need to be evaluated to compute the τ-values, which is bluntly unrealistic for the considered cost allocation problem. By utilizing some key features in the τ-value calculation process, the proposed estimated τ-value method can significantly reduce the number of evaluated sub-coalitions, meanwhile, achieving a high estimation accuracy.

To summarize, this chapter is dedicated to proposing a cooperative operation framework for VPPs and charging stations with different ownerships. To handle the interest conflicts between different stakeholders, an EV user incentive program and a cost allocation method are proposed in this chapter. To this end, the original contributions of this chapter can be summarized as follow:

- A multi-stakeholder VPP-CSs system consisting of a distributed generator-based VPP and multiple charging stations is investigated. A cooperative operation framework is proposed to handle the interactive day-ahead offering and real-time balancing problems of the VPP-CSs system.

- An EV user incentive program is proposed. Compared to the methods in chapter 4, the incentive program proposed in this chapter can achieve more EV user cost reduction, higher EV energy flexibility utilization, and lower total system cost
- An estimated τ-value cost allocation method is proposed to efficiently address the cost allocation problem of the VPP-CSs system.

The remainder of this chapter is organized as follows: Section 5.2 presents the proposed VPP-CSs operation framework and the EV user incentive program. Section 5.3 gives the detailed problem formulations of the day-ahead offering and real-time dispatching models. Section 5.4 provides the estimated τ-value cost allocation method. Numerical results are given and discussed in Section 5.5. Section 5.6 concludes this chapter.

5.2 Problem Description

This section first presents an overview of the investigated VPP-CSs system, then provides the details of the proposed EV user incentive program.

5.2.1 VPP-CSs System

The configuration of the considered VPP-CSs system is presented in Fig. 5.1.

This chapter considers a distributed generator-based VPP (with both wind and thermal power plants) and multiple charging stations (with level 2 charging rate) to form a VPP-CSs system. Due to the heavy capital cost of energy storage devices (Rahman et al. 2020), only renewable generators and thermal power plants are considered to form the VPP, and energy storage devices are not included in the VPP configuration. In this system, the stakeholders include the VPP, the charging stations, and EV users. The VPP can directly manage the wind and thermal power plants to participate in electricity markets. The charging stations can directly manage the charging/discharging behavior of EVs. In this configuration, the charging stations can indirectly benefit from the competitive market price through the VPP. The VPP benefits from charging stations by indirectly making use of the energy flexibility of EVs. Due to the small

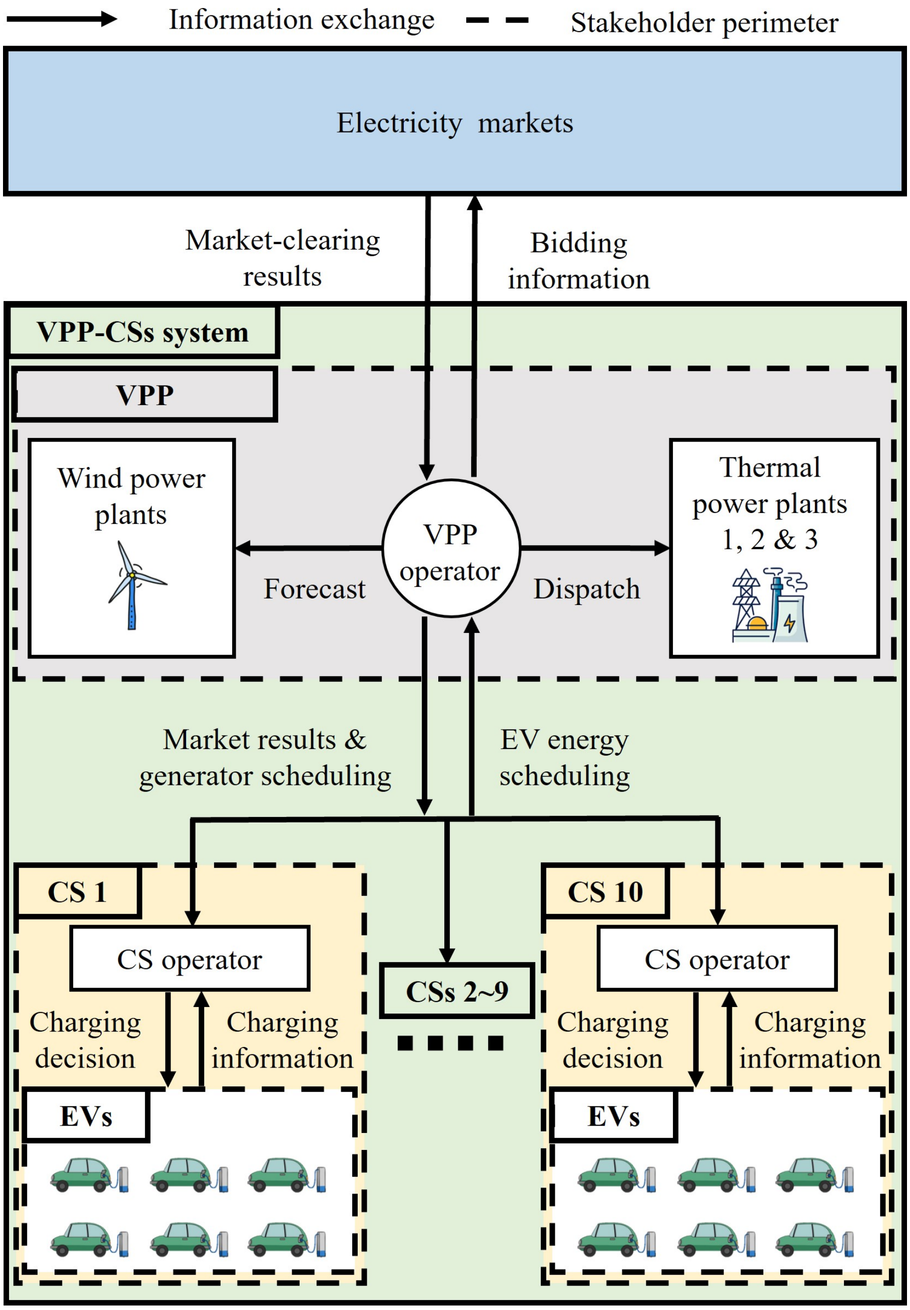

Figure 5.1: Configuration of the VPP-CSs system

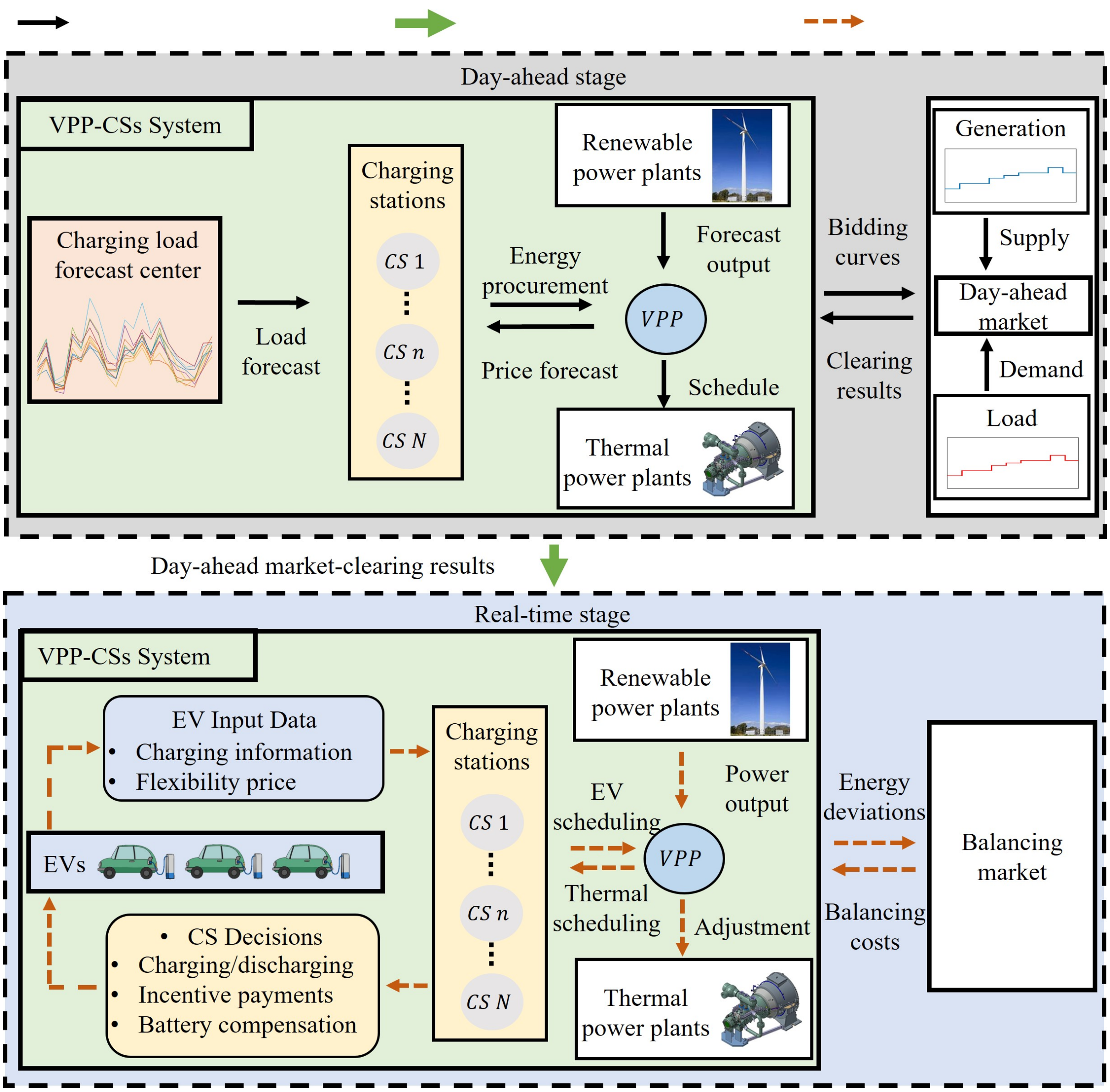

Figure 5.2: Operation framework of the considered VPP-CSs system.

capacities of individual EVs, EV users are not involved in the market operation. To address the interests of EV users, the contribution of EV users is financially remunerated through an incentive program.

The proposed operation framework for the VPP-CSs system is summarized in Fig. 5.2. The considered VPP-CSs system participates in both the day-ahead energy market and the balancing market. Under this framework, the considered VPP-CSs system needs to face uncertainties in market price, renewable generation, and EV charging demand.

In the day-ahead market, the investigated VPP-CSs system acts as a price-taker who submits offering curves to the market operator. The submitted offering curves should contain price-quantity pairs that reflect how much energy the VPP-CSs system is willing to sell to or buy from the day-ahead market at different market-clearing prices. In the balancing market, due to uncertainties in renewable generation and EV charging demand, the VPP-CSs system is considered a deviator. The balancing market settles the energy deviations of the considered VPP-CSs system by using penalty prices. Specifically, energy surplus will be sold at a lower price, and energy deficiency needs to be compensated at a higher price (Kardakos, Simoglou, and Bakirtzis 2015):

$$\lambda_t^+ = \psi^+ \cdot \lambda_t^{DA} \tag{5.1}$$

$$\lambda_t^- = \psi^- \cdot \lambda_t^{DA} \tag{5.2}$$

$$\psi^+ \geq 1 \tag{5.3}$$

$$\psi^- \leq 1 \tag{5.4}$$

where λ_t^{DA} is the day-ahead energy market-clearing price at time t; The balancing prices for energy deficiency and energy surplus are given by λ_t^+ and λ_t^-, respectively. Parameters ψ^+ and ψ^- are the market penalty coefficients, which can reflect how severely the market penalizes energy deviations.

In the day-ahead stage, charging stations need to forecast the market price and charging demand. Based on the forecast information, charging stations can schedule their energy procurement plans under both market price and EV charging demand uncertainties to minimize their energy procurement cost. After charging stations complete their energy procurement plans, the VPP collects the charging station energy procurement plans to develop the aggregated VPP-CSs system offering curves under uncertain prices and renewable power generation. Before developing the aggregated offering curve, the VPP needs to predict the market price and renewable energy production. With the forecast information and charging station energy plans, the VPP can schedule the thermal power plants and offer different energy quantities at different price scenarios to maximize its profit. Once the market is cleared, the VPP gets paid by the market for energy sales or pays the market for energy procurements at the market-clearing price. Besides, the charging stations should also pay the VPP for their scheduled energy procurements or get paid for energy sales at the market-clearing price.

To handle uncertainties in the day-ahead stage, uncertainties in renewable productions and EV charging demands are modeled using intervals. Each interval is characterized by a forecast value (i.e., fv_t^r for renewable production and fv_t^{cs} for charging station charging demand) and an uncertainty coefficient that indicates the accuracy of the forecasts (i.e., σ^{DA} for renewable production and σ^{CS} for charging station charging demand), as shown below:

$$\left(1-\sigma^{DA}\right) fv_t^r \leq u_t^r \leq \min\left\{\left(1+\sigma^{DA}\right) fv_t^r, P^{r,ic}\right\} \tag{5.5}$$

$$\left(1-\sigma^{CS}\right) fv_t^{cs} \leq u_t^{cs} \leq \min\left\{\left(1+\sigma^{CS}\right) fv_t^{cs}, P^{cs,ic}\right\} \tag{5.6}$$

where u_t^r and u_t^{cs} represent the renewable power production and EV charging demand, respectively. The installed renewable power generation capacity is given by $P^{r,ic}$, and the charging station service capacity is given by $P^{cs,ic}$.

Besides, the market price uncertainty is modeled using representative scenarios. The representative price scenarios are selected to cover price scenarios ordered from high to low in an unbiased manner (Alahyari, Ehsan, and Mousavizadeh 2019). To this end, the charging station day-ahead energy scheduling problems can be formulated as stochastic minimax regret problems, which minimize the expected worst-case regret under both EV charging demand and market price uncertainties. For the VPP, the day-ahead offering problems can be formulated as minimax regret optimization problems that minimize the worst-case regret regarding uncertain renewable power generation.

In the real-time stage, the VPP and charging stations cooperatively schedule the thermal power plants and EV charging plans to minimize energy deviation costs resulting from the renewable output and EV charging demand forecast errors. In this stage, the market prices and EV charging information become known parameters, the remaining uncertain factor is renewable production. To handle the renewable uncertainty and keep up with the constantly updated EV charging information, a rolling horizon optimization approach is developed in this chapter. In the rolling horizon approach, the generator generation and EV charging decisions are continuously optimized to minimize the total operation cost. Notably, in this VPP-CSs system, the generator generation can be directly controlled, but the charging power of EVs cannot be arbitrarily changed since EVs belong to EV users instead of the VPP-CSs system. Hence, an EV user incentive program is proposed in the next subsection to remunerate EV users in exchange for EV charging power control rights.

5.2.2 EV User Incentives

By controlling the charging and discharging of batteries, EVs can play an important role in reshaping the aggregated load profile of the VPP-CSs system. However, controlling EV charging and discharging behaviors requires cooperation from EV users who wish to recharge their EVs as quickly as possible. Hence, a well-designed incentive program is of great significance to encourage EV user participation in smart charging and improve the overall profitability of the VPP-CSs system.

Existing incentive programs can be categorically classified as static and dynamic programs. Static incentive programs have the advantages of being simple and consistent, but dynamic programs can offer more controllability for charging station operators to improve their profitability. By combining the strengths of both static and dynamic programs, the method proposed in chapter 4 shows promising performances in encouraging EV energy flexibility utilization.

However, two factors can undermine the performance of the original methods proposed in chapter 4. Firstly, the V2G operation is not considered. The original method only utilizes the EV charging flexibility and ignores the discharging flexibility. As the V2G technology matures, the importance of utilizing EV discharging flexibility has been intensively researched (Sovacool et al. 2018; Heilmann and Friedl 2021; Bibak and Tekiner-Moğulkoç 2021). Hence, the first improvement of the proposed incentive program is to encourage the V2G operation. Besides, the original method adopts the uniform pricing mechanism, which can discourage flexibility utilization on some occasions. By using the uniform pricing mechanism, the variation in EV users' willingness to respond to system regulation signals cannot be reflected, hence, reducing the efficiency of incentive programs in encouraging EV users. Compared to the uniform pricing mechanism, the pay-as-bid mechanism is more efficient in reflecting different EV users' willingness to offer their energy flexibility. Therefore, the second improvement in the proposed incentive program is to adopt the pay-as-bid mechanism to encourage more proactive EV users' participation. The proposed incentive program details are presented next.

In the considered framework, EV users buy energy from charging stations to recharge their EVs. Meanwhile, EV users can get paid by selling their EV energy flexibility to charging stations. If the time-of-use pricing is applied to affect the charging behavior of EV users, EV users will need to wait for low-price hours to recharge their EVs if they wish to reduce their charging bills. Making EV users wait can disturb their parking and travel plans, which causes inconvenience for EV users. Hence, the energy retail price at charging stations for EV users to recharge their EVs is always the same. To encourage EV users to respond to regulation signals from charging stations, incentives are used in the proposed incentive program to acquire EV battery access rights and control the charging process of EVs. In the proposed incentive program, the remuneration is based on the pay-as-bid and pay-as-use principles. That is, the payment for using the EV charging and discharging flexibility depends on both the EV user offering price γ_m (\$/kWh) and the quantity of adopted energy flexibility (kWh).

The adopted charging energy flexibility is the load shifted between different periods, and the adopted discharging energy flexibility is the energy injected back into the grid from EVs. Through the proposed incentive program, charging stations will remunerate EV users for adopting their energy flexibility. Besides, battery degradation will also be compensated when discharging energy flexibility is adopted. The payment computations are schematically illustrated in Fig. 5.3, which shows how much will EV users be remunerated for adopting their energy flexibility. Fig. 5.3a shows the EV charging load before (left) and after (right) the scheduling. In hours 13 and 14, the charging station not only reduces the EV charging power but also discharges the EV to inject power back into the grid. In hours 15 to 18, the EV charging power is increased to fulfill the EV charging demand. These EV power changes are summarized in Fig.

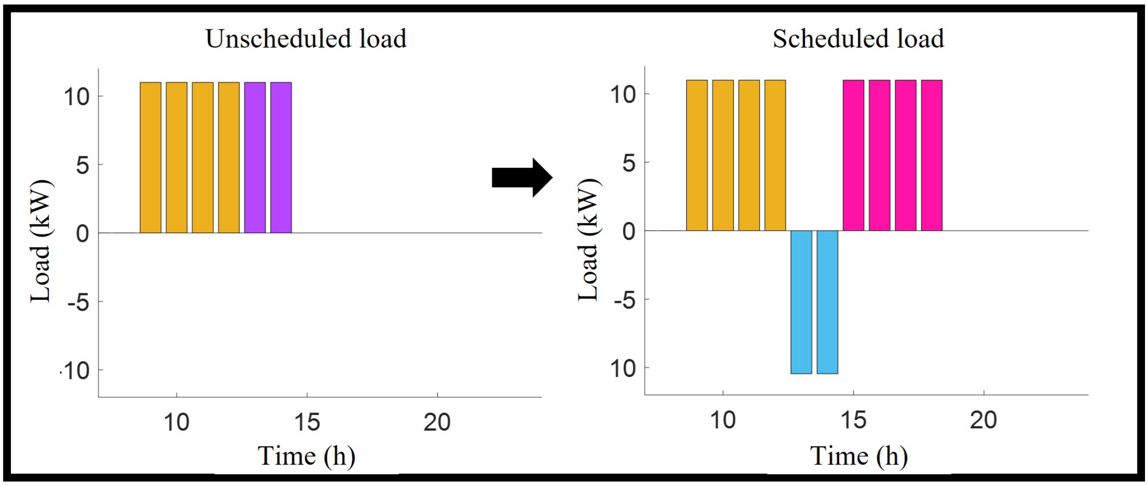

(a) Load scenarios

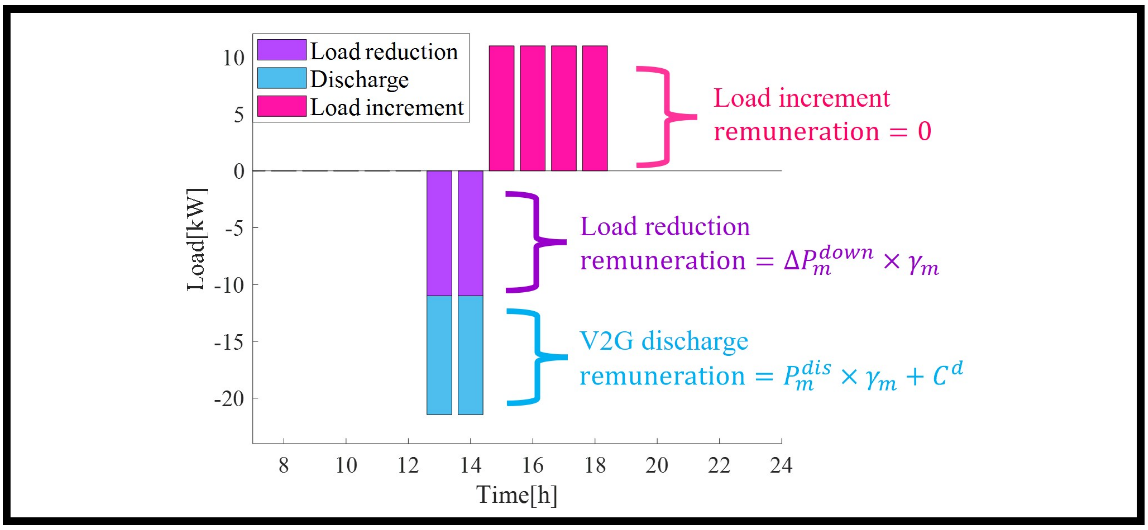

(b) Load change results

Figure 5.3: Payments for using EV energy flexibility

5.3b, in which one can observe that the EV user gets remunerated for both the reduced charging power (adopted charging energy flexibility) and the scheduled discharging power (adopted discharging energy flexibility).

Notably, increasing the EV charging load cannot generate remuneration for EV users. This is because EV users always tend to recharge their EVs as quickly as possible to reduce their range anxiety (Chung et al. 2018), and increasing the charging power can rarely cause inconvenience to EV users.

When energy flexibility is adopted, the payment for EV user m is based on the adopted energy flexibility and the offering prices γ_m. To obtain the energy flexibility adopting results, the unscheduled charging load should be computed first. It is assumed that in the unscheduled charging scenario, EV users would recharge their EVs at the maximum charging power immediately after they arrive at the charging stations to mitigate their range anxieties. In the unscheduled charging scenario, the maximum charging power continues until EVs are fully charged. The charging load in the unscheduled charging scenario is defined as the unscheduled charging load $P^{us}_{m,t}$. In the unscheduled charging scenario, the unscheduled charging load $P^{us}_{m,t}$ of EV user m at time t can be summarized as follows:

$$P^{us}_{m,t} = \begin{cases} 0 & : SOC_{m,t-1} = SOC^{max} \\ \frac{SOC^{max}_m - SOC_{m,t}}{Cap^{ev}_m} & : P^{max}_m > \frac{SOC^{max}_m - SOC_{m,t}}{Cap^{ev}_m \Delta t} \\ P^{max}_m & : P^{max}_m \leq \frac{SOC^{max}_m - SOC_{m,t}}{Cap^{ev}_m \Delta t} \end{cases} \tag{5.7}$$

where SOC^{max} is the maximum SOC of EV m, P^{max}_m is the maximum charging rate of energy for EV m, and Cap_m is the battery capacity of EV m. The SOC of EV m at each scheduling period t is given by $SOC_{m,t}$, and Δt is the length of a scheduling time interval.

By using Eq (5.7), the upward $\Delta P^u_{m,t}$ and downward $\Delta P^d_{m,t}$ power changes can be obtained by comparing the scheduled load $P^s_{m,t}$ with the unscheduled load $P^{us}_{m,t}$:

$$\Delta P^u_{m,t} - \Delta P^d_{m,t} = P^s_{m,t} - P^{us}_{m,t} \tag{5.8}$$

In this formulation, the unscheduled EV charging load is used as the baseline to calculate the adopted EV energy flexibility, which further determines the financial remuneration of EV users.

Since EV users always tend to recharge their battery as quickly as possible, adding charging loads within the maximum EV charging power to the no-load periods will not cause inconvenience to EV users. Hence, the incentive payment $\omega_{m,t}$ only considers downward changes $\Delta P^d_{m,t}$:

$$\omega_{m,t} = \Delta P^d_{m,t} \gamma_m \Delta t \tag{5.9}$$

where γ_m is the flexibility offering price of EV user m.

When V2G operation is involved, the battery degradation cost will also be included in the payment:

$$\omega_{m,t} = (\Delta P^{d}_{m,t} + P^{dis}_{m,t})\gamma_m \Delta t + C^{bd}_{m,t} \tag{5.10}$$

where the battery degradation cost is denoted by $C^{bd}_{m,t}$. In this chapter, the battery degradation cost is modeled by using the battery investment cost C^{bi}_{m} and the total life cycles n^{lc} (Das et al. 2020):

$$C^{bd}_{m,t} = \frac{P^{dis}_{m,t}\Delta t}{E_m} C^{bi}_{m} \tag{5.11}$$

$$E_m = n^{lc} Cap^{ev}_{m} \tag{5.12}$$

where the prospective lifetime energy output of EV m is denoted by E_m, which is given by Eq (5.12). Terms n^{lc} and Cap^{ev}_{m} represent the battery life cycles and energy capacity of EV m, respectively.

5.3 Problem Formulation

This section firstly presents the day-ahead charging station scheduling and VPP offering problems, then gives the real-time VPP-CSs cooperative balancing problem.

5.3.1 Charging Station Day-Ahead Energy Scheduling

For charging stations, both the market price and EV charging demand uncertainties need to be considered in the day-ahead charging station scheduling problem. In this chapter, the market price is modeled by representative scenarios, and the EV charging demand is modeled using confidence intervals. Hence, the day-ahead scheduling problem for charging stations is formulated as a stochastic minimax regret problem based on the forecasts. In stochastic minimax regret problems, the expected maximum regret is minimized under both market price and EV charging demand uncertainties:

$$\min_{P_{n,t}^{DA,cs}} \sum_{t\in 1:24} \left\{ f^{DA}\left(P_{n,t}^{DA,cs}\right) + \max_{u_t^{cs}} \sum_{k\in K} \pi_k \min_{P_{n,t}^{DA,cs,u} P_{n,t}^{B,u}, P_{n,t}^{B}} \left[f^B\left(P_{n,t}^{B}\right) - f^{DA}\left(P_{n,t}^{DA,cs,u}\right) - f^B\left(P_{n,t}^{B,u}\right) \right] \right\} \tag{5.13}$$

$$f^{DA}(P_t^{DA}) = \lambda_{k,t}^{DA,f} \cdot P_t^{DA} \tag{5.14}$$

$$f^B(P_t^B) = \begin{cases} \left|P_t^B \lambda_t^+\right| & : P_t^B \geq 0 \\ -\left|P_t^B \lambda_t^-\right| & : P_t^B \leq 0 \end{cases} \tag{5.15}$$

s.t.

$$\text{(5.1)–(5.4), (5.6)} \tag{5.16}$$

$$P_{n,t}^{DA,cs} + P_{n,t}^{B} = u_t^{cs} \tag{5.17}$$

$$P_{n,t}^{DA,cs,u} + P_{n,t}^{B,u} = u_t^{cs} \tag{5.18}$$

$$(1-\sigma^{CS}) f v_{n,t}^{cs} \leq P_{n,t}^{DA,cs} \leq min\left\{(1-\sigma^{CS}) f v_{n,t}^{cs}, P_n^{cs,ic}\right\} \tag{5.19}$$

$$\pi_1 + \pi_2 + ... + \pi_K = 1 \tag{5.20}$$

where $P_{n,t}^{DA,cs}$ and $P_{n,t}^{B,cs}$ represent the energy procurement and balancing market energy deviation of charging station n at time t, respectively. Correspondingly, the optimal charging station solutions under the charging demand scenario u_t^{cs} are represented by $P^{DA,cs,u}$ and $P_{n,t}^{B,cs}$, respectively. The probability of price scenario k is given by π_k. Functions $f^{DA}(P_t^{DA})$ and $f^B(P_t^B)$ are the day-ahead energy procurement cost and energy balancing cost, respectively.

Constraints (5.17) and (5.18) are energy-balancing constraints. Constraint (5.19) provides a reasonable range for energy procurements to reduce the searching domain without affecting optimality. Constraint (5.20) ensures that the summation of all scenario probabilities equals to one.

After charging stations complete their day-ahead energy procurement scheduling, the scheduling results $P_{n,t}^{DA,cs}$ of each charging station n are reported to the VPP to form an aggregated VPP-CSs offering strategy in the day-ahead energy market.

5.3.2 VPP Day-Ahead Bidding

In the day-ahead stage, after collecting the charging station energy scheduling plans, the VPP needs to develop an aggregated offering strategy confronting price and renewable uncertainties. Based on the forecast information, the offering problem of the VPP is divided into two levels to handle these uncertainties. In the upper level, different price scenarios are generated as the inputs of the lower-level problem to acquire several price-quantity pairs for constructing offering curves. In the lower-level problem, the VPP optimizes the offering quantity and thermal productions for each forecast market price scenario $\lambda_{k,t}^{DA}$ under renewable output uncertainty. At the lower level, the VPP offering problem is formulated as minimax regret optimization problems. In the minimax regret problems, the maximum regret of the worst-case renewable generation is minimized for a given market price scenario $\lambda_{k,t}^{DA}$ at time t:

$$\min_{P_t^{DA},P_{i,t}^{G}} \left\{ \left[\sum_{i \in I} f^G(P_{i,t}^G) - f^{DA}(P_t^{DA}) \right] + \max_{u_t^r} \left\{ \min_{P_t^{DA,u},P_{i,t}^{G,u},P_t^{B,u},P_t^B} \left\{ \begin{array}{l} f^B(P_t^B) - \sum_{i \in I} f^G(P_{i,t}^{G,u}) \\ +f^{DA}(P_t^{DA,u}) - f^B(P_t^{B,u}) \end{array} \right\} \right\} \right\} \tag{5.21}$$

$$f^G(P_{i,t}^G) = c_i(P_{i,t}^G)^2 + b_i P_{i,t}^G + a_i \tag{5.22}$$

s.t.

$$(5.1) - (5.5), (5.14), (5.15) \tag{5.23}$$

$$P_t^{B,u} + \sum_i P_{i,t}^{G,u} + u_t^r - \sum_{n \in N} P_{n,t}^{DA,cs} = P_t^{DA,u} \tag{5.24}$$

$$P_t^B + \sum_i P_{i,t}^G + u_t^r - \sum_{n \in N} P_{n,t}^{DA,cs} = P_t^{DA} \tag{5.25}$$

$$y_i^u P_i^{G,min} \le P_{i,t}^{G,u} \le y_i^u P_i^{G,max} \tag{5.26}$$

$$y_i P_i^{G,min} \le P_{i,t}^G \le y_i P_i^{G,max} \tag{5.27}$$

$$[y_i^u, y_i] \in (0, 1) \tag{5.28}$$

where P_t^{DA}, $P_{i,t}^G$, P_t^B and u_t^r represent the market offering energy, the energy production of thermal power plant i, balancing market energy deviation, and renewable production at time t, respectively. Similarly, terms with a superscript u, including P_t^{DA}, $P_{i,t}^G$ and P_t^B, are the optimal VPP solutions under the scenario u_t^r. The binary variables $[y_i^u, y_i]$ are the on/off status indicators of the thermal generators. Term $P_{n,t}^{DA,cs}$ is the reported day-ahead energy procurement of charging station n at time t. The thermal generator fuel cost is given by $f^G(P_{i,t}^G)$ in (5.22).

Constraints (5.24) and (5.25) are energy-balancing constraints. Constraints (5.26) to (5.27) are the power limit and unit commitment constraints of the thermal generators.

In the upper level, several price scenarios $k \in K$ are generated as inputs of the problem (5.21) – (5.28). After solving the lower-level minimax regret offering problem K times with different price scenarios, several optimal offering quantities can be obtained. To construct the VPP-CSs day-ahead offering curves, these optimal offering quantities are paired with the corresponding price scenarios to form price-quantity pairs as the building blocks of offering curves.

Notably, in the day-ahead stage, to be consistent with the market-clearing resolution, the scheduling time interval for the thermal power plants, renewable power plants, and charging stations is set to be one hour.

5.3.3 VPP-CSs Real-Time Balancing

In the real-time stage, the VPP-CSs system needs to balance energy deviations resulting from the forecast errors to minimize the total cost. In the real-time stage, the market has been cleared, the connected EV charging information becomes available, and the EV charging/discharging load can be controlled by the EV charging stations. Hence, the only uncertainty remaining in this stage is renewable energy production. Besides, The EV energy scheduling problem should keep updated with EV charging information to meet the energy requirements of each EV. Therefore, the real-time VPP-CSs coordinated balancing problem is formulated as a rolling horizon optimization problem to handle the constantly updated EV charging information and renewable production forecast. Notably, to keep pace with the updated EV charging and renewable forecast information, only the first step in the solution of each scheduling horizon will be implemented. Hence, a real-time rolling horizon optimization problem needs to be solved for every scheduling period. In the real-time rolling horizon optimization model, to keep pace with the constantly updated EV charging and renewable forecast information, the optimization horizon is set to be 8 hours, and the scheduling resolution is set to be 15 minutes (Su, Lie, and Zamora 2020; Wang et al. 2022b). That is, in the real-time stage, the scheduling horizon for all energy resources is 15 minutes.

In the real-time coordinated balancing problem, the VPP-CSs system simultaneously schedules the generator generation and EV charging/discharging power to minimize the total system costs, which include the fuel cost, EV user incentive cost, and energy deviation cost.

$$\min_{P_{i,t}^{G}, P_t^{B,vc}, \Delta P_{m,t}^{d}, \Delta P_{m,t}^{u}, P_{m,t}^{dis}} \left\{ \sum_{t \in T} \left[\sum_{i \in I} f^G(P_{i,t}^{G}) + f^B(P_t^{B,vc}) + \sum_{m \in M} \omega_{m,t} \right] \right\} \tag{5.29}$$

$$(5.1)\text{–}(5.4), (5.7)\text{–}(5.12), (5.15), (5.22), (5.27), (5.28) \tag{5.30}$$

$$P_t^{DA} - \sum_{n \in N} P_{n,t}^{DA,cs} = \sum_{i \in I} P_{i,t}^{G} + f v_t^{r,rt} + P_t^{B,vc} - \sum_{m \in M} \left[\frac{P_{m,t}^{us} + \Delta P_{m,t}^{u} - \Delta P_{m,t}^{d}}{\eta} - \eta P_{m,t}^{dis} \right] \tag{5.31}$$

$$-RD_i \leq P_{i,t}^{G} - P_{i,t-1}^{G} \leq RU_i \tag{5.32}$$

$$-P_m^{dis,max} \leq P_{m,t}^{us} + \Delta P_{m,t}^{u} - \Delta P_{m,t}^{d} - P_{m,t}^{dis} \leq P_m^{max} \tag{5.33}$$

$$P_{m,t}^{us} + \Delta P_{m,t}^{u} - \Delta P_{m,t}^{d} \leq P_{m}^{max} \tag{5.34}$$

$$\sum_{t \in T} \left(\Delta P_{m,t}^{u} - \Delta P_{m,t}^{d} - P_{m,t}^{dis} \right) = 0 \tag{5.35}$$

$$SOC_{m,t} = SOC_{m,t-1} + \frac{P_{m,t}^{us} + \Delta P_{m,t}^{u} - \Delta P_{m,t}^{d} - P_{m,t}^{dis}}{Cap_{m}^{ev}} \Delta t \tag{5.36}$$

$$SOC_{m}^{min} \leq SOC_{m,t} \leq SOC_{m}^{max} \tag{5.37}$$

$$\Delta P_{m,t}^{u} \Delta P_{m,t}^{d} = 0 \tag{5.38}$$

$$\Delta P_{m,t}^{u} P_{m,t}^{dis} = 0 \tag{5.39}$$

$$\left[\Delta P_{m,t}^{u}, \Delta P_{m,t}^{d}, P_{m,t}^{dis} \right] \geq 0 \tag{5.40}$$

where the entire scheduling horizon is given by T. The energy deviation of the VPP-CSs system at time t is denoted by $P_{t}^{B,vc}$. The real-time renewable production forecast at time t is given by $fv_{t}^{r,rt}$. The reduced charging power, the increased charging power, and the discharged power of EV m at time t are given by $\Delta P_{m,t}^{d}$, $\Delta P_{m,t}^{u}$, and $P_{m,t}^{dis}$, respectively. The charging and discharging efficiency are given by η. Parameters RD_i and RU_i denote the ramp-down and ramp-up capabilities of thermal power plant i. The power limits of EV m are given by P_m^{max} and $P_m^{dis,max}$, respectively.

Constraint (5.31) is the energy-balancing constraint. The thermal power plant ramping capability is restricted by constraint (5.32). Constraints (5.33) and (5.34) limit the EV power. Constraint (5.35) ensures that the EVs are fully charged within the parking duration. Constraints (5.36) and (5.37) are the SOC constraints of EVs. Constraints (5.38) – (5.40) guarantee the rationality of the optimization results.

The solution methodology for day-ahead minimax regret problems can be referred to chapter 3. As a mixed-integer quadratic programming problem, the real-time balancing problem can be readily solved by commercial solvers such as GUROBI (*GUROBI optimizer* 2022). Besides, to efficiently solve the real-time scheduling problem for large EV fleets, the distributed solution approach (Wang et al. 2022b) based on the ADMM algorithm is applied. Hence, the solution methodology to the formulated optimization problems is not provided in this chapter.

5.4 Cost Allocation Method

This section first develops a τ-value cost allocation method, then proposes a maximum right cost estimation approach to reduce the computational burden of calculating the τ-values.

5.4.1 τ-value Cost Allocation

The VPP and charging stations cooperatively minimize the total cost, which includes the thermal generator fuel cost, the EV user incentive cost, and the energy deviation cost. Because the VPP and charging stations have different ownerships, a fair cost allocation mechanism to share the total cost among the players is the key to stabilize this VPP-CSs coalition. In this sub-section, a τ-value method is developed to solve the cooperative game problem and allocate the costs among players.

In this cooperative game problem, the VPP and charging stations represent the players in the game. That is, each stakeholder is a player in the game. The goal of this game is to analyze the contributions of each stakeholder and allocate the cost to the VPP and charging stations based on their contributions.

Firstly, the VPP-CSs system is considered as a grand coalition Z. In this grand coalition, each player corresponds to a VPP or a charging station. Besides, the cost generated from any sub-coalition $S \in Z$ is defined as the characteristic function $v : 2^Z \to R$ with $v(\emptyset) = 0$. Then, a cooperative game can be defined as the ordered pair $\langle Z, v \rangle$, in which the real number $v(S)$ represents the cost generated from the members of S when they cooperate.

In this cooperative game $\langle Z, v \rangle$, for each player $l \in Z$ in the sub-coalition $S : \{S \in Z, l \in S\}$, the marginal cost contribution $M_l(S, v)$ of player l to the coalition S is:

$$M_l(S, v) = v(S) - v(S \backslash \{l\}) \tag{5.41}$$

where the last term represents the cost generated by the rest members of S without player l. When the considered sub-coalition is the grand coalition Z, this marginal contribution of player l is defined as its utopia cost $M_l^u(Z, v)$:

$$M_l^u(Z, v) = v(Z) - v(Z \backslash \{l\}) \tag{5.42}$$

The utopia cost represents the cost contribution of a considered player to the total cost of the grand coalition. Namely, when a new player is added to the grand coalition, the utopia cost of the added new player is the increment of the total grand coalition cost due to the addition of this new player. The utopia cost $M_l^u(Z, v)$ is the minimum cost player l should pay. Because if player l wants to pay less, then it is more advantageous for other players in the grand coalition Z to remove player l. Hence, the utopia cost $M_l^u(Z, v)$ provides a lower bound of the cost allocated to player l. Next, an upper bound of the cost allocated to player l is found by identifying the maximum cost player l should pay.

The remainder $R(S, l)$ of player l in a sub-coalition S is defined as the cost remanent for player l in the coalition S if all other players $h : \{h \in S, h \neq l\}$ only pay their utopia costs:

$$R(S,l) = v(S) - \sum_{h \in S \setminus \{l\}} M_h^u(Z,v) \tag{5.43}$$

Then, for each player $l \in Z$, the maximum right cost $M_l^{mrc}(v)$ is defined as the minimum remainder player l can have from all possible sub-coalitions that contain player l:

$$M_l^{mrc}(v) = \min_{S:l \in S} R(S,l) \tag{5.44}$$

The maximum right cost of player l is the maximum cost player l needs to pay in the grand coalition. Because if player l pays more than $M_l^{mrc}(v)$, then the sub-coalition S with $R(S,l) = M_l^{mrc}(v)$ would form a more solid coalition by making all other players in S pay their utopia costs. Hence, $M_l^{mrc}(v)$ can serve as an upper bound of the cost allocated to the player l.

After obtaining the utopia costs and maximum right costs, the lower and upper bounds of costs allocated to the VPP and each charging station can be determined. With these upper and lower bounds, it is reasonable to find a compromise between the lower and upper bounds to be the solution for the cost allocation problem. By using the lower and upper bounds of costs allocated to players, the τ-values for each player $l \in Z$ can be computed such that each player pays a cost that lies between their lower and upper cost bounds:

$$\tau_l(v) = \phi M_l^{mrc}(v) + (1 - \phi) M_l^u(Z,v) \tag{5.45}$$

where the coefficient $\phi \in [0,1]$ can be uniquely determined by satisfying the efficiency criterion:

$$\sum_{l \in Z} \tau_l(v) = v(Z) \tag{5.46}$$

where $v(Z)$ is the total cost generated by the grand coalition. In the cost allocation problem, the obtained τ-value $\tau_l(v)$ for player l is the cost allocated to that player.

Notably, the stakeholders in the cooperative game problem only include the VPP and charging stations. Thus, the cost allocation method only handles the cost allocation problem between the VPP and charging stations. For EV users, they participate in the scheduling process through the proposed incentive program, and their contributions are rewarded through the incentive program. Hence, EV users are not included in the cost allocation problem.

5.4.2 Proposed Maximum Right Cost Estimation Approach

In the conventional τ-value method, computing the maximum right costs requires evaluating the characteristic function $v : 2^Z \to R$ for 2^Z times, which is unrealistic for the considered cost allocation problem. To keep the computational burden under control, an estimation method is proposed to use fewer coalition samples to estimate the maximum right costs. By utilizing some characteristics in the τ-value calculation process, the proposed estimation approach can reduce the number of evaluated coalitions from two dimensions, including reducing the number of players considered for sampling and reducing the number of considered coalition sizes.

The first attempt to reduce the computational burden is to reduce the number of considered players. When calculating the remainder $R(S, l)$ for player l in coalition S, the decisive factors include the utopia costs $M_h^u(Z, v)$ of other players and the total cost $v(S)$ generated from coalition S. Hence, it is straightforward to imply that smaller remainders for player l can be achieved with smaller total costs $v(S)$ and larger utopia costs $M_h^u(Z, v)$ of other players in the coalition S. Based on this implication, the attractiveness $Attractiveness(h, l)$ of player h to player l is defined as the opposite of $R(S, l)$, in which the coalition S only consists of players l and h:

$$Attractiveness(h, l) = M_h^u(Z, v) - v(l + h) \tag{5.47}$$

The attractiveness $Attractiveness(h, l)$ serves as a measure of how attractive it is for player l to cooperate with player h. The less player l needs to pay by cooperating with player h, the more attractive player h is to player l. By evaluating all two-member coalitions, one can obtain an attractive matrix $AttM$ that records the attractiveness of all players to other players in the grand coalition. With the attractiveness matrix, the coalition sampling for calculating the maximum right costs can be more instructive. That is, when choosing members to form coalitions with player l, one can selectively consider those players with large attractiveness $Attractiveness(h, l)$ to player l.

To select attractive players to form coalitions with player l, players $h \in Z\backslash\{l\}$ are ordered based on their attractiveness to player l. In the decreasingly ordered list $OAttM_l = \{h_1^l \dots h_j^l \dots h_{Z-1}^l\}$, the jth element h_j^l is the jth attractive member to player l. Then, the players that will be selected for sampling can be shortlisted by finding a number J, which determines how many players will be considered when estimating the maximum right cost for player l. The number of considered shortlisted players is constrained by the value of J. More specifically, only the first J attractive players in $OAttM_l = \{h_1^l \dots h_j^l \dots h_{Z-1}^l\}$ will be considered to form coalition samples with player l. Setting the value of J is meant to filter out the members that are less likely to yield better maximum right cost estimation, which can reduce the computational burden for estimation.

On the one hand, increasing J can increase the sampling domain, which may provide closer estimations of the actual maximum right costs. On the other hand, a larger J will increase the computational burden by enlarging the sampling domain. Hence, it is of vital importance to find a proper value of J to meet the estimation accuracy requirements while avoiding unbearable computational burdens. In the proposed estimation approach, the optimal value of J can be uniquely determined by the number of considered coalition sizes, as will be shown later in Eq (5.49).

The number of considered coalition sizes is another factor that can affect the computational burden for estimating the maximum right costs. Considering more coalition sizes will increase the computational burden. The process of determining the minimum number of considered coalition sizes is given next.

For each player l, coalitions with increasing sizes are formed by gradually adding members according to $OAttM_l$. Meanwhile, the remainder for player l under each coalition size $|S|$ is recorded to generate a remainder matrix $RM(l, |S|)$. In each row of the remainder matrix $RM(l, |S|)$, the global minimum remainder for player l can be found. For different coalition sizes, the difference between the global minimum remainder and the local minimum remainder found before this coalition size can shed some light on the maximum right cost estimation accuracy because the true maximum right cost is the global minimum remainder obtained from a larger coalition sample domain. Hence, to determine the number of coalition sizes for evaluation, one only needs to identify a maximum coalition size $|S|_{max}$, such that for all players $l \in Z$, the maximum deviation between the global minimum remainder and the local minimum remainder found before this coalition size is below the given accuracy threshold ε_τ:

$$\max_{l \in Z} \left\{ \frac{\min[RM(l, |S| \leq |S|_{max})]}{\min[RM(l, S \leq Z)]} - 1 \right\} \leq \varepsilon_\tau \tag{5.48}$$

In this condition, the numerator refers to the local minimum of player l in the remainder matrix, considering only coalition sizes $|S| \leq |S|_{max}$, and the denominator is the global minimum of player l in the remainder matrix considering all coalition sizes. Hence, this condition can be satisfied by taking into account a sufficient number of coalition sizes. However, if too many coalition sizes need to be considered to satisfy this condition, a larger threshold ε_τ may need to be employed, thus compromising a certain degree of accuracy in exchange for a reduced computational burden.

After identifying the maximum evaluated coalition size $|S|_{max}$, the optimal value of J can be determined.

$$J = |S|_{max} - 1 \tag{5.49}$$

The optimal value of J is given by (5.49) because the considered player l must be included in all sampled sub-coalitions, and at least $(|S|_{max} - 1)$ extra members are needed to form a sub-coalition with size $|S|_{max}$.

After determining J and $|S|_{max}$, one can estimate the maximum right cost for player l by evaluating all possible coalitions S_{sample} that can be formed by player l and members in $\{h_1^l \dots h_j^l \dots h_J^l\}$:

$$estM_l^{mrc}(v) = \min_{S_{sample}, l \in S_{sample}} R(S_{sample}, l) \tag{5.50}$$

where $estM_l^{mrc}(v)$ represents the estimated maximum right cost for player l. To this end, the estimated τ-values for each player can be obtained by replacing the $M_l^{mrc}(v)$ in (45) with $estM_l^{mrc}(v)$.

The proposed estimated τ-value cost allocation method can be summarized as follows:

Step 1: Set the remainder deviation threshold ε_τ.

Step 2: Calculate the utopia costs for all players $l \in Z$.

Step 3: Derive the attractive matrix $AttM(h,l)$ and create the ordered list $OAttM_l$ for each player.

Step 4: Derive the remainder matrix $RM(l,|S|)$.

Step 5: Obtain the considered coalition size $|S|_{max}$, derive shortlisted member size J through (5.48) and (5.49).

Step 6: For each player l, evaluate all possible coalitions formed by l and members in $\{h_1^l \dots h_j^l \dots h_J^l\}$, derive the estimated maximum right costs for all players from (5.50).

Step 7: Obtain the estimated τ-values from (5.45) and (5.46) and allocate the cost based on the estimated τ-values.

The flowchart for applying the estimated τ-value cost allocation method is summarized in Fig. 5.4.

Under the proposed estimation approach, the maximum number of required evaluations N_{max}^{eval} is reduced from 2^Z to:

$$N_{max}^{eval} = C_Z^2 + (Z^2 - 3Z + 1) + Z \sum_{|S|=3}^{|S|_{max}} C_J^{|S|-1} \tag{5.51}$$

where the first term is for deriving the attractiveness matrix $AttM(h,l)$. The second term is for developing the remainder matrix $RM(l,Z)$ and utopia costs $M_h^u(Z,v)$. The third term is for estimating other possible coalitions. Notably, (5.51) only gives a theoretical upper bound for the number of required evaluations. When applying the proposed estimation approach, the sampled coalitions for estimating the maximum right costs may overlap with each other, and these repeatedly sampled coalitions only need to be evaluated once. Besides, based on

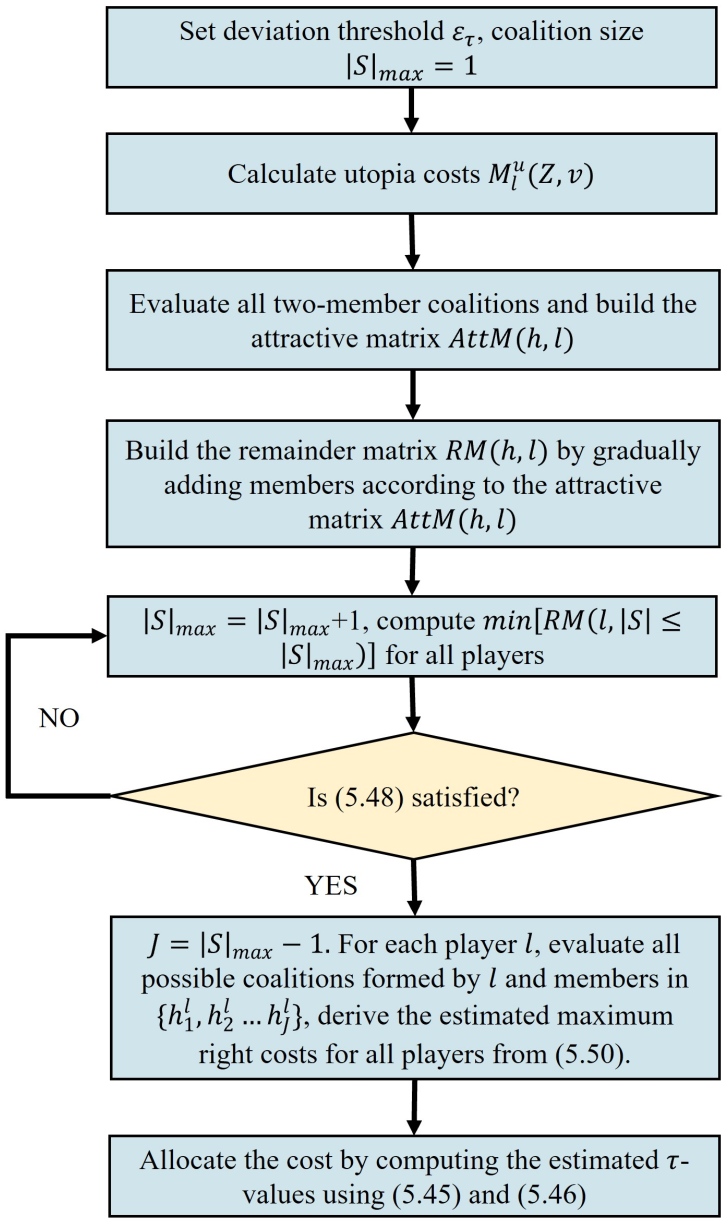

Figure 5.4: Flowchart of the estimated τ-value cost allocation method.

(5.51), as more players join this coalition, the computational complexity of the proposed cost allocation method becomes $O(n^2)$, whereas the computational complexity of the conventional τ-value method is $O(2^n)$.

5.5 Case Study

5.5.1 Experiment Setup

The considered VPP-CSs system consists of a distributed generator-based VPP and 10 charging stations. The generator parameters are given in Table 5.1. The day-ahead forecast renewable generation (*Wind Generation Data* 2019) and market price scenarios (*Day Ahead Auction Prices* 2019) are presented in Fig. 5.5, which are generated from ARIMA models (Wang et al. 2021b) by using historical data. As in chapter 3, the market penalty coefficients are also set to $\psi^+ = 1.5$ and $\psi^- = 0.5$ to moderately penalize the energy deviations. Fig. 5.5b also shows the forecast charging station load profiles generated by using the k-means scenario reduction method (Gray and Morsi 2014). Negative charging station loads in Fig. 5.5b suggest that charging stations would discharge the EVs at those high average forecast price periods. The number of price scenarios generated to construct the offering curves is set to five. Uncertainty coefficients σ^{DA} and σ^{CS} are set to 0.3.

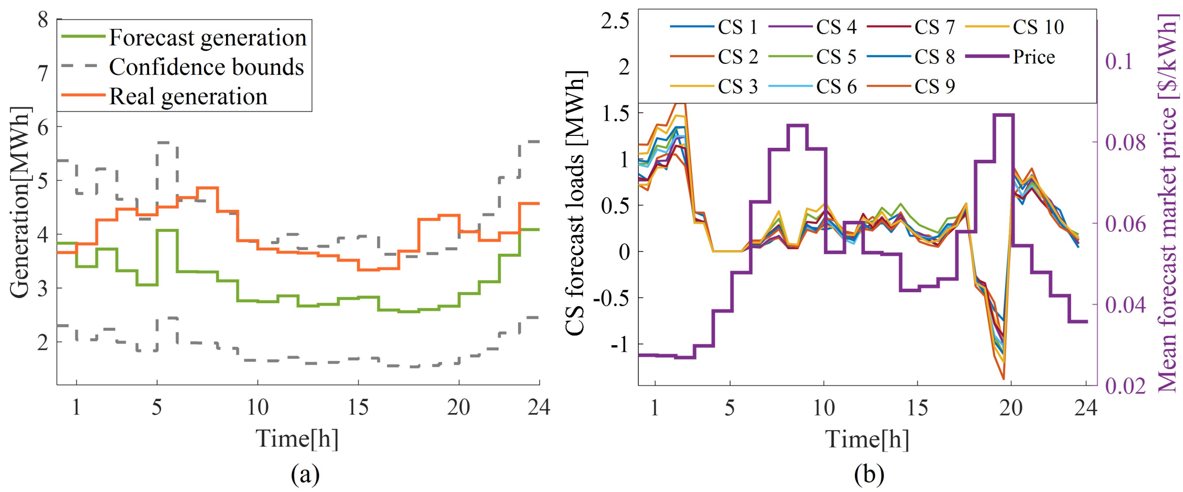

Figure 5.5: (a) day-ahead renewable generation information, (b) forecast charging station load profiles and average forecast market price

Table 5.1: Generator Characteristics

Generator	P_{max} [MW]	$EcoP_{min}$ [MW]	RU [MW/h]	RD [MW/h]	$a[\$/h]$	$b[\$/MWh]$	$c[(\$/MWh)^2]$
TP 1	9	1	3	3	120	40	1.10
TP 2	7	1	2.5	2.5	100	45	1.15
TP 3	5	1	2	2	80	50	1.20
WP	6	0	/	/	/	/	/

TP: thermal power plant; WP: wind power plant

In the real-time stage, the scheduling horizon is set to 8 hours with a scheduling resolution of 15 minutes (Su, Lie, and Zamora 2020). The real-time EV charging data is obtained from the same dataset of chapter 4. It is assumed that the number of EVs charging in each charging station follows the uniform distribution $U(160, 240)$. In total, 2,031 EVs are generated for the considered 10 charging stations. The EV user offering prices γ_m for energy flexibility are assumed to follow the normal distribution with mean and variance equal to half of the average market energy prices. The EV charging price is set to 1.5 times of the average day-ahead energy market price. The charging and discharging efficiency of EVs is set to be 0.95. In the cost allocation stage, the remainder deviation threshold ε_τ is set to be 0.01.

5.5.2 Numerical Results

Fig. 5.6 gives several typical offering curves from the VPP-CSs system and the day-ahead market-clearing results. The offering curves in Fig. 5.6 correspond to low (hour 5), medium (hour 14), and high (hour 18) average forecast prices, respectively. In hour 5, the VPP-CSs system decides not to turn on the thermal power plants for some low-price scenarios, making the first three steps offer the same energy in the market. Thus, the offering curve for hour 5 only has three price-quantity pairs. In hour 14, the forecast price scenarios are distributed in a range that allows the VPP-CSs system to offer a different quantity at each price scenario, leading to a five-step offering curve for hour 14. Hour 18 has high forecast prices, making it offer at full capacity for the last two price scenarios. Thus, only four price-quantity pairs are observed in that offering curve.

The day-ahead market-clearing results are presented in Fig. 5.6b together with the total sched-

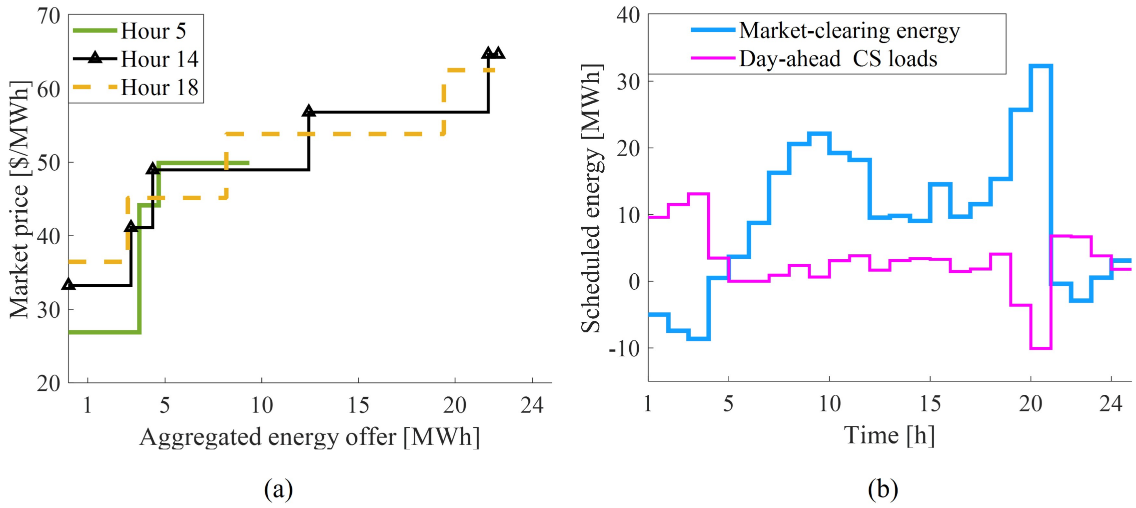

Figure 5.6: (a) typical offering curves, (b) day-ahead scheduling results

uled day-ahead charging station loads. Due to low average forecast prices, the aggregated VPP-CSs loads are negative in hours 1 to 4, suggesting that the considered VPP-CSs system is a consumer that imports energy from the grid. When forecast prices are high enough, to maximize the total profit, the VPP-CSs system not only offers its energy generation but also offers discharged EV energy to the market, such as in hours 19 and 20. In some hours, the market energy exchange is nearly zero, because the generated energy is used to satisfy EV charging demands, such as hours 4, 21, and 23.

The revenues and costs of the VPP-CSs system are shown in Fig. 5.7. The revenues include the day-ahead market revenue, EV charging revenue, and the balancing market revenue when there is an energy surplus. The costs include fuel costs, EV incentive costs, EV energy discharging costs, and balancing market costs when there is an energy deficiency. The largest revenue comes from the day-ahead market, which is $16,366 in total. The revenue for charging EVs is $5,930. Because the forecast renewable power generation is much lower than the actual renewable power output, the total balancing cost is $-650, which suggests that the VPP-CSs system is earning money from the balancing market under the dual pricing rule. The largest cost of the VPP-CSs system is the fuel cost, which is $11,251 in total. The total EV incentive cost is $964, which is mostly concentrated at high-price hours 19 and 20. Throughout the operating day, each EV user gets an average incentive payment of $0.475, which is 16.3% of their average charging cost ($2.920). Overall, the net profit of the VPP-CSs system over the day is $10,731.

The VPP load profile and revenue are also presented in Fig. 5.7. In Fig. 5.7, there are some

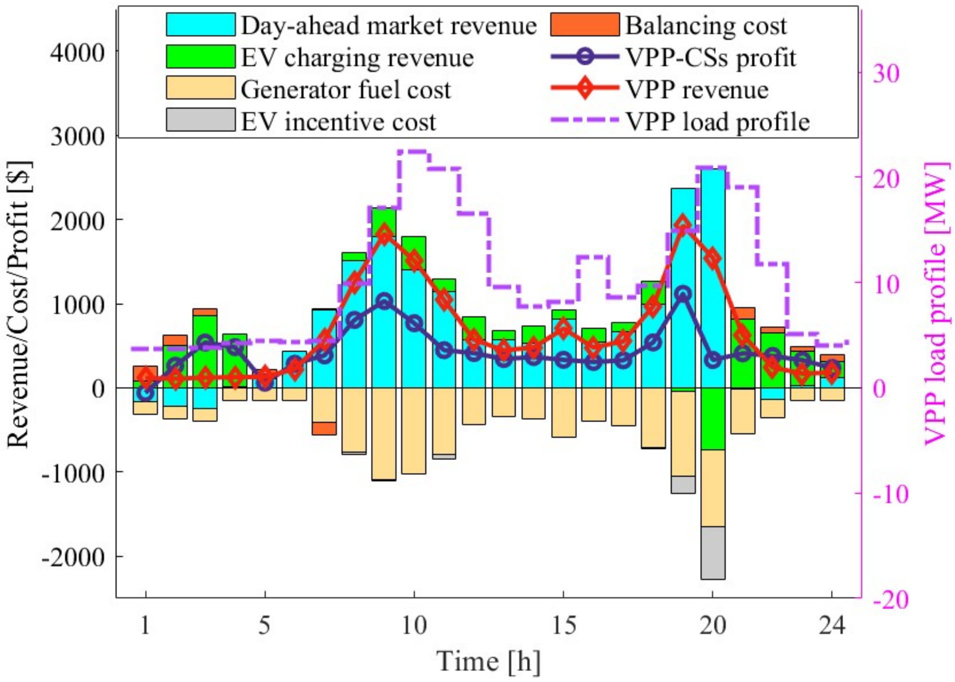

Figure 5.7: Optimization results of the VPP-CSs system

mismatches between the VPP revenue and VPP load profile. For example, the VPP produces the most energy in hour 10, whereas its revenue in hour 10 is not the highest. Such mismatches are caused by the energy prices in the electricity market. Due to the volatile energy prices, producing the same energy may lead to different VPP revenues.

Define the τ-value estimation accuracy θ_l for player l as (5.52), the average estimation accuracy by using the proposed estimated τ-value method can reach 99.2%.

$$\theta_l = 1 - \sqrt{\left(\frac{\tau_l^{est} - \tau_l^{conv}}{\tau_l^{conv}}\right)^2} \tag{5.52}$$

where τ_l^{est} and τ_l^{conv} are τ-values of player l obtained from the estimated and conventional τ-value methods, respectively.

By applying the estimated τ-value method and the conventional τ-value method, the profits of each player in the VPP-CSs system are presented in Fig. 5.8a. In Fig. 5.8a, the results obtained from the estimated and conventional τ-value methods are very close to each other, which further confirms that the proposed method can achieve accurate estimations.

To prove the performance of the proposed cooperative VPP-CSs operation framework, the profits of the non-cooperative case (VPP and each charging station operate separately) are

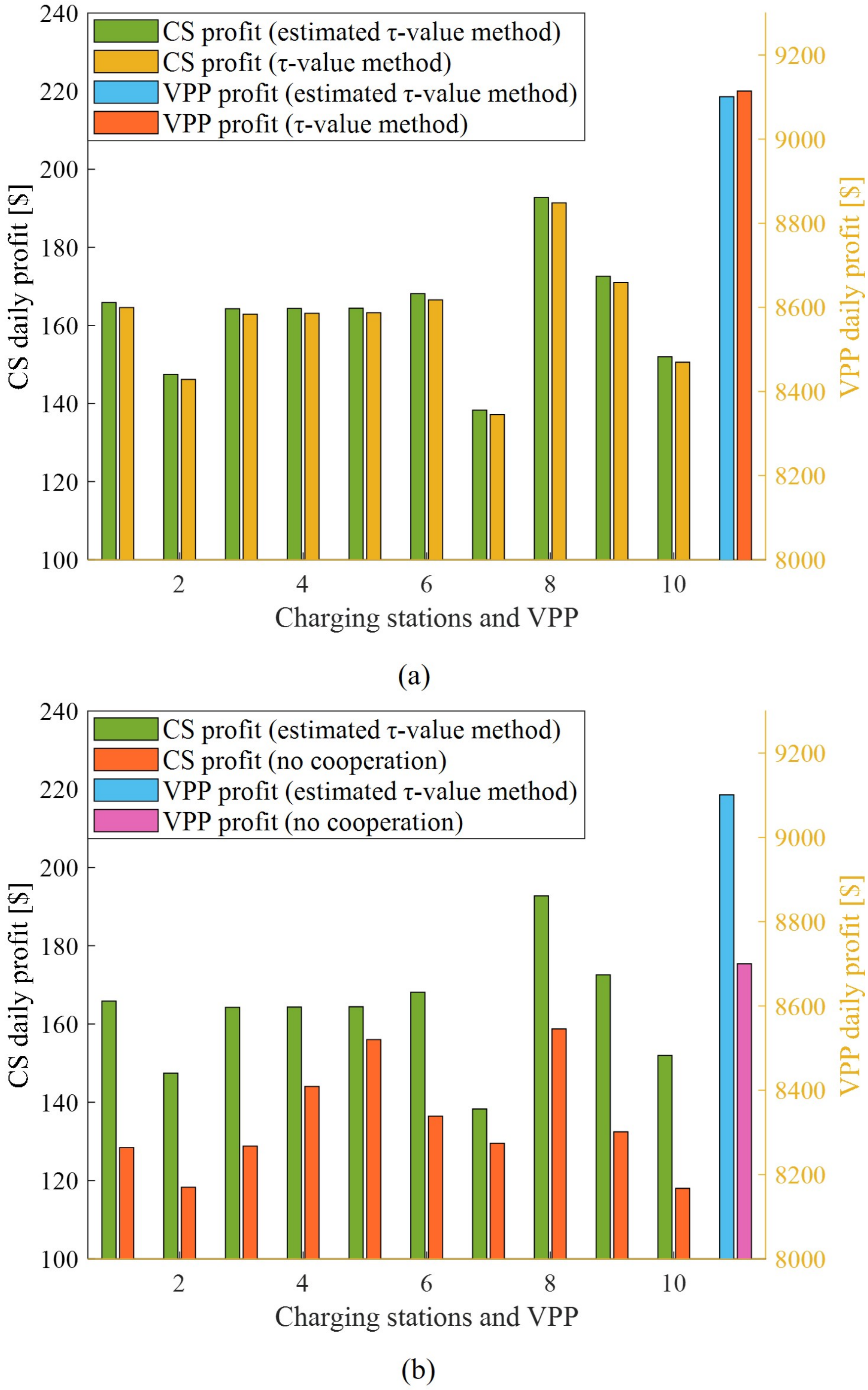

Figure 5.8: (a) Profits using the estimated τ-value method and standard τ-value method, (b) profits using the estimated τ-value method and under no cooperation.

Table 5.2: Comparison of different cooperative levels

Cooperative level	Deviation cost [$]	Incentive cost [$]	CS profit[$]	VPP profit [$]	Total profit [$]
Non-cooperative	-401	1,397	1350.8 (100%)	8700.2 (100%)	10,051 (100%)
Semi-cooperative	-523	1,398	1472.8 (109.0%)	8700.2 (100%)	10,173 (101.2%)
Cooperative	-650	964	1630.0 (120.7%)	9101.0 (104.6%)	10,731 (106.8%)

provided in Fig. 5.8b. The VPP profit increment is $400.8 as compared to the case of no cooperation ($8,700.2). The charging station profit increments are distributed from $8.4 to $37.4 with an average value of $27.9. Considering that the average charging station profit without cooperation is $135.1, the average charging station profit is increased by 20.7% through the proposed cooperative operation. As compared to the non-cooperation case, the proposed cooperative framework increases the total profit of the VPP-CSs system by 6.8%, from $10,051 to $10,731.

To further confirm the benefits of charging stations in collaborating with the VPP, the case in which the charging stations form a coalition without involving the VPP (semi-cooperative, case 2) is also investigated. The results are presented in Table 5.2 together with the non-cooperative case (VPP and each charging station operate separately, case 1) and the proposed cooperative framework (case 3). Notably, the data in Table 5.2 is the aggregated result of both the VPP and charging stations.

Comparing case 2 with case 1, the cooperation among charging stations can moderately reduce the total balancing cost of charging stations, and the incentive payment remains almost the same. Hence, in the semi-cooperative case, the profit increment mainly comes from the cross-balancing effect among the charging stations. When VPP is involved in the coalition, on the one hand, the cross-balancing effect is more significant. On the other hand, the VPP can absorb the charging station deviations at lower costs, hence, reducing both the balancing cost and the EV incentive cost. Consequently, in the cooperative case, the involvement of the VPP can bring a huge benefit to charging stations, as shown in Table 5.2.

Notably, it is assumed that charging stations can participate in the wholesale market in all

Table 5.3: Comparison of different incentive programs

VPP-CSs system	Benchmark	With V2G	With pay-as-bid	Proposed
Total revenue [$]	21,211	21,494	21,715	22,296
Total cost [$]	10,928	11,113	11,123	11,565
Total profit [$]	10,283 (100%)	10,381 (100.9%)	10,592 (103.0%)	10,731 (104.4%)
Incentive Payment [$]	489	716	630	964
Adopted energy flexibility [kWh]	15,686	20,774	22,114	30,090

cases. Whereas in practical scenarios, charging stations are generally not allowed to access the wholesale market due to their small capacities. In that case, they must face higher electricity prices from the distribution network operator.

To verify the superiority of the proposed incentive program, four incentive programs are evaluated in this chapter. Program 1 is the benchmark incentive program proposed in chapter 4, in which the V2G operation is not considered, and the uniform pricing mechanism is used. In program 2, the V2G operation is added on top of the benchmark program. In program 3, the uniform pricing in the benchmark program is replaced with the pay-as-bid mechanism. Program 4 is the proposed incentive program, which concurrently adopts the V2G operation and the pay-as-bid rule. The optimization results of different programs are summarized in Table 5.3.

By comparing program 2 with the benchmark, one can observe that with the V2G operation, the profit of the VPP-CSs system is increased by $98, and the incentive payment for EV users is increased by $227. These economic benefits are generated by adopting EV discharging energy flexibility through the V2G operation. The advantage of the pay-as-bid rule can be demonstrated by comparing program 3 with the benchmark. In program 3, the pay-as-bid rule allows 6,428 kWh more EV energy flexibility to be adopted as compared to the uniform pricing mechanism, suggesting that the pay-as-bid rule is more efficient in encouraging the utilization of EV energy flexibility. With an increased EV energy flexibility utilization rate, the total profit of the VPP-CSs system and the total incentive payment for EV users are increased by $309 and $141, respectively. When both the V2G operation and pay-as-bid are considered, as in the proposed incentive program, the incentive payment for EV users almost doubled (from $489 to

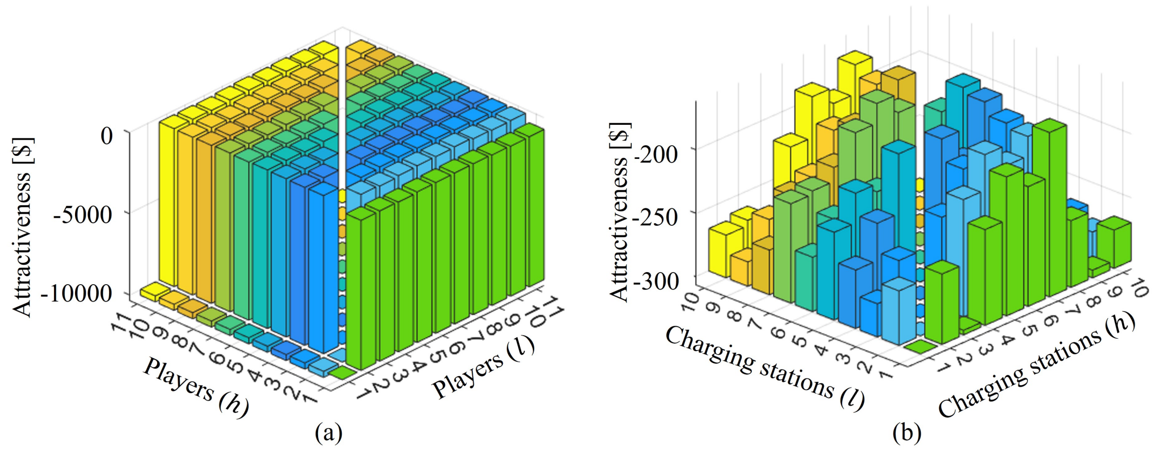

Figure 5.9: Attractive matrix for (a) all players and (b) charging stations only.

$964). For the VPP-CSs system, its total profit is also increased by $448, which is 4.4% of its total profit. Besides, by using the proposed incentive program, the adopted EV energy flexibility is almost twice of the adopted EV energy flexibility from the benchmark, which confirms its superiority in encouraging the utilization of EV energy flexibility.

5.5.3 τ-value Estimation

This sub-section provides some analysis of the proposed estimation approach. The obtained attractiveness matrix is presented in Fig. 5.9. In Fig. 5.9a, the VPP is set to be player 1, and charging stations are set to be players 2 to 11. As shown in Fig. 5.9a, the attractiveness of charging stations to the VPP is much smaller than their attractiveness to other charging stations. This is because the VPP has much larger remainders than charging stations in all cases. Besides, the VPP's attractiveness to other charging stations is also obviously lower than the attractiveness of charging stations to other charging stations. This is because the utopia cost of the VPP is much lower than the total cost of any two-player coalition that includes the VPP and a charging station. To show the variance of the attractiveness matrix more clearly, the rest part of the attractiveness matrix without the VPP is presented in Fig. 5.9b, which shows that the attractiveness between different players can be very different. Fig. 5.9b also gives straightforward information on which players are more attractive to the considered player when estimating the maximum right cost for player l. Notably, in the diagonals of Fig. 5.9, the attractiveness is not presented because they represent one-member coalitions.

The remainders for all players under different coalition sizes are shown in Fig. 5.10. Fig.

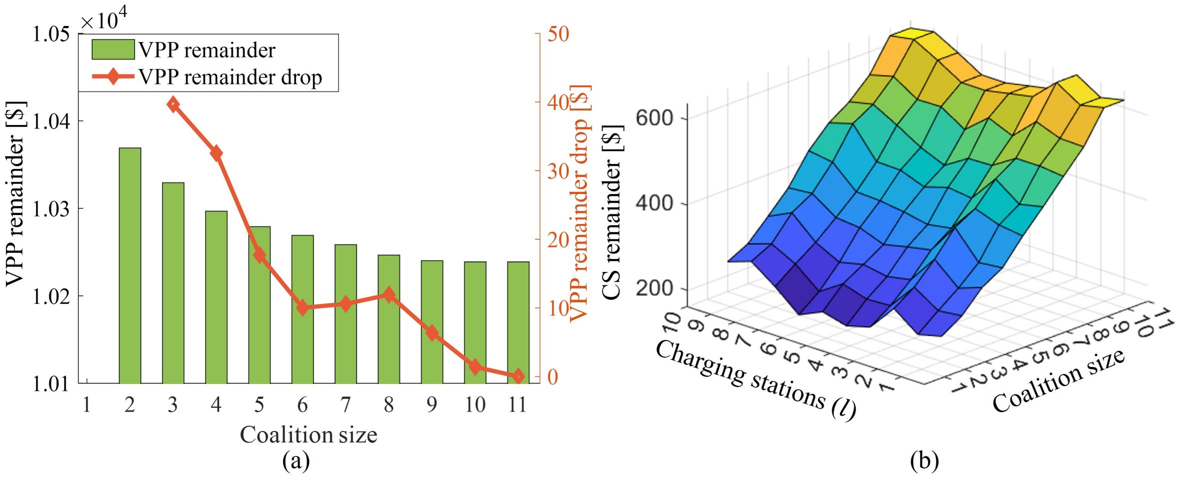

Figure 5.10: (a) Remainders and remainder drops for the VPP, (b) remainders for charging stations.

5.10a provides the remainders for the VPP. One can observe that the remainder for the VPP gradually decreases with increasing coalition sizes until coalition sizes 10 and 11, in which the VPP remainder reaches $10,238.9. Besides, Fig. 5.10a also shows that with increasing coalition sizes, the VPP remainder drops most significantly when coalition sizes are small, which suggests that cooperation with more attractive charging stations can give more remainder drops for the VPP. The remainders of charging stations are shown in Fig. 5.10b, which tells that the remainders of charging stations are always increasing with enlarged coalition sizes. Hence, the global minimum remainders of charging stations are all obtained by forming two-member coalitions of charging station l and its most attractive player h_1^l.

The ratios between the estimated τ-values and the actual τ-values under different $|S|_{max}$ and J are presented in Fig. 11. In Fig. 5.11, the VPP is player 1, and charging stations are players 2 to 11. Because $|S|_{max}$ is uniquely related to J, only J is used to represent each $|S|_{max}$ and J combination. As shown in Fig. 11, when $J = 2$, the maximum deviation of the estimated τ-value from the true τ-value is about 2%. The τ-value estimation deviations are gradually reduced with increased coalition samples. Such deviation reduction is less significant for larger estimation sizes, suggesting that the marginal effect of considering larger coalition sizes is decreasing.

By using the proposed τ-value estimation approach, the minimum $|S|_{max}$ and J that can satisfy this accuracy threshold are 4 and 3, respectively. In that case, the maximum number of coalitions that should be evaluated in the estimation process is $N_{max}^{eval} = 188$, which is much less than

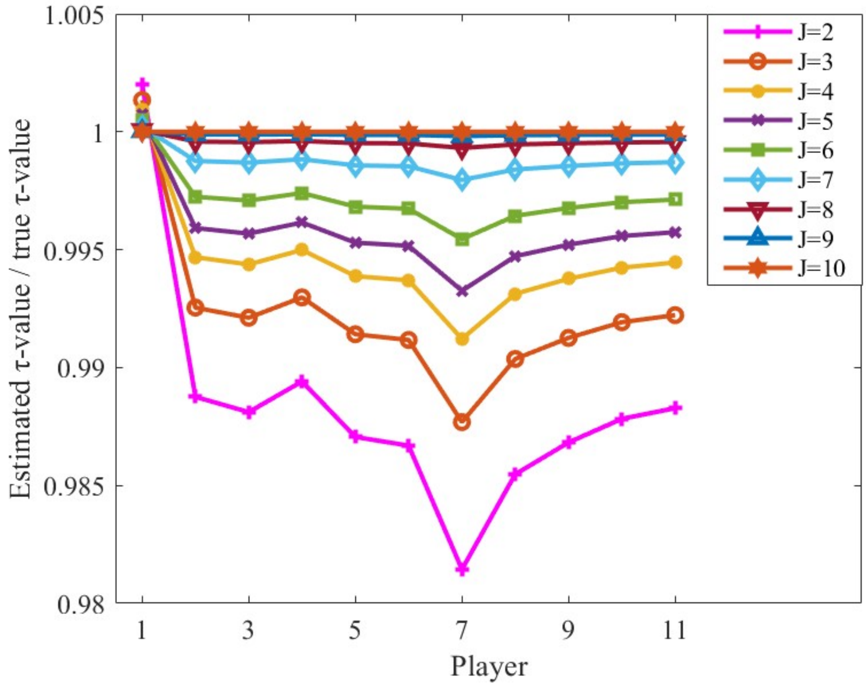

Figure 5.11: Estimated deviations under different J and $|S|_{max}$.

2,048 evaluations of the conventional τ-value method. To show the scalability of the proposed cost allocation method, the required numbers of evaluations using the conventional τ-value method, the coalitional τ-value method (Casas-Méndez et al. 2003), and the proposed estimation approach are presented in Fig. 5.12. In the coalitional τ-value method, it is assumed that there are three prior unions, including the VPP and two charging station unions. In Fig. 5.12, as the coalition size grows, the conventional τ-value method becomes computationally impractical because of its exponential computational complexity. Compared with the coalitional τ-value method, the proposed estimated τ-value method suffers slightly more computational burden at small coalition sizes ($N \leq 10$). As the number of players grows, the computational burden of the coalitional τ-value method also grows exponentially, whereas the number of computations of the proposed method remains to be low.

Notably, under the distributed solution approach, the proposed methods have good scalability concerning the number of EVs. The solution time for the real-time scheduling problem is mainly affected by the charging station that has the most EVs to be scheduled. Normally, it takes a few seconds to solve a single real-time scheduling problem. Besides, evaluating a single sub-coalition requires solving the real-time scheduling problem 96 times. On average, evaluating one sub-coalition takes 198.9s.

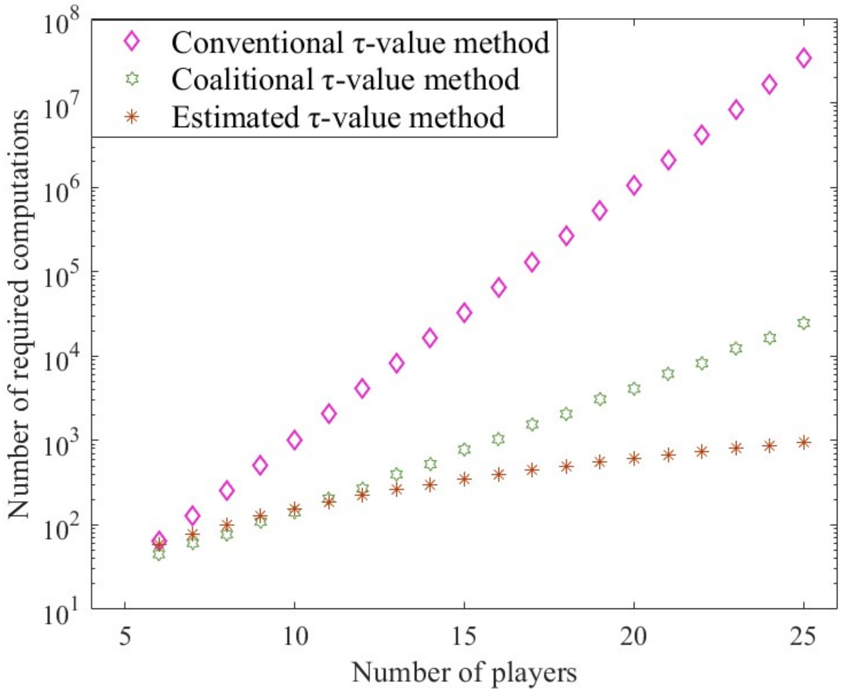

Figure 5.12: Computational performance comparison.

5.6 Chapter Summary

This chapter is devoted to proposing a cooperative operation framework for VPPs and charging stations that have different interests. To support the flexible operation of the considered VPP-CSs system, an EV user incentive program is proposed for acquiring EV energy flexibility. To efficiently address the conflicting interests between different stakeholders, an estimated τ-value cost allocation method is also proposed.

In the cooperative framework, the cross-balancing effect that can reduce the deviation cost is obvious among the players. To fully make use of this cross-balancing effect, large EV charging management platforms should be established to collectively manage the charging load of larger EV fleets. Besides, new electricity market products should be designed to further unleash the potential of EV energy flexibility. As compared to the case of no cooperation, the average charging station profit and VPP profit has been increased by 20.7% and 4.6%, respectively, achieving a win-win situation for all members. For the proposed EV user incentive program, numerical results suggest that both the V2G operation and pay-as-bid strategy can enhance the profitability of the considered system. But the improvement from adopting the pay-as-bid strategy (3.0%) is more obvious than involving the V2G operation (0.9%). For the considered VPP-CSs system, compared to the conventional τ-value method, the proposed τ-value estimation approach can reduce the computational burden from 2047 evaluations to 188 evaluations, meanwhile, achieving an average of 99.2% estimation accuracy. As compared to the coalitional τ-value method, the proposed method can also significantly reduce the computational burden for large coalitions. The computational burden reduction of the proposed method will become more significant as the size of the coalition grows.

Based on the methods developed in previous chapters, this chapter further proposes a multi-stakeholder operation framework for VPP and EV charging stations to coordinately manage DERs to improve the financial benefits of all stakeholders. To this end, the methodologies developed in this thesis provide DER operators with solutions for several important problems, including exchanging energy and energy flexibility with the electricity markets, handling uncertainties in DER operation, and effectively coordinating different DER components as well as stakeholders to operate as a whole system.

Chapter 6

Conclusion

Power systems are transforming to provide cleaner, cheaper, and more reliable electricity, and developing DERs is becoming a key enabler for supporting the upgrade of power systems. Because of the distributed and stochastic nature of DERs, better energy management methods need to be developed to seize the opportunities and deal with the challenges brought by the massive integration of DERs.

The primary objective of this thesis is to propose economic operation strategies for VPPs and EV charging stations to improve the financial benefits of managing the energy and energy flexibility of DERs. To realize the target, this thesis first proposes an optimal VPP operation framework considering multiple electricity markets under multiple uncertainties. Then, an EV charging station energy management strategy is proposed by taking EV user incentives into account. Based on the methods proposed for VPPs and EV charging stations, the operation of a multi-stakeholder VPP-CSs system is further investigated to allow cooperation between VPPs and EV charging stations.

The methods proposed in this thesis can help VPP and EV charging station operators improve their financial benefits by effectively managing the DER energy and interacting with the electricity markets. The major contributions of this thesis can be summarized as follows:

(1) An optimal VPP operation regime considering multiple electricity markets and multiple uncertainties is proposed. The proposed operation regime includes a day-ahead market bidding model and a real-time energy scheduling model. In the day-ahead bidding stage, the developed price-dependent offering strategy improves the bidding flexibility of the VPP in the energy

market. Also, the proposed stochastic minimax regret optimization model utilizes a combination of scenarios and confidence intervals to describe the uncertainties, making it advantageous for problems where some uncertainties have accurate probability distributions while others do not. In the real-time energy scheduling stage, the proposed self-adaptive algorithm optimally determines the size of the confidence intervals in a look-back-and-adjust manner. The proposed methods improve the decision-making flexibility of the VPP in both market participation and energy scheduling problems, which significantly enhances the VPP's profitability.

(2) An EV charging station energy management strategy with an EV user incentive program is proposed. Besides, an optimal pricing model is developed to help the EV charging station optimally determine the incentive price that can maximize its financial benefit. To deal with the dimensionality of the EV charging station operation problem, an ADMM algorithm with adaptive penalty factors is further proposed. As compared to traditional static and dynamic incentive programs, the proposed EV charging station operation strategy simultaneously realizes simplicity, consistency, and controllability in the interactions with EV users, making the proposed methods highly potential for practical implementations.

(3) A mutually beneficial operation framework is proposed for VPPs considering EV charging stations. The proposed operation framework handles the conflicting interests of different stakeholders by using the cooperative game theory. To support the flexible operation of the investigated VPP-CSs system, an EV user incentive program is proposed. The cost allocation problem between different stakeholders is addressed by using the τ-value method. To facilitate practical applications of the proposed methods, the computational intractability of the τ-value method is addressed by a proposed estimation approach. The proposed VPP-CSs operation allows VPPs to integrate EV fleets to perform similar functionalities of energy storage systems, hence, reducing the capital cost of building additional energy storage devices. EV charging stations can also benefit from this cooperation and improve their financial gains.

In the future, several interesting topics can be further investigated as the extension of the methods proposed in this thesis, including:

(1) More energy flexibility products can be considered to diversify the income sources. This thesis only considers energy and reserve products, which cannot fully exploit the potential of DERs. Some other electricity market products such as frequency regulation service, voltage regulation service, and ramping flexibility (Wang and Hobbs 2014) service can be involved in

the operation to increase the profitability of managing DERs.

(2) Real-world data can be used and analyzed by machine-learning techniques to replace some assumptions in this thesis. For example, the EV user price preferences are assumed to follow the normal distribution, which may not be accurate in general. If real-world EV user charging price data can be acquired, some machine-learning techniques such as neural networks and decision tree models can be applied to estimate the price sensitivity of EV users.

(3) The economic analysis in this work only considers the operation stage. Future works can extend the analysis horizon to include the cost of investment, maintenance, reuse, recycling, and disposal of DERs to analyze the economics over a longer period.

(4) This thesis is based on steady-state analysis, the time-varying features such as system voltage and frequency during operation may also be included in further research.

References

Aasgård, Ellen Krohn et al. (2019). "Hydropower bidding in a multi-market setting". In: *Energy Systems* 10, pp. 543–565.

Abbasi, Mohammad Hossein et al. (2019). "Coordinated operation of electric vehicle charging and wind power generation as a virtual power plant: A multi-stage risk constrained approach". In: *Applied Energy* 239, pp. 1294–1307.

Aboli, Reza, Ramezani, Maryam, and Falaghi, Hamid (2019). "Joint optimization of day-ahead and uncertain near real-time operation of microgrids". In: *International Journal of Electrical Power & Energy Systems* 107, pp. 34–46.

Alahyari, Arman, Ehsan, Mehdi, and Mousavizadeh, MirSaeed (2019). "A hybrid storage-wind virtual power plant (VPP) participation in the electricity markets: A self-scheduling optimization considering price, renewable generation, and electric vehicles uncertainties". In: *Journal of Energy Storage* 25, p. 100812.

Aliasghari, Parinaz, Mohammadi-Ivatloo, Behnam, and Abapour, Mehdi (2020). "Risk-based scheduling strategy for electric vehicle aggregator using hybrid Stochastic/IGDT approach". In: *Journal of Cleaner Production* 248, p. 119270.

Baringo, Ana and Baringo, Luis (2016). "A stochastic adaptive robust optimization approach for the offering strategy of a virtual power plant". In: *IEEE Transactions on Power Systems* 32.5, pp. 3492–3504.

Baringo, Ana, Baringo, Luis, and Arroyo, Jose M (2018a). "Day-ahead self-scheduling of a virtual power plant in energy and reserve electricity markets under uncertainty". In: *IEEE Transactions on Power Systems* 34.3, pp. 1881–1894.

Baringo, Ana, Baringo, Luis, and Arroyo, José M (2018b). "Self scheduling of a virtual power plant in energy and reserve electricity markets: A stochastic adaptive robust optimization approach". In: *2018 Power Systems Computation Conference (PSCC)*. IEEE, pp. 1–7.

Behi, Behnaz et al. (2021). "Advanced monitoring and control system for virtual power plants for enabling customer engagement and market participation". In: *Energies* 14.4, p. 1113.

Bhuiyan, Erphan A et al. (2021). "Towards next generation virtual power plant: Technology review and frameworks". In: *Renewable and Sustainable Energy Reviews* 150, p. 111358.

Bibak, Bijan and Tekiner-Moğulkoç, Hatice (2021). "A comprehensive analysis of Vehicle to Grid (V2G) systems and scholarly literature on the application of such systems". In: *Renewable Energy Focus* 36, pp. 1–20.

Boyd, Stephen et al. (2011). "Distributed optimization and statistical learning via the alternating direction method of multipliers". In: *Foundations and Trends® in Machine learning* 3.1, pp. 1–122.

Braslavsky, Julio H, Wall, Josh R, and Reedman, Luke J (2015). "Optimal distributed energy resources and the cost of reduced greenhouse gas emissions in a large retail shopping centre". In: *Applied Energy* 155, pp. 120–130.

Brinkel, NBG et al. (2020). "Impact of rapid PV fluctuations on power quality in the low-voltage grid and mitigation strategies using electric vehicles". In: *International Journal of Electrical Power & Energy Systems* 118, p. 105741.

Camal, Simon, Michiorri, Andrea, and Kariniotakis, George (2018). "Optimal offer of automatic frequency restoration reserve from a combined PV/wind virtual power plant". In: *IEEE Transactions on Power Systems* 33.6, pp. 6155–6170.

Cao, Yan et al. (2020). "Optimal scheduling of electric vehicles aggregator under market price uncertainty using robust optimization technique". In: *International Journal of Electrical Power & Energy Systems* 117, p. 105628.

Casas-Méndez, Balbina et al. (2003). "An extension of the τ-value to games with coalition structures". In: *European Journal of Operational Research* 148.3, pp. 494–513.

Chen, Bokan et al. (2014). "Robust optimization for transmission expansion planning: Minimax cost vs. minimax regret". In: *IEEE Transactions on Power Systems* 29.6, pp. 3069–3077.

Chen, Xia, Hou, Yunhe, and Hui, SY Ron (2016). "Distributed control of multiple electric springs for voltage control in microgrid". In: *IEEE Transactions on Smart Grid* 8.3, pp. 1350–1359.

Chung, Hwei-Ming et al. (2018). "Electric vehicle charge scheduling mechanism to maximize cost efficiency and user convenience". In: *IEEE Transactions on Smart Grid* 10.3, pp. 3020–3030.

Dabbagh, Saeed Rahmani and Sheikh-El-Eslami, Mohammad Kazem (2015). "Risk-based profit allocation to DERs integrated with a virtual power plant using cooperative Game theory". In: *Electric Power Systems Research* 121, pp. 368–378.

Das, Ridoy et al. (2020). "Multi-objective techno-economic-environmental optimisation of electric vehicle for energy services". In: *Applied Energy* 257, p. 113965.

Day Ahead Auction Prices (2019). Nordpoolgroup. URL: `https://www.nordpoolgroup.com/Marketdata1/GB/Auction-prices/UK/Hourly/?view=table` (visited on 03/07/2021).

DER classification (2021). AEMC. URL: `https://www.aemc.gov.au/energy-system/electricity/electricity-system/distributed-energy-resources` (visited on 12/07/2022).

Divshali, Poria Hasanpor and Evens, Corentin (2020). "Stochastic bidding strategy for electrical vehicle charging stations to participate in frequency containment reserves markets". In: *IET Generation, Transmission & Distribution* 14.13, pp. 2566–2572.

Dong, Xiaohong et al. (2018). "A charging pricing strategy of electric vehicle fast charging stations for the voltage control of electricity distribution networks". In: *Applied energy* 225, pp. 857–868.

Duan, Xiaoyu, Hu, Zechun, and Song, Yonghua (2020). "Bidding strategies in energy and reserve markets for an aggregator of multiple EV fast charging stations with battery storage". In: *IEEE Transactions on Intelligent Transportation Systems* 22.1, pp. 471–482.

Dubey, Anamika et al. (2015). “Determining time-of-use schedules for electric vehicle loads: A practical perspective”. In: *IEEE Power and Energy Technology Systems Journal* 2.1, pp. 12–20.

Fachrizal, Reza et al. (2020). “Smart charging of electric vehicles considering photovoltaic power production and electricity consumption: A review”. In: *ETransportation* 4, p. 100056.

Fan, Lei et al. (2014). “Min-max regret bidding strategy for thermal generator considering price uncertainty”. In: *IEEE Transactions on Power Systems* 29.5, pp. 2169–2179.

Fan, Shuai et al. (2020). “Optimal coordination of virtual power plant with photovoltaics and electric vehicles: A temporally coupled distributed online algorithm”. In: *Applied energy* 277, p. 115583.

Fathabadi, Hassan (2017). “Novel solar powered electric vehicle charging station with the capability of vehicle-to-grid”. In: *Solar Energy* 142, pp. 136–143.

Ferruzzi, Gabriella et al. (2016). “Optimal bidding in a Day-Ahead energy market for Micro Grid under uncertainty in renewable energy production”. In: *Energy* 106, pp. 194–202.

Fleten, Stein-Erik and Kristoffersen, Trine Krogh (2007). “Stochastic programming for optimizing bidding strategies of a Nordic hydropower producer”. In: *European Journal of Operational Research* 181.2, pp. 916–928.

Foroughi, Mehdi et al. (2021). “A bi-level model for optimal bidding of a multi-carrier technical virtual power plant in energy markets”. In: *International Journal of Electrical Power & Energy Systems* 125, p. 106397.

Gazijahani, Farhad Samadi and Salehi, Javad (2017). “Optimal bilevel model for stochastic risk-based planning of microgrids under uncertainty”. In: *IEEE Transactions on Industrial Informatics* 14.7, pp. 3054–3064.

Giuntoli, Marco and Poli, Davide (2013). “Optimized thermal and electrical scheduling of a large scale virtual power plant in the presence of energy storages”. In: *IEEE Transactions on Smart Grid* 4.2, pp. 942–955.

Global electric car stock (2022). IEA. URL: `https://www.iea.org/data-and-statistics/charts/global-electric-car-stock-2010-2021` (visited on 10/12/2022).

Gray, Matthew K and Morsi, Walid G (2014). "Power quality assessment in distribution systems embedded with plug-in hybrid and battery electric vehicles". In: *IEEE Transactions on Power Systems* 30.2, pp. 663–671.

GUROBI optimizer (2022). GUROBI. URL: `https://www.gurobi.com/products/gurobi-optimizer` (visited on 01/15/2022).

Hadayeghparast, Shahrzad, Farsangi, Alireza SoltaniNejad, and Shayanfar, Heidarali (2019). "Day-ahead stochastic multi-objective economic/emission operational scheduling of a large scale virtual power plant". In: *Energy* 172, pp. 630–646.

Hajebrahimi, Ali et al. (2020). "Scenario-wise distributionally robust optimization for collaborative intermittent resources and electric vehicle aggregator bidding strategy". In: *IEEE transactions on power systems* 35.5, pp. 3706–3718.

Hashemi, Behzad, Shahabi, Majid, and Teimourzadeh-Baboli, Payam (2019). "Stochastic-based optimal charging strategy for plug-in electric vehicles aggregator under incentive and regulatory policies of DSO". In: *IEEE Transactions on Vehicular Technology* 68.4, pp. 3234–3245.

Hedegaard, Rasmus Elbæk, Pedersen, Theis Heidmann, and Petersen, Steffen (2017). "Multimarket demand response using economic model predictive control of space heating in residential buildings". In: *Energy and Buildings* 150, pp. 253–261.

Heidari, Rahmat, Seron, Maria M, and Braslavsky, Julio H (2017). "Ultimate boundedness and regions of attraction of frequency droop controlled microgrids with secondary control loops". In: *Automatica* 81, pp. 416–428.

Heilmann, C and Friedl, G (2021). "Factors influencing the economic success of grid-to-vehicle and vehicle-to-grid applications—A review and meta-analysis". In: *Renewable and Sustainable Energy Reviews* 145, p. 111115.

Heinisch, Verena et al. (2021). “Smart electric vehicle charging strategies for sectoral coupling in a city energy system”. In: *Applied Energy* 288, p. 116640.

Hoque, Md Murshadul et al. (2021). “Transactive coordination of electric vehicles with voltage control in distribution networks”. In: *IEEE Transactions on Sustainable Energy* 13.1, pp. 391–402.

Hu, Zechun et al. (2016). “Pricing mechanisms design for guiding electric vehicle charging to fill load valley”. In: *Applied Energy* 178, pp. 155–163.

IEA (2022). *World Energy Outlook 2022*. Tech. rep. URL: `https://www.iea.org/reports/world-energy-outlook-2022` (visited on 03/13/2023).

Injeti, Satish Kumar and Thunuguntla, Vinod Kumar (2020). “Optimal integration of DGs into radial distribution network in the presence of plug-in electric vehicles to minimize daily active power losses and to improve the voltage profile of the system using bio-inspired optimization algorithms”. In: *Protection and Control of Modern Power Systems* 5, pp. 1–15.

Iqbal, Sheeraz et al. (2020). “V2G strategy for primary frequency control of an industrial microgrid considering the charging station operator”. In: *Electronics* 9.4, p. 549.

Jafari, Mehran and Foroud, Asghar Akbari (2020). “A medium/long-term auction-based coalition-forming model for a virtual power plant based on stochastic programming”. In: *International Journal of Electrical Power & Energy Systems* 118, p. 105784.

Jia, Youwei et al. (2019). “A retroactive approach to microgrid real-time scheduling in quest of perfect dispatch solution”. In: *Journal of Modern Power Systems and Clean Energy* 7.6, pp. 1608–1618.

Jia, Youwei et al. (2020). “A novel retrospect-inspired regime for microgrid real-time energy scheduling with heterogeneous sources”. In: *IEEE Transactions on Smart Grid* 11.6, pp. 4614–4625.

Jiang, Ruiwei et al. (2013). “Two-stage minimax regret robust unit commitment”. In: *IEEE Transactions on Power Systems* 28.3, pp. 2271–2282.

Jin, Jiangliang and Xu, Yunjian (2020). “Optimal policy characterization enhanced actor-critic approach for electric vehicle charging scheduling in a power distribution network”. In: *IEEE Transactions on Smart Grid* 12.2, pp. 1416–1428.

Jirdehi, Mehdi Ahmadi et al. (2020). “Different aspects of microgrid management: A comprehensive review”. In: *Journal of Energy Storage* 30, p. 101457.

Jovanovic, Raka and Bayram, Islam Safak (2019). “Scheduling electric vehicle charging at park-and-ride facilities to flatten duck curves”. In: *2019 IEEE Vehicle Power and Propulsion Conference (VPPC)*. IEEE, pp. 1–5.

Ju, Liwei et al. (2016a). “A bi-level stochastic scheduling optimization model for a virtual power plant connected to a wind–photovoltaic–energy storage system considering the uncertainty and demand response”. In: *Applied energy* 171, pp. 184–199.

Ju, Liwei et al. (2016b). “Multi-objective stochastic scheduling optimization model for connecting a virtual power plant to wind-photovoltaic-electric vehicles considering uncertainties and demand response”. In: *Energy Conversion and Management* 128, pp. 160–177.

Ju, Liwei et al. (2019). “A multi-objective robust scheduling model and solution algorithm for a novel virtual power plant connected with power-to-gas and gas storage tank considering uncertainty and demand response”. In: *Applied Energy* 250, pp. 1336–1355.

Jun, PL, Jun, DongDong, and Linpeng, Nie (2019). “Decision-making model of virtual power plant for participating in spot market transaction based on hybrid stochastic and robust approach”. In: *Am. J. Environ. Resour. Econ* 4.1, p. 32.

Kardakos, Evaggelos G, Simoglou, Christos K, and Bakirtzis, Anastasios G (2015). “Optimal offering strategy of a virtual power plant: A stochastic bi-level approach”. In: *IEEE Transactions on Smart Grid* 7.2, pp. 794–806.

Karimyan, Peyman et al. (2016). “Stochastic approach to represent distributed energy resources in the form of a virtual power plant in energy and reserve markets”. In: *IET Generation, Transmission & Distribution* 10.8, pp. 1792–1804.

Kasaei, Mohammad Javad, Gandomkar, Majid, and Nikoukar, Javad (2017). "Optimal management of renewable energy sources by virtual power plant". In: *Renewable energy* 114, pp. 1180–1188.

Khooban, Mohammad Hassan et al. (2017). "A new load frequency control strategy for micro-grids with considering electrical vehicles". In: *Electric Power Systems Research* 143, pp. 585–598.

Ko, Kab Seok, Han, Sekyung, and Sung, Dan Keun (2016). "Performance-based settlement of frequency regulation for electric vehicle aggregators". In: *IEEE Transactions on Smart Grid* 9.2, pp. 866–875.

Kong, Peng-Yong and Karagiannidis, George K (2016). "Charging schemes for plug-in hybrid electric vehicles in smart grid: A survey". In: *IEEE Access* 4, pp. 6846–6875.

Kong, Xiangyu et al. (2019). "Bi-level multi-time scale scheduling method based on bidding for multi-operator virtual power plant". In: *Applied Energy* 249, pp. 178–189.

Kong, Xiangyu et al. (2020). "Robust stochastic optimal dispatching method of multi-energy virtual power plant considering multiple uncertainties". In: *Applied Energy* 279, p. 115707.

Koraki, Despina and Strunz, Kai (2017). "Wind and solar power integration in electricity markets and distribution networks through service-centric virtual power plants". In: *IEEE Transactions on Power Systems* 33.1, pp. 473–485.

Koufakis, Alexandros-Michail et al. (2019). "Offline and online electric vehicle charging scheduling with V2V energy transfer". In: *IEEE Transactions on Intelligent Transportation Systems* 21.5, pp. 2128–2138.

Kouka, Karima et al. (2020). "Dynamic energy management of an electric vehicle charging station using photovoltaic power". In: *Sustainable Energy, Grids and Networks* 24, p. 100402.

Li, Desheng et al. (2020). "An energy management strategy with renewable energy and energy storage system for a large electric vehicle charging station". In: *Etransportation* 6, p. 100076.

Li, Jianwei et al. (2017). “Design/test of a hybrid energy storage system for primary frequency control using a dynamic droop method in an isolated microgrid power system”. In: *Applied Energy* 201, pp. 257–269.

Li, Sichen et al. (2022). “EV Charging Strategy Considering Transformer Lifetime via Evolutionary Curriculum Learning-Based Multiagent Deep Reinforcement Learning”. In: *IEEE Transactions on Smart Grid* 13.4, pp. 2774–2787.

Li, Yang et al. (2018). “Optimal operation strategy for integrated natural gas generating unit and power-to-gas conversion facilities”. In: *IEEE Transactions on Sustainable Energy* 9.4, pp. 1870–1879.

Liang, Zheming and Guo, Yuanxiong (2016). “Robust optimization based bidding strategy for virtual power plants in electricity markets”. In: *2016 IEEE Power and Energy Society General Meeting (PESGM)*. IEEE, pp. 1–5.

Limmer, Steffen and Rodemann, Tobias (2019). “Peak load reduction through dynamic pricing for electric vehicle charging”. In: *International Journal of Electrical Power & Energy Systems* 113, pp. 117–128.

Liu, Guodong, Xu, Yan, and Tomsovic, Kevin (2015). “Bidding strategy for microgrid in day-ahead market based on hybrid stochastic/robust optimization”. In: *IEEE Transactions on Smart Grid* 7.1, pp. 227–237.

Liu, Hong et al. (2015). “An optimization strategy of controlled electric vehicle charging considering demand side response and regional wind and photovoltaic”. In: *Journal of Modern Power Systems and Clean Energy* 3.2, pp. 232–239.

Liu, Wei-Li et al. (2019). “Coordinated charging scheduling of electric vehicles: a mixed-variable differential evolution approach”. In: *IEEE Transactions on Intelligent Transportation Systems* 21.12, pp. 5094–5109.

Liu, Wenjie et al. (2021). “Optimal reserve management of electric vehicle aggregator: Discrete bilevel optimization model and exact algorithm”. In: *IEEE Transactions on Smart Grid* 12.5, pp. 4003–4015.

Liu, Zhaoxi et al. (2018). "Two-stage optimal scheduling of electric vehicle charging based on transactive control". In: *IEEE Transactions on Smart Grid* 10.3, pp. 2948–2958.

Luis, Baringo and Morteza, Rahimiyan (2021). *Virtual Power Plants and Electricity Markets.*

Luo, Yugong et al. (2020). "Charging scheduling strategy for different electric vehicles with optimization for convenience of drivers, performance of transport system and distribution network". In: *Energy* 194, p. 116807.

Ma, Jiayi et al. (2017). "Ultra-short-term wind generation forecast based on multivariate empirical dynamic modeling". In: *IEEE Transactions on Industry Applications* 54.2, pp. 1029–1038.

Mashhour, Elaheh and Moghaddas-Tafreshi, Seyed Masoud (2010). "Bidding strategy of virtual power plant for participating in energy and spinning reserve markets—Part I: Problem formulation". In: *IEEE Transactions on Power Systems* 26.2, pp. 949–956.

Mei, Jie et al. (2019). "Coalitional game theory based local power exchange algorithm for networked microgrids". In: *Applied energy* 239, pp. 133–141.

Merritt, Noel Richard, Chakraborty, Chandan, and Bajpai, Prabodh (2017). "New voltage control strategies for VSC-based DG units in an unbalanced microgrid". In: *IEEE Transactions on Sustainable Energy* 8.3, pp. 1127–1139.

Ministry of, Power (2021). *Handbook of Electric Vehicle Charging Infrastructure Implementation.* Tech. rep. URL: `https://evstory.b-cdn.net/wp-content/uploads/2022/07/HandbookforEVChargingInfrastructureImplementation081221.pdf` (visited on 03/13/2023).

Moghaddam, Zeinab et al. (2017). "Smart charging strategy for electric vehicle charging stations". In: *IEEE Transactions on transportation electrification* 4.1, pp. 76–88.

Moghaddam, Zeinab et al. (2019). "A coordinated dynamic pricing model for electric vehicle charging stations". In: *IEEE Transactions on Transportation Electrification* 5.1, pp. 226–238.

Mouli, GR Chandra, Bauer, Pavol, and Zeman, Miro (2016). "System design for a solar powered electric vehicle charging station for workplaces". In: *Applied Energy* 168, pp. 434–443.

Muhtadi, Abir et al. (2021). "Distributed energy resources based microgrid: Review of architecture, control, and reliability". In: *IEEE Transactions on Industry Applications* 57.3, pp. 2223–2235.

Muñoz, Edgar Ramos et al. (2016). "Electric vehicle charging algorithms for coordination of the grid and distribution transformer levels". In: *Energy* 113, pp. 930–942.

Naval, Natalia and Yusta, Jose M (2021). "Virtual power plant models and electricity markets-A review". In: *Renewable and Sustainable Energy Reviews* 149, p. 111393.

Navigant (2019). *Global DER Overview*. Tech. rep. URL: `https://www.navigantresearch.com/reports/global-der-overview` (visited on 12/25/2022).

Nezamabadi, Hossein and Setayesh Nazar, Mehrdad (2016). "Arbitrage strategy of virtual power plants in energy, spinning reserve and reactive power markets". In: *IET Generation, Transmission & Distribution* 10.3, pp. 750–763.

Nguyen, Hieu Trung, Le, Long Bao, and Wang, Zhaoyu (2018). "A bidding strategy for virtual power plants with the intraday demand response exchange market using the stochastic programming". In: *IEEE Transactions on Industry Applications* 54.4, pp. 3044–3055.

Nosratabadi, Seyyed Mostafa, Hooshmand, Rahmat-Allah, and Gholipour, Eskandar (2016). "Stochastic profit-based scheduling of industrial virtual power plant using the best demand response strategy". In: *Applied energy* 164, pp. 590–606.

– (2017). "A comprehensive review on microgrid and virtual power plant concepts employed for distributed energy resources scheduling in power systems". In: *Renewable and Sustainable Energy Reviews* 67, pp. 341–363.

Nunes, Pedro and Brito, MC (2017). "Displacing natural gas with electric vehicles for grid stabilization". In: *Energy* 141, pp. 87–96.

Nwulu, Nnamdi I and Xia, Xiaohua (2017). "Optimal dispatch for a microgrid incorporating renewables and demand response". In: *Renewable energy* 101, pp. 16–28.

Olival, PC, Madureira, André Guimarães, and Matos, Manuel (2017). “Advanced voltage control for smart microgrids using distributed energy resources”. In: *Electric power systems research* 146, pp. 132–140.

Oliveira Farias, Héricles Eduardo et al. (2021). “Combined Framework with Heuristic Programming and Rule-Based Strategies for Scheduling and Real Time Operation in Electric Vehicle Charging Stations”. In: *Energies* 14.5, p. 1370.

Ottesen, Stig Ødegaard, Tomasgard, Asgeir, and Fleten, Stein-Erik (2018). “Multi market bidding strategies for demand side flexibility aggregators in electricity markets”. In: *Energy* 149, pp. 120–134.

Pandžić, Hrvoje et al. (2013). “Offering model for a virtual power plant based on stochastic programming”. In: *Applied Energy* 105, pp. 282–292.

Peik-Herfeh, Malahat, Seifi, H, and Sheikh-El-Eslami, MK (2013). “Decision making of a virtual power plant under uncertainties for bidding in a day-ahead market using point estimate method”. In: *International Journal of Electrical Power & Energy Systems* 44.1, pp. 88–98.

Peikherfeh, Malahat, Seifi, Hossein, and Sheikh-El-Eslami, Mohammad Kazem (2011). “Optimal dispatch of distributed energy resources included in a virtual power plant for participating in a day-ahead market”. In: *2011 International Conference on Clean Electrical Power (ICCEP)*. IEEE, pp. 204–210.

PJM thirty minute reserve (2019). P. J. M. Interconnection. URL: `https://www.pjm.com/-/media/committees-groups/committees/oc/20180306/20180306-item-19-30-minutereserves.ashx` (visited on 09/11/2020).

Pourghaderi, Niloofar et al. (2018). “Commercial demand response programs in bidding of a technical virtual power plant”. In: *IEEE Transactions on Industrial Informatics* 14.11, pp. 5100–5111.

Pourghaderi, Niloofar et al. (2021). “Reliability-based optimal bidding strategy of a technical virtual power plant”. In: *IEEE Systems Journal* 16.1, pp. 1080–1091.

Qiu, Jing et al. (2017). “Optimal scheduling for prosumers in coupled transactive power and gas systems”. In: *IEEE Transactions on Power Systems* 33.2, pp. 1970–1980.

Quint, Ryan et al. (2019). “Transformation of the grid: The impact of distributed energy resources on bulk power systems”. In: *IEEE Power and Energy Magazine* 17.6, pp. 35–45.

Rahimi, Mahdi, Ardakani, Fatemeh Jahanbani, and Ardakani, Ali Jahanbani (2021). “Optimal stochastic scheduling of electrical and thermal renewable and non-renewable resources in virtual power plant”. In: *International Journal of Electrical Power & Energy Systems* 127, p. 106658.

Rahimiyan, Morteza and Baringo, Luis (2015). “Strategic bidding for a virtual power plant in the day-ahead and real-time markets: A price-taker robust optimization approach”. In: *IEEE Transactions on Power Systems* 31.4, pp. 2676–2687.

Rahman, Hasimah A et al. (2015). “Operation and control strategies of integrated distributed energy resources: A review”. In: *Renewable and Sustainable Energy Reviews* 51, pp. 1412–1420.

Rahman, Md Mustafizur et al. (2020). “Assessment of energy storage technologies: A review”. In: *Energy Conversion and Management* 223, p. 113295.

Rajendran, Gowthamraj et al. (2021). “A comprehensive review on system architecture and international standards for electric vehicle charging stations”. In: *Journal of Energy Storage* 42, p. 103099.

Rassaei, Farshad, Soh, Wee-Seng, and Chua, Kee-Chaing (2015). “Demand response for residential electric vehicles with random usage patterns in smart grids”. In: *IEEE Transactions on Sustainable Energy* 6.4, pp. 1367–1376.

Rezaei, Navid et al. (2020). “Economic energy and reserve management of renewable-based microgrids in the presence of electric vehicle aggregators: A robust optimization approach”. In: *Energy* 201, p. 117629.

Richardson, David B (2013). “Electric vehicles and the electric grid: A review of modeling approaches, Impacts, and renewable energy integration”. In: *Renewable and Sustainable Energy Reviews* 19, pp. 247–254.

Rui, Tao et al. (2019). “A distributed charging strategy based on day ahead price model for PV-powered electric vehicle charging station”. In: *Applied Soft Computing* 76, pp. 638–648.

Sadati, S Muhammad Bagher et al. (2019). “Bi-level model for operational scheduling of a distribution company that supplies electric vehicle parking lots”. In: *Electric Power Systems Research* 174, p. 105875.

Sadeghi, Saleh et al. (2021). “Optimal bidding strategy of a virtual power plant in day-ahead energy and frequency regulation markets: A deep learning-based approach”. In: *International Journal of Electrical Power & Energy Systems* 127, p. 106646.

Saner, Can Berk, Trivedi, Anupam, and Srinivasan, Dipti (2022). “A cooperative hierarchical multi-agent system for EV charging scheduling in presence of multiple charging stations”. In: *IEEE Transactions on Smart Grid* 13.3, pp. 2218–2233.

Sarker, Mushfiqur R, Dvorkin, Yury, and Ortega-Vazquez, Miguel A (2015). “Optimal participation of an electric vehicle aggregator in day-ahead energy and reserve markets”. In: *IEEE transactions on power systems* 31.5, pp. 3506–3515.

Shabanzadeh, Morteza, Sheikh-El-Eslami, Mohammad-Kazem, and Haghifam, Mahmoud-Reza (2015). “The design of a risk-hedging tool for virtual power plants via robust optimization approach”. In: *Applied Energy* 155, pp. 766–777.

– (2017). “An interactive cooperation model for neighboring virtual power plants”. In: *Applied energy* 200, pp. 273–289.

Shafie-Khah, Miadreza et al. (2015). “Optimal behavior of electric vehicle parking lots as demand response aggregation agents”. In: *IEEE Transactions on Smart Grid* 7.6, pp. 2654–2665.

Shafiekhani, Morteza et al. (2019). "Strategic bidding of virtual power plant in energy markets: A bi-level multi-objective approach". In: *International Journal of Electrical Power & Energy Systems* 113, pp. 208–219.

Shamshirband, Mehdi, Salehi, Javad, and Gazijahani, Farhad Samadi (2018). "Decentralized trading of plug-in electric vehicle aggregation agents for optimal energy management of smart renewable penetrated microgrids with the aim of CO2 emission reduction". In: *Journal of Cleaner Production* 200, pp. 622–640.

Sharma, Satish and Abhyankar, AR (2016). "Loss allocation for weakly meshed distribution system using analytical formulation of Shapley value". In: *IEEE Transactions on Power Systems* 32.2, pp. 1369–1377.

Shayegan-Rad, Ali, Badri, Ali, and Zangeneh, Ali (2017). "Day-ahead scheduling of virtual power plant in joint energy and regulation reserve markets under uncertainties". In: *Energy* 121, pp. 114–125.

Sheidaei, F and Ahmarinejad, A (2020). "Multi-stage stochastic framework for energy management of virtual power plants considering electric vehicles and demand response programs". In: *International Journal of Electrical Power & Energy Systems* 120, p. 106047.

Shi, Ye et al. (2018). "Model predictive control for smart grids with multiple electric-vehicle charging stations". In: *IEEE Transactions on Smart Grid* 10.2, pp. 2127–2136.

Shin, MyungJae, Choi, Dae-Hyun, and Kim, Joongheon (2019). "Cooperative management for PV/ESS-enabled electric vehicle charging stations: A multiagent deep reinforcement learning approach". In: *IEEE Transactions on Industrial Informatics* 16.5, pp. 3493–3503.

Singh, Bhim et al. (2020). "Implementation of solar PV-battery and diesel generator based electric vehicle charging station". In: *IEEE Transactions on Industry Applications* 56.4, pp. 4007–4016.

Singh, Shakti, Jagota, Shubhangi, and Singh, Mukesh (2018). "Energy management and voltage stabilization in an islanded microgrid through an electric vehicle charging station". In: *Sustainable cities and society* 41, pp. 679–694.

Solanke, Tirupati Uttamrao et al. (2020). “A review of strategic charging–discharging control of grid-connected electric vehicles”. In: *Journal of Energy Storage* 28, p. 101193.

Song, Yanqiu, Shangguan, Lingzhi, and Li, Guijun (2021). “Simulation analysis of flexible concession period contracts in electric vehicle charging infrastructure public-private-partnership (EVCI-PPP) projects based on time-of-use (TOU) charging price strategy”. In: *Energy* 228, p. 120328.

Sovacool, Benjamin K et al. (2018). “The neglected social dimensions to a vehicle-to-grid (V2G) transition: a critical and systematic review”. In: *Environmental Research Letters* 13.1, p. 013001.

Stekli, Joseph et al. (2022). “Distributed energy resource participation in electricity markets: A review of approaches, modeling, and enabling information and communication technologies”. In: *Energy Strategy Reviews* 43, p. 100940.

Su, Jun, Lie, TT, and Zamora, Ramon (2019). “Modelling of large-scale electric vehicles charging demand: A New Zealand case study”. In: *Electric Power Systems Research* 167, pp. 171–182.

– (2020). “A rolling horizon scheduling of aggregated electric vehicles charging under the electricity exchange market”. In: *Applied energy* 275, p. 115406.

Sun, Baojun (2021). “A multi-objective optimization model for fast electric vehicle charging stations with wind, PV power and energy storage”. In: *Journal of Cleaner Production* 288, p. 125564.

Tajeddini, Mohammad Amin, Rahimi-Kian, Ashkan, and Soroudi, Alireza (2014). “Risk averse optimal operation of a virtual power plant using two stage stochastic programming”. In: *Energy* 73, pp. 958–967.

Tan, Xiaoqi et al. (2017). “Optimal scheduling of battery charging station serving electric vehicles based on battery swapping”. In: *IEEE Transactions on Smart Grid* 10.2, pp. 1372–1384.

Tan, Zhongfu et al. (2020). “Dispatching optimization model of gas-electricity virtual power plant considering uncertainty based on robust stochastic optimization theory”. In: *Journal of Cleaner Production* 247, p. 119106.

Tastu, Julija et al. (2011). “Spatio-temporal analysis and modeling of short-term wind power forecast errors”. In: *Wind Energy* 14.1, pp. 43–60.

TIDE: Take control of your energy bills the smart way (2022). Green Energy UK. URL: `https://www.greenenergyuk.com/tideabout` (visited on 02/07/2022).

Torreglosa, Juan P et al. (2016). “Decentralized energy management strategy based on predictive controllers for a medium voltage direct current photovoltaic electric vehicle charging station”. In: *Energy Conversion and Management* 108, pp. 1–13.

Toubeau, Jean-François, De Grève, Zacharie, and Vallée, François (2017). “Medium-term multimarket optimization for virtual power plants: A stochastic-based decision environment”. In: *IEEE Transactions on Power Systems* 33.2, pp. 1399–1410.

Vahedipour-Dahraie, Mostafa et al. (2020). “Risk-averse optimal energy and reserve scheduling for virtual power plants incorporating demand response programs”. In: *IEEE Transactions on Smart Grid* 12.2, pp. 1405–1415.

Vasirani, Matteo et al. (2013). “An agent-based approach to virtual power plants of wind power generators and electric vehicles”. In: *IEEE Transactions on Smart Grid* 4.3, pp. 1314–1322.

Vayá, Marina González and Andersson, Göran (2015). “Self scheduling of plug-in electric vehicle aggregator to provide balancing services for wind power”. In: *IEEE Transactions on Sustainable Energy* 7.2, pp. 886–899.

Wang, Beibei and Hobbs, Benjamin F (2014). “A flexible ramping product: Can it help real-time dispatch markets approach the stochastic dispatch ideal?” In: *Electric Power Systems Research* 109, pp. 128–140.

Wang, Haifeng et al. (2021a). “Optimal scheduling of electric vehicles charging in battery swapping station considering wind-photovoltaic accommodation”. In: *Electric Power Systems Research* 199, p. 107451.

Wang, Han, Riaz, Shariq, and Mancarella, Pierluigi (2020). “Integrated techno-economic modeling, flexibility analysis, and business case assessment of an urban virtual power plant with multi-market co-optimization”. In: *Applied Energy* 259, p. 114142.

Wang, Han et al. (2021b). “Two-stage minimax regret-based self-scheduling strategy for virtual power plants”. In: *2021 IEEE Power & Energy Society General Meeting (PESGM)*. IEEE, pp. 1–5.

Wang, Han et al. (2022a). “A Hybrid Incentive Program for Managing Electric Vehicle Charging Flexibility”. In: *IEEE Transactions on Smart Grid* 14.1, pp. 476–488.

Wang, Han et al. (2022b). “Electric Vehicle Charging Scheduling Strategy for Supporting Load Flattening under Uncertain Electric Vehicle Departures”. In: *Journal of Modern Power Systems and Clean Energy*.

Wang, Han et al. (2022c). “Optimal operating regime of an electric vehicle aggregator considering reserve provision”. In: *Energy Reports* 8, pp. 353–362.

Wang, Jianing et al. (2022d). “Virtual power plant containing electric vehicles scheduling strategies based on deep reinforcement learning”. In: *Electric power systems research* 205, p. 107714.

Wang, Jianxiao et al. (2017a). “Optimal bidding strategy for microgrids in joint energy and ancillary service markets considering flexible ramping products”. In: *Applied Energy* 205, pp. 294–303.

Wang, Jianxiao et al. (2017b). “Robust bidding strategy for microgrids in joint energy, reserve and regulation markets”. In: *2017 IEEE Power & Energy Society General Meeting*. IEEE, pp. 1–5.

Wang, Mingshen et al. (2020). “Electric vehicle aggregator modeling and control for frequency regulation considering progressive state recovery”. In: *IEEE Transactions on Smart Grid* 11.5, pp. 4176–4189.

Wang, Yuchang and Thompson, John S (2018). “Two-stage admission and scheduling mechanism for electric vehicle charging”. In: *IEEE Transactions on Smart Grid* 10.3, pp. 2650–2660.

Wei, Congying et al. (2018). "A bi-level scheduling model for virtual power plants with aggregated thermostatically controlled loads and renewable energy". In: *Applied Energy* 224, pp. 659–670.

Wenzel, George et al. (2017). "Real-time charging strategies for an electric vehicle aggregator to provide ancillary services". In: *IEEE Transactions on Smart Grid* 9.5, pp. 5141–5151.

Wind Generation Data (2019). FindGrid. URL: `https://data.fingrid.fi/open-dataforms/search/en/?selected_datasets=181` (visited on 06/14/2021).

Wozabal, David and Rameseder, Gunther (2020). "Optimal bidding of a virtual power plant on the Spanish day-ahead and intraday market for electricity". In: *European Journal of Operational Research* 280.2, pp. 639–655.

Wu, Fei and Sioshansi, Ramteen (2019). "A stochastic operational model for controlling electric vehicle charging to provide frequency regulation". In: *Transportation Research Part D: Transport and Environment* 67, pp. 475–490.

Wu, Qiuwei et al. (2018). "Transactive real-time electric vehicle charging management for commercial buildings with PV on-site generation". In: *IEEE Transactions on Smart Grid* 10.5, pp. 4939–4950.

Wu, Yu et al. (2022). "Hierarchical operation of electric vehicle charging station in smart grid integration applications—An overview". In: *International Journal of Electrical Power & Energy Systems* 139, p. 108005.

Xu, Shaolun et al. (2019). "Decentralized charging control strategy of the electric vehicle aggregator based on augmented Lagrangian method". In: *International Journal of Electrical Power & Energy Systems* 104, pp. 673–679.

Yang, Dechang et al. (2020a). "Bidding strategy for virtual power plant considering the large-scale integrations of electric vehicles". In: *IEEE Transactions on Industry Applications* 56.5, pp. 5890–5900.

Yang, Jiajia et al. (2020b). “A penalty scheme for mitigating uninstructed deviation of generation outputs from variable renewables in a distribution market”. In: *IEEE Transactions on Smart Grid* 11.5, pp. 4056–4069.

Yang, Xiyun and Zhang, Yanfeng (2021). “A comprehensive review on electric vehicles integrated in virtual power plants”. In: *Sustainable Energy Technologies and Assessments* 48, p. 101678.

Yao, Leehter, Lim, Wei Hong, and Tsai, Teng Shih (2016). “A real-time charging scheme for demand response in electric vehicle parking station”. In: *IEEE Transactions on Smart Grid* 8.1, pp. 52–62.

You, Pengcheng et al. (2015). “Optimal cooperative charging strategy for a smart charging station of electric vehicles”. In: *IEEE Transactions on Power Systems* 31.4, pp. 2946–2956.

You, Shi, Traeholt, Chresten, and Poulsen, Bjarne (2009). “A market-based virtual power plant”. In: *2009 International Conference on Clean Electrical Power*. IEEE, pp. 460–465.

Yu, Songyuan et al. (2019). “Uncertainties of virtual power plant: Problems and countermeasures”. In: *Applied energy* 239, pp. 454–470.

Yuan, Zhi-Peng et al. (2022). “Data-Driven Risk-Adjusted Robust Energy Management for Microgrids Integrating Demand Response Aggregator and Renewable Energies”. In: *IEEE Transactions on Smart Grid* 14.1, pp. 365–377.

Zamani, Ali Ghahgharaee et al. (2016). “Stochastic operational scheduling of distributed energy resources in a large scale virtual power plant”. In: *International Journal of Electrical Power & Energy Systems* 82, pp. 608–620.

Zeng, Bo and Zhao, Long (2013). “Solving two-stage robust optimization problems using a column-and-constraint generation method”. In: *Operations Research Letters* 41.5, pp. 457–461.

Zhang, Chenghua et al. (2018). “Peer-to-Peer energy trading in a Microgrid”. In: *Applied Energy* 220, pp. 1–12.

Zhang, Lei and Li, Yaoyu (2015a). “A game-theoretic approach to optimal scheduling of parking-lot electric vehicle charging”. In: *IEEE Transactions on Vehicular Technology* 65.6, pp. 4068–4078.

– (2015b). “Optimal management for parking-lot electric vehicle charging by two-stage approximate dynamic programming”. In: *IEEE Transactions on Smart Grid* 8.4, pp. 1722–1730.

Zhang, Runfan and Hredzak, Branislav (2020). “Distributed dynamic clustering algorithm for formation of heterogeneous virtual power plants based on power requirements”. In: *IEEE Transactions on Smart Grid* 12.1, pp. 192–204.

Zhang, Zhien et al. (2020). “Advances in carbon capture, utilization and storage”. In: *Applied Energy* 278, p. 115627.

Zhao, Haotian et al. (2020). “Aggregating additional flexibility from quick-start devices for multi-energy virtual power plants”. In: *IEEE Transactions on Sustainable Energy* 12.1, pp. 646–658.

Zhao, Tianyang et al. (2017). “Real-time optimal energy and reserve management of electric vehicle fast charging station: Hierarchical game approach”. In: *IEEE Transactions on Smart Grid* 9.5, pp. 5357–5370.

Zheng, Liran et al. (2021). “A Charging Strategy for Electric Vehicle Fast Charging Station to Mitigate Distribution Transformer Aging and Reduce Operation Cost”. In: *2021 IEEE Industry Applications Society Annual Meeting (IAS)*. IEEE, pp. 1–8.

Zheng, Yanchong, Wang, Yubin, and Yang, Qiang (2023). “Two-phase operation for coordinated charging of electric vehicles in a market environment: From electric vehicle aggregators’ perspective”. In: *Renewable and Sustainable Energy Reviews* 171, p. 113006.

Zheng, Yanchong et al. (2019). “Integrating plug-in electric vehicles into power grids: A comprehensive review on power interaction mode, scheduling methodology and mathematical foundation”. In: *Renewable and Sustainable Energy Reviews* 112, pp. 424–439.

Zheng, Yanchong et al. (2020). “Day-ahead bidding strategy for electric vehicle aggregator enabling multiple agent modes in uncertain electricity markets”. In: *Applied Energy* 280, p. 115977.

Zhou, Bin et al. (2020). “Optimal coordination of electric vehicles for virtual power plants with dynamic communication spectrum allocation”. In: *IEEE Transactions on Industrial Informatics* 17.1, pp. 450–462.

Zhou, Yuzhou, Zhai, Qiaozhu, and Wu, Lei (2022). “Optimal operation of regional microgrids with renewable and energy storage: Solution robustness and nonanticipativity against uncertainties”. In: *IEEE Transactions on Smart Grid* 13.6, pp. 4218–4230.

Zhou, Zhenyu et al. (2019). “Blockchain and computational intelligence inspired incentive-compatible demand response in internet of electric vehicles”. In: *IEEE Transactions on Emerging Topics in Computational Intelligence* 3.3, pp. 205–216.

Appendix A

Appendix Chapter

A.1 Two-Stage Minimax Regret Problem Reformulation

The original two-stage minimiax regret problem is as follows:

$$\min_{y} \left\{ f_1(y) + \max_{u} \left\{ \min_{x} f_2(x) - \min_{y^u, x^u} \left[f_1(y) + f_2(x^u) \right] \right\} \right\} \tag{A.1}$$

Firstly, the inner minimization problem is transformed into a maximization problem, this can be achieved by altering the sign of the optimal solution cost functions and turn it into a maximization problem. Hence, equation (A.1) can be written as:

$$\min_{y} \left\{ f_1(y) + \max_{u} \left\{ \max_{y^u, x^u} \left[-f_1(y) - f_2(x^u) \right] + \min_{x} f_2(x) \right\} \right\} \tag{A.2}$$

The optimal solutions y^u and x^u are dependent on the uncertainty realizations u. Because both the uncertainty realization u and optimal solutions under u are optimization variables, and both are maximization problems, the second inner maximization problem can be integrated for the optimal solution under scenario u into the middle maximization problem. Following this operation, equation (A.2) is equivalent to equation (A.3):

$$\min_{y} \left\{ f_1(y) + \max_{u,y^u,x^u} \left\{ \min_{x} \left[f_2(x) - f_1(y) - f_2(x^u) \right] \right\} \right\} \tag{A.3}$$

In equation (A.3), the worst-case uncertainty realization u, the optimal first-stage decision y^u and second-stage decision x^u under u are all decision variables of the middle maximization problem. To this end, by considering a lifted uncertain vector ζ that represents all the variables in the middle maximization problem, equation (A.3) can be reformulated as:

$$\min_{y} \left\{ f_1(y) + \max_{\zeta} \left\{ \min_{x} \left[f_2(x) - f_1(y) - f_2(x^u) \right] \right\} \right\} \tag{A.4}$$

A.2 Bilinear Term Transformation

The Bilinear term $\beta \Delta P_{m,t}^{d}$ is the product of two bounded continuous variables β and $\Delta P_{m,t}^{d}$. To transform it into the product of a binary variable $y_{m,t}^{d}$, a continuous variable β, and a constant $P_{m,t}^{us}$, the optimality condition can be utilized. Firstly, when $\Delta P_{m,t}^{d} > 0$, from the objective function one can conclude that:

$$\lambda_m^{out} - \lambda_m^{in} > \beta \tag{A.5}$$

where λ_m^{out} is the market price when the load is shifted out, and λ_m^{in} is the market price when the load is shifted in. In this case, the profit improvement $\Delta Profit$ from shifting the load $\Delta P_{m,t}^{d}$ is:

$$\Delta Profit = \Delta P_{m,t}^{d} (\lambda_m^{out} - \lambda_m^{in} - \beta) \tag{A.6}$$

The profit change $\Delta Profit$ is an increasing function of $\Delta P_{m,t}^{d}$. Hence, in the optimal solution, the value of $\Delta P_{m,t}^{d}$ is either 0 or its maximum possible value $P_{m,t}^{us}$. To this end, the continuous variable $\Delta P_{m,t}^{d}$ can be transformed into the product of a binary variable $y_{m,t}^{d}$ and a constant $P_{m,t}^{us}$.